From the:

Comprehensive Pneumology Center (CPC), Helmholtz Center Munich

and the

Institute of Experimental Pneumology, Ludwig-Maximilians-Universität München

Director: Dr. Ali Önder Yildirim

Dissertation

zum Erwerb des Doctor of Philosophy (Ph.D.) an der

Medizinischen Fakultät der

Ludwig-Maximilians-Universität zu München

Harnessing primary human bronchial epithelial cell culture for studies of airway epithelial injury and regeneration

vorgelegt von:

Ashesh Anjankumar Chakraborty

aus:

Ahmedabad, India

Jahr:

2022

Mit Genehmigung der Medizinischen Fakultät der

Ludwig-Maximilians-Universität zu München

First evaluator (1. TAC member): *PD Dr. Claudia Staab-Weijnitz*

Second evaluator (2. TAC member): *Prof. Dr. rer. nat. Alexander Dietrich*

Dean: **Prof. Dr. med. Thomas Gudermann**

Datum der Verteidigung:

19.06.2023

Affidavit

LMU LUDWIG-MAXIMILIANS-UNIVERSITÄT MÜNCHEN | Dean's Office Medical Faculty | MMRS

Affidavit

Chakraborty, Ashesh Anjankumar
Surname, first name

Germany
Country

I hereby declare, that the submitted thesis entitled:

Harnessing primary human bronchial epithelial cell culture for studies of airway epithelial injury and regeneration

is my own work. I have only used the sources indicated and have not made unauthorised use of services of a third party. Where the work of others has been quoted or reproduced, the source is always given.

I further declare that the dissertation presented here has not been submitted in the same or similar form to any other institution for the purpose of obtaining an academic degree.

Munich, 10.07.2023
place, date

Ashesh Anjankumar Chakraborty
Signature doctoral candidate

Confirmation of congruency

LMU LUDWIG-MAXIMILIANS-UNIVERSITÄT MÜNCHEN | Dean's Office Medical Faculty | MMRS

Confirmation of congruency between printed and electronic version of the doctoral thesis

Chakraborty, Ashesh Anjankumar
Surname, first name

Germany
Country

I hereby declare, that the submitted thesis entitled:

Harnessing primary human bronchial epithelial cell culture for studies of airway epithelial injury and regeneration

is congruent with the printed version both in content and format.

Munich, 10.07.2023
place, date

Ashesh Anjankumar Chakraborty
Signature doctoral candidate

Table of contents

Summary

The human airway epithelium provides the first interaction site for inhaled toxicants and pathogens and plays an important role in the development of both acute and chronic lung diseases including major global causes of death like chronic obstructive pulmonary disease and lung cancer. In such diseased conditions, the normal architecture of the airways is distorted, and restoration of the normal airway structure is desirable. However, the underlying mechanisms involved in adult human airway regeneration are poorly understood. To date, our knowledge about acute airway epithelial injury and subsequent regeneration mechanisms has been heavily dependent on the use of mouse models where exposure to *e.g.* polidocanol (PDOC) or naphthalene (NA) causes unspecific or cell type-specific depletion of bronchial epithelial cells followed by regeneration. Such acute injury to the airway epithelium is often related to suffering and distress for the animals. In addition, the airway structure, size, cell type composition, and progenitor stem cells involved differ between mice and humans. Therefore, the aim of this thesis was to develop human-derived models and elucidate novel mechanisms underlying human bronchial epithelial regeneration using organotypic culture of primary human bronchial epithelial cells (phBECs) at air-liquid interface (ALI).

Upon airway epithelial injury, the human airway progenitor basal cells present in the airway epithelium undergo proliferation and regenerate the damaged epithelium. Similarly, during *in vitro* differentiation of phBECs into a full-blown epithelium, basal cells proliferate and differentiate to form a functional bronchial epithelium featuring all major cell types. Therefore, normal *in vitro* differentiation of phBECs serves, to some extent, as a model of airway injury. In the first part of the study (chapter 1), this airway basal cell differentiation model was applied to study underlying mechanisms in bronchial epithelial regeneration. This model is, however, limited in terms of physiological relevance, because it does not represent an injury on a fully differentiated epithelium; it also does not allow for second hit studies. Therefore, in the second part of this thesis work (chapter 2) a novel human *in vitro* model for airway epithelial injury and regeneration was established.

In chapter 1, unbiased proteomic analysis from human airway basal cell differentiation into a fully functional bronchial epithelium showed an overall inhibition of the cholesterol biosynthesis pathway during the differentiation phase. Hence, we aimed to investigate the role of the cholesterol biosynthesis pathway in the differentiation of airway epithelial basal cells into a full-blown bronchial epithelium. To address this aim, we differentiated phBECs in the continuous presence of supplemented cholesterol (CHOL) for 21 days. Chronic CHOL treatment resulted in an increased club cell population in comparison to time-matched vehicle control during the differentiation phase as monitored via immunofluorescent stainings.

In the second part of the study chapter 2, differentiated phBECs were treated with either NA or PDOC. In contrast to the mouse model, 0.35 mM NA treatment did not induce any cell death in differentiated phBECs, let alone specifically deplete club cells. PDOC treatment, however, led to a marked loss of cells with a half-maximal effective concentration (EC50) of 0.047% PDOC. Treatment of differentiated phBECs with 0.04% PDOC led to initial cell depletion and was followed by subsequent regeneration of a functional epithelium, as evident by the rise of differentiated cell types such as ciliated, goblet, and club cells at an expense of basal cells, and the restoration of epithelial barrier integrity during the regeneration phase. In a proof-of-concept approach, the inhibition of Notch signalling by the ɣ-secretase inhibitor DAPT during the regeneration phase blunted differentiation towards secretory cell types such as club and goblet cells.

In conclusion, this thesis work has identified cholesterol as a potential regulator of bronchial epithelial cell fate and established a novel human *in vitro* model for studying airway epithelial injury and regeneration. Inhibition of Notch signalling on the established regeneration model post PDOC injury abolished secretory cell formation serving as a proof-of-concept that the established human *in vitro* model is suitable to study mechanisms of airway epithelial injury and repair.

1. Introduction

1.1 Human airways structure and function

The human conducting airway epithelium provides the first line of defence against inhaled toxins, particles, and pathogens present in the outside environment. Upon inhalation of these toxicants, the conducting airways provide numerous defence mechanisms where these toxicants are trapped and removed either via mucociliary clearance. Furthermore, the epithelial cells present in the airways contain xenobiotic metabolizing enzymes namely cytochrome P 450 enzymes, glutathione S transferases, and epoxide hydrolases which are also involved in the detoxification of these toxicants in the airways (Castell et al., 2005; Hiemstra et al., 2018). However, repeated exposure of such toxicants to the airways may disrupt lung homeostasis and could lead to a cascade of events such as oxidative stress, altered airways epithelial barrier integrity, excessive radical formation (reactive oxygen/nitrogen species), altered epithelial differentiation and defective epithelial microbial defence mechanisms (Castell et al., 2005; Hiemstra et al., 2018; Romieu et al., 2008).

1.1.1 Major airways cell types

In general, the human lung is divided into two regions, defined as the conducting airways and the respiratory airways. The conducting airways contain the trachea, the bronchi, and the conducting bronchioles. The conducting airways are lined with a pseudostratified epithelium containing cell types such as ciliated, goblet, club, and basal cells. However, as airways generation increases, the airways' structure and the cell type composition also change from pseudostratified epithelium to simple columnar or cuboidal epithelium containing predominantly secretory cells, mainly club cells, and fewer ciliated cells. Basal cells are considered progenitors for the other cell types in the conducting airways (BéruBé et al., 2010; Chakraborty et al., 2022) (Figure 1a). Club cells are non-ciliated epithelial cells have been associated with several protective roles such as secretion of anti-inflammatory and immunomodulatory proteins. Club cells also serve as progenitors for ciliated cells in the airway. Furthermore, they are

also involved in the detoxification of inhaled toxicants via Xenobiotic metabolizing enzymes (XME's) (Rokicki et al., 2016). Goblet cells are the mucus producing cells involved in the maintenance of epithelial barrier via the secretion of mucus. They are also involved in the secretion of anti-microbial proteins, cytokines and chemokines in the airways (Davis & Wypych, 2021). Another predominant cell type ciliated cells account for over 50% of all cells in the human conducting airways and plays an important role in the maintenance of airway homeostasis. They contain about 300 motile cilia per cell and are involved in the removal of mucus and other debris from the airways via ciliary beating (Schamberger et al., 2015). The respiratory airways contain the respiratory bronchioles and the alveoli, which in turn consist of alveolar type I (AT I) and type II (AT II) cells. While AT1 cells are essential for facilitating gas exchange between the human lung and blood capillaries, AT II cells produce surfactant and are the progenitors for the rise of AT I cells in the respiratory airways.

1.1.2 Rare cell types in human airways

With the advent of single cell technologies, several rare cell types have been described for the conducting airways in the last decade. For instance, pulmonary neuroendocrine cells (PNECs) are a rare epithelial cell population randomly distributed in the airways and represent less than 1% of the total lung epithelial cell population (Branchfield et al., 2016; Mou et al., 2021; Song et al., 2012; Weichselbaum et al., 2005). PNECs are also involved in the maintenance of innate immunity in airways by releasing neuropeptides and neurotransmitters against inhaled environmental stimuli. Under normal conditions PNEC numbers remain low, however, it has been reported that there is an increase in the number of PNECs during lung diseases such as asthma, chronic obstructive pulmonary disease, bronchopulmonary dysplasia, cystic fibrosis, and pulmonary hypertension (Cutz et al., 2007; Gu et al., 2014; Sunday et al., 2004).

Another rare airways cell type, the tuft cell or brush cell, is rarely found in the tracheal region but absent from the lower respiratory airways until damage (Rane et al., 2019; Strine & Wilen, 2022). Tuft cells are known to be involved in acetylcholine, eicosanoid and IL 25 synthesis in the airways (Davis & Wypych, 2021). Additionally, tuft cells are also responsible to detect bacteria and aller-

gens in the airways and induce neuroinflammation and anti-bacterial response against them (Billipp et al., 2021).

Pulmonary ionocytes consist of less than 2% of the total cell type population found in the human airways. Airways epithelial basal cells or tuft cells are the progenitors for pulmonary ionocytes. Pulmonary ionocytes rely on Notch signalling for their differentiation and express cystic fibrosis transmembrane conductance regulator and forkhead box I1 (Davis & Wypych, 2021; Plasschaert et al., 2018). Finally, another cell type termed hillock cells are generally found in the conducting airways and corresponds to keratin 13^{+} cells. These cells are considered to be highly proliferative and also express markers associated with cell adhesion and squamous cell differentiation (Davis & Wypych, 2021; Deprez et al., 2020; Plasschaert et al., 2018).

1.2 Aberrant repair of the airway epithelium plays a central role in chronic lung disease development

1.2.1 Chronic Obstructive Pulmonary Disease (COPD)

Chronic obstructive pulmonary disease is the third leading cause of death worldwide according to the World Health Organization, and the trend is still rising (www.WHO.org) (Lopez et al., 2006). Cigarette smoking is one of the well-established major risk factors for the cause of COPD. However, other contributing risk factors include genetic predisposition (alpha 1 antitrypsin deficiency), air pollution, occupational-related exposures, and exposure to the toxic gases from biomass fuel combustion (Salvi & Barnes, 2009). COPD is characterized by airflow limitation, which is slowly progressive and mostly irreversible. The airflow limitation is caused due to the combination of emphysema (loss of alveolar structure due to the alveolar wall destruction), and small airway diseases. In COPD disease condition, several physiological and pathological changes observed include shortening of cilia and impaired mucociliary clearance (Thomas et al., 2021), reduced ciliated cell count and squamous cell metaplasia (Schamberger et al., 2015), epithelial barrier integrity dysfunction (Carlier et al., 2018), goblet cell hyperplasia leading to increased mucus secretion (Shaykhiev, 2019), and increased extracellular matrix deposition (Pini et al., 2014).

Aberrant repair takes place in such diseased condition, but the underlying mechanisms are not fully understood. The reactivation of developmental signalling pathways as one of the aberrant repair mechanisms have been studied in COPD such as Notch (Boucherat et al., 2016; Tilley et al., 2009), TGF-β1 (Dijke et al., 2002; Disler et al., 2019; Springer et al., 2004; I. M. Wang et al., 2008; Zandvoort et al., 2006), and Wnt has also been observed in COPD (Boucherat et al., 2016). A study carried out by Carlier et al., showed an upregulation of the Wnt/β-catenin pathway in the airway epithelium of COPD patients as compared to never smokers and control smokers. Furthermore, they also reported that the extrinsic activation of the Wnt/β-catenin pathway in the airway epithelial cells from COPD leads to epithelial barrier integrity dysfunction, inhibited epithelial differentiation, and also induced epithelial-to-mesenchymal transition (Carlier et al., 2018).

Therefore, based on the above-mentioned evidences, it suggests that an alteration of the conducting airways takes place in COPD pathogenesis and the aberrant repair observed contributes to the disease progression in part via the reactivation of the developmental signalling pathways as mentioned above, but to a large extent is not well understood.

1.2.2 Idiopathic Pulmonary Fibrosis (IPF)

Idiopathic pulmonary fibrosis is a devastating chronic lung disease with limited treatment options and a median survival rate approximately between 2-5 years after the first diagnosis. The incidence for IPF is estimated to be about 10 in 100,000 per year and the trend is continuously rising. Cigarette smoking is considered as one of the major risk factors in IPF (Sauleda et al., 2018). It is believed that the fibrotic response observed in IPF is triggered by repeated injuries to the airways epithelium, which further leads to the release of profibrotic mediators such as TGF-β1, myofibroblast differentiation, and excessive deposition of ECM components in the alveolar region causing impaired gas exchange.

Historically, IPF was believed to be caused by repetitive injuries to the respiratory epithelium; however, recent evidence has shown that the bronchial epithelium is also involved in IPF disease development and progression (Chakraborty et al., 2022). In IPF, several changes in the airways function have been report-

ed such as impaired mucociliary clearance, dysfunction of airways epithelial barrier integrity, thickening of basement membrane, honeycomb cyst formation, and increased ECM components deposition (Figure 1b). Honeycomb cysts formations are located close to the fibrotic areas in the alveolar region which are enriched with $KRT5^{+}KRT14^{+}CC10^{-}$ cells replacing normal alveolar epithelium in a process generally termed bronchiolization (Evans et al., 2016). Honeycomb cysts are generally of two types: 1) Honeycomb mucociliary: composed of the pseudostratified layer containing p63+KRT5+ basal, ciliated, and *MUC5B* expressing goblet cells (Prasse et al., 2019; Seibold et al., 2013; Smirnova et al., 2016). 2) Honeycomb basaloid: composed of stratified hyperplastic basal cells positive for KRT5, and KRT14 (Smirnova et al., 2016) (Figure 1b). An alteration of airways epithelial barrier integrity is observed in IPF, a study reported an increased claudin-2, a tight junction protein in the IPF bronchiolar regions (Zou et al., 2020). Furthermore, a study investigated the expression of protein kinase D (a negative regulator of airways barrier integrity) and reported increased expression in IPF bronchiolar region as compared to control (Gan et al., 2013, 2014). Airways epithelial senescence is implicated in IPF pathogenesis which is generally caused due to repetitive injuries to the epithelium and the cell cycle arrest of the progenitor stem cells (Selman & Pardo, 2014). Recent single-cell RNA seq studies have shown hyperplastic basal cell populations present in the bronchiolar region are involved in the expression of genes related to cell cycle growth arrest and senescence (Adams et al., 2020; DePianto et al., 2021; Habermann et al., 2020).

Figure 1

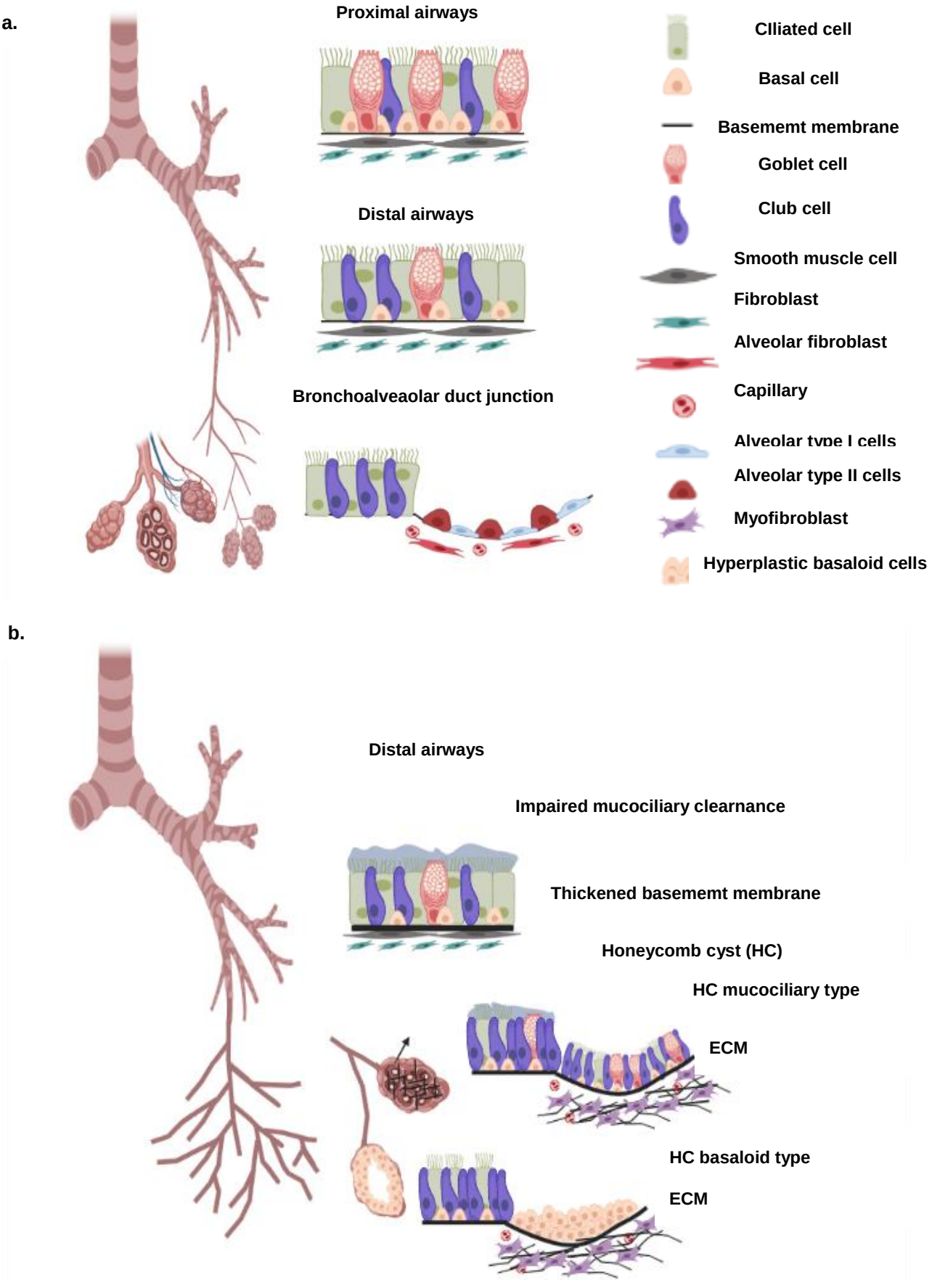
a.
Proximal airways
Distal airways
Bronchoalveaolar duct junction
Clliated cell
Basal cell
Basememt membrane
Goblet cell
Club cell
Smooth muscle cell
Fibroblast
Alveolar fibroblast
Capillary
Alveolar type I cells
Alveolar type II cells
Myofibroblast
Hyperplastic basaloid cells
b.
Distal airways
Impaired mucociliary clearnance
Thickened basememt membrane
Honeycomb cyst (HC)
HC mucociliary type
ECM
HC basaloid type
ECM

Figure 1: Graphical illustration of airways in healthy lung and IPF. (a) Healthy lung representing the normal cell type composition in the proximal, and the distal airways as well as in the bronchioalveolar duct junction. (b) IPF lung representing dilated bronchioles, thickened basement membrane and impaired mucociliary clearance in the distal airways, two different types of honeycomb cysts (HC: mucociliary type, and basaloid type), and the deposition of extracellular matrix (ECM) in the alveolar region. Figure was created using with biorender. This figure has been published in Chakraborty *et al.*, Cells, 2022 under an open access Creative Commons CC BY 4.0 license.

Furthermore, an increased expression of proapoptotic markers such as caspase 3, bax, and p53 and downregulation of anti-apoptotic marker such as bcl-2 has been reported in the bronchial epithelial cells from IPF patients, indicating apoptosis as a key event in the airways epithelium leading to delayed re-epithelization observed in IPF(Plataki et al., 2005). The reactivation of developmental signalling pathways has been implicated in IPF pathogenesis, such as activation of Notch signalling promoting aberrant epithelial repair (Vaughan et al., 2014), induction of TGF-β1 signalling leading to cell senescence (Minagawa et al., 2011), and Wnt signalling in airways remodeling (Königshoff et al., 2008).

Hence, based on the above-mentioned evidences, it suggest that the conducting airways are deregulated in IPF pathogenesis including thickening of basement membrane, impaired mucociliary clearance and honeycomb cyst formation. Aberrant airway epithelial repair via the reactivation of developmental pathways has been observed in IPF, but to a greater extent is not well understood.

1.2.3 Lung cancer

According to a WHO report, cancer is the leading cause of death worldwide accounting for nearly 10 million cases, out of which lung cancer-related death accounts for approximately 2.26 million cases (www.WHO.org). Lung cancer is generally classified into two major types, defined as Small cell and Non-Small Cell carcinoma. The major histological types included in non-small cell carcinoma involve squamous cell carcinoma, large cell carcinoma, and adenocarcinoma (Wistuba et al., 2000). The human airways epithelium is well known to be involved in the development of preneoplastic lesions prior to lung carcinoma development, and the pathological changes observed in the airway's epithelium include squamous cell dysplasia and hyperplasia. Wang and colleagues investigated the histological patterns of bronchial epithelial dysplasia from lung resection specimens with lung carcinoma. They showed increased expression of the bronchial epithelial cell dysplasia from the lung resection specimen positive for cytokeratin 7, 8, 10, 13, 17, and 18. Furthermore, they also found overexpression of p53 and Ki67 in these bronchial epithelial cell dysplasia (G. F. Wang et al., 2006). Smoking-associated COPD is considered to be one of the major risk factors for the cause of Lung cancer (Rooney & Sethi, 2011). CXCL14, an airway epithelium-derived chemokine regulates functions related to inflammation and carcinogenesis. A study used differentiated airways epithelial cells treated with smoke extract led to an induction of CXCL14, which further exerted its effect on airways basal cells and compromised the stemness property of basal cells. Interestingly, the same study also reported CXCL14 upregulation in two lung cancer cohorts (adenocarcinoma and squamous cell carcinoma) (Shaykhiev et al., 2013). Therefore, it suggests that the inflammation response observed in lung cancer leads to the release of cytokines which may further affect the airways basal stem cells to undergo repair and may cause cell cycle growth arrest. In lung cancer, the reactivation of developmental signalling pathways also takes place. A study has investigated the role of hedgehog signalling in lung cancer by collecting the lung tissue sections from lung cancer patients and determined the expression of hedgehog components such as SHH and GLI, and found them overexpressed in patients with lung cancer (Watkins et al., 2003). Besides hedgehog signalling, another developmental signalling pathway, Notch has also been reported to be deregulated in lung cancer. Studies have

reported overexpression of Notch-3 (Dang et al., 2000), gain-of-function mutation of Notch-1, and the suppression of NUMB protein (repressor of Notch signalling) (Westhoff et al., 2009) in tissue sections from lung cancer patients.

1.3 Acute lung injury and its implications on the human conducting airways

There is growing evidence that airway epithelial cells are involved in the pathogenesis of acute lung injury. As mentioned before, the airway epithelium provides the first line of defense against inhaled toxins, viruses and other environmental related exposures. The toll like receptor present on the airway epithelium upon interaction with the inhaled toxicants undergoes activation and initiates inflammatory response by releasing cytokines and chemokines, increased reactive radical formation and neutrophil activation (Ekstrand-Hammarström et al., 2007; Greene & McElvaney, 2005). Furthermore, an increased protease release and reduced antiprotease activity affecting tight junction protein E-cadherin is also observed in the pathogenesis of acute lung injury (McGuire et al., 2003). Therefore, it points clearly that an alteration in conducting airways is not only limited to chronic lung diseases but also observed in acute lung injury, so it is important to understand the mechanisms involved in adult human airway regeneration.

1.4 Aims of this thesis

Overall, it makes it clear that the airway epithelium injury and aberrant repair are central to the development of lung diseases including COPD and lung cancer which also account for major death burdens according to the WHO, but the underlying mechanisms in adult human airway regeneration is not well understood. In order to better understand these questions, the overall aim of the study has been divided into two specific aims as mentioned below

Chapter 1: Investigate the role of cholesterol biosynthesis pathway in human airway basal cell differentiation

Chapter 2: To establish a human in vitro model for airway epithelial injury and regeneration

2. Chapter 1: The role of cholesterol biosynthesis pathway in the human airway basal cell differentiation

The below mentioned work was performed by me and in part carried out by the master thesis student Ms Juliana Giraldo at Staab-Weijnitz Lab under my direct supervision and guidance in the laboratory.

2.1 Introduction

The molecular signalling pathways such as TGF-β, BMP, WNT, Hedgehog, and Notch play an important role in the maintenance of progenitor stem cells in the airways and initiate them to undergo proliferation and differentiation during the developmental stages of the lung. In addition, during lung development, the Notch signalling pathway determines the balance between ciliated and secretory cells in the human conducting airways (Chakraborty et al., 2022; Rackley & Stripp, 2012). These signalling pathways largely remain quiescent during a postnatal stage but undergo reactivation during an injury response and initiate the repair by inducing proliferation and differentiation of the progenitor stem cells in the airways (Chakraborty et al., 2022; Fernandez & Eickelberg, 2012). Aberrant repair via the reactivation of the development pathways have been shown in several chronic lung diseases, but the underlying mechanisms in the airway regeneration are not well studied.

Human airway basal cell differentiation have been used in the past for chronic injury studies using cigarette smoke (Mastalerz et al., 2022; Schamberger et al., 2015). So therefore, we take advantage of the airway basal cell differentiation model and investigated the underlying mechanisms of the conducting airway injury.

2.2 Results

2.2.1 Proteome analysis suggests a role for cholesterol biosynthesis in bronchial epithelial cell differentiation

To assess mechanisms underlying bronchial epithelial cell differentiation in an unbiased, global approach, we performed a proteome analysis on differentiating phBECs at the ALI, collecting total protein at day 0, 7, 14, 21, and 28, and subjecting the samples to label-free tandem mass spectrometry (MS/MS). Proteins with significantly altered levels (Log Fold change: < -1 or > +1, *p*-value < 0.05) were subjected to pathway enrichment analysis using Ingenuity pathway analysis (IPA Tool; Ingenuity®Systems, Redwood City, CA, USA; http://www.ingenuity.com).Here, we observed an overall inhibition of cholesterol biosynthesis pathway in comparison to day 0 during the differentiation phase (Figure 2). We therefore reasoned that supplementing CHOL during airways basal cell differentiation may alter differentiation routes and final airways cell composition.

Figure 2

a.

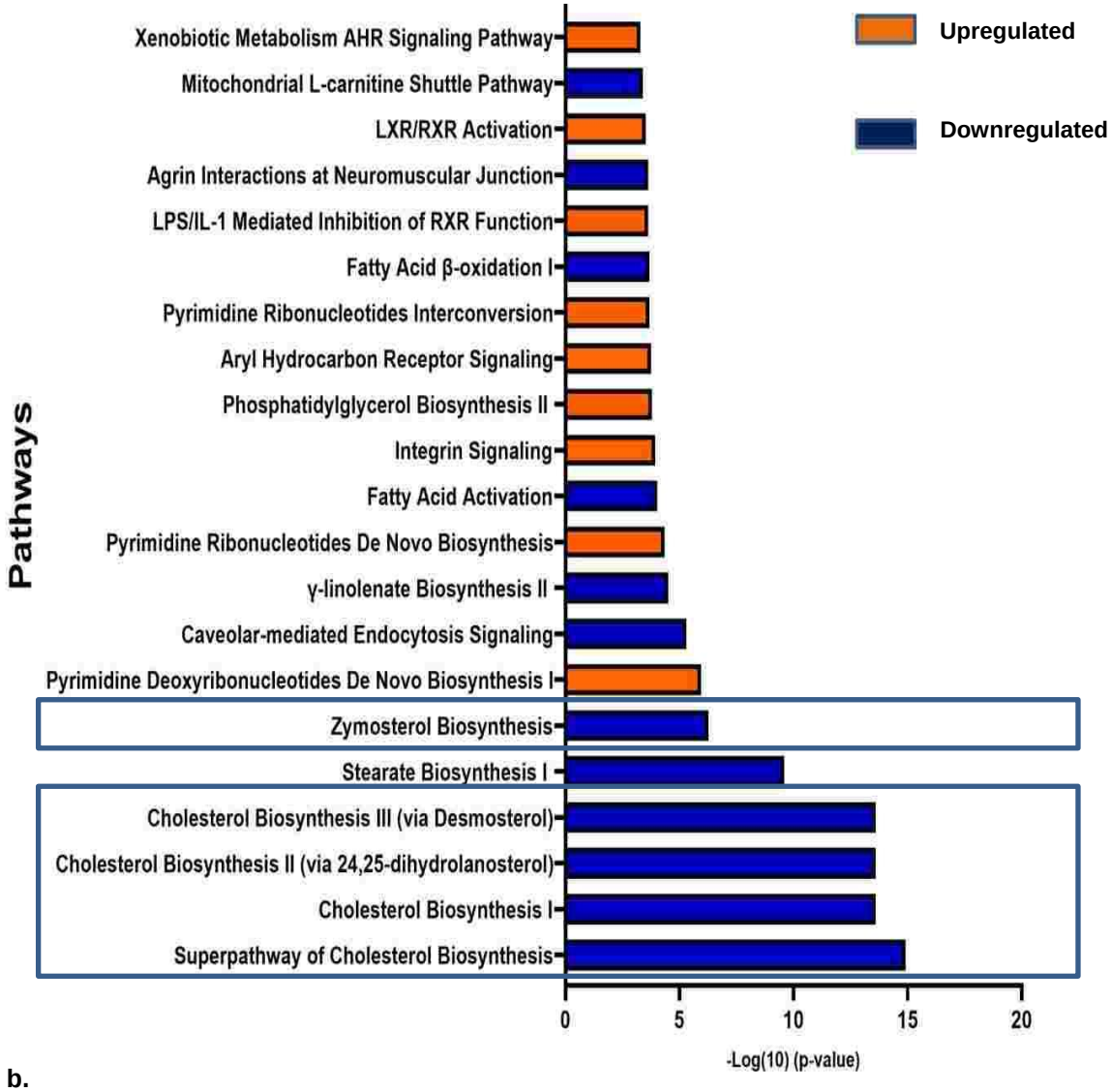
Upregulated
Downregulated
Pathways
Xenobiotic Metabolism AHR Signaling Pathway
Mitochondrial L-carnitine Shuttle Pathway
LXR/RXR Activation
Agrin Interactions at Neuromuscular Junction
LPS/IL-1 Mediated Inhibition of RXR Function
Fatty Acid β-oxidation I
Pyrimidine Ribonucleotides Interconversion
Aryl Hydrocarbon Receptor Signaling
Phosphatidylglycerol Biosynthesis II
Integrin Signaling
Fatty Acid Activation
Pyrimidine Ribonucleotides De Novo Biosynthesis
γ-linolenate Biosynthesis II
Caveolar-mediated Endocytosis Signaling
Pyrimidine Deoxyribonucleotides De Novo Biosynthesis I
Zymosterol Biosynthesis
Stearate Biosynthesis I
Cholesterol Biosynthesis III (via Desmosterol)
Cholesterol Biosynthesis II (via 24,25-dihydrolanosterol)
Cholesterol Biosynthesis I
Superpathway of Cholesterol Biosynthesis
0
5
10
15
20
-Log(10) (p-value)

b.

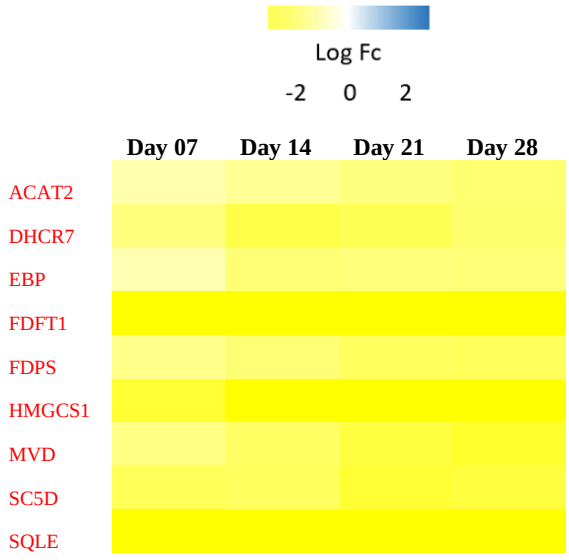
Log Fc
-2
0
2
Day 07
Day 14
Day 21
Day 28
ACAT2
DHCR7
EBP
FDFT1
FDPS
HMGCS1
MVD
SC5D
SQLE

Figure 2: Ingenuity pathway analysis from differentiating phBECs at ALI condition. (a) List of top 20 deregulated signalling pathways from differentiating phBECs proteome data. Data are presented as –log (10) (*p*-value) for the corresponding signalling pathways. The analysis was performed using Ingenuity Pathway Analysis (IPA Tool; Ingenuity®Systems, Redwood City, CA, USA; http://www.ingenuity.com). (b) Protein hits related to cholesterol biosynthesis pathway from differentiating phBECs via IPA analysis. All the proteins were significant ($p<0.05$) and the statistical analysis was obtained using fischer exact test p value.

From previous and my own studies (Mastalerz et al., 2022), we know that at ALI, the human bronchial epithelium is fully differentiated after 21 days, after which only few changes are observed in terms of cell type composition and gene expression. Therefore, we differentiated phBECs at ALI condition for 21 days under the influence of chronic CHOL exposure during the entire differentiation phase. phBECs treated with CHOL chronically were harvested at day 7, 14 and 21, and the cell type-specific composition was determined at both transcript level by qRT-PCR and at protein level by immunofluorescent staining. The epithelial barrier integrity was assessed using TEER analysis during the entire differentiation phase (Figure 3).

Figure 3

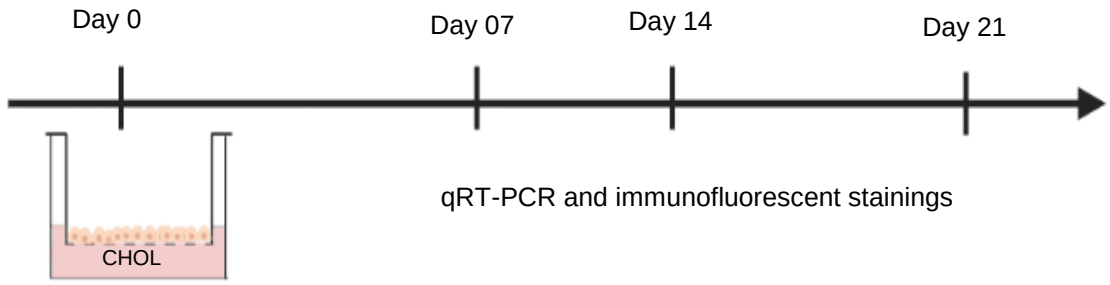

Figure 3: Schematic overview of the chronic CHOL treatment performed via the basolateral compartment of the insert during phBECs differentiation.

2.2.2 phBECs treated with vehicle control (absolute ethanol) in culture medium shows cytotoxicity at higher concentrations

Normal physiological and pathological cholesterol levels found in human blood can be as high as 100 mg/dl (2.6 mM) and 500 mg/dl (12.9 mM), respectively (National Cholesterol Education Program (NCEP), 2001). However, the solubility of CHOL is limited in aqueous solutions while it is moderately soluble in organic solvents. Therefore, we used absolute ethanol as an organic solvent to dissolve CHOL at the maximum soluble stock concentration of 16 mM (Domańska et al., 1994). As ethanol has been shown to be cytotoxic *in vitro* (Timm et al., 2013), we first set out to determine the maximal non-toxic ethanol concentration which would allow for the application of the highest cell culture-compatible concentration of cholesterol.

Figure 4

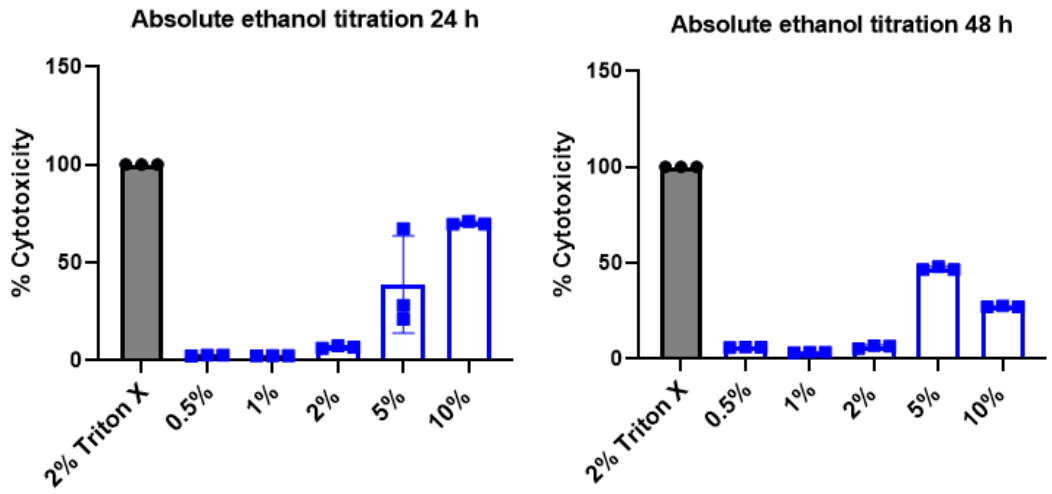

Figure 4: phBECs exposed to absolute ethanol titrations in PneumaCult-ALI medium shows cytotoxicity at higher concentration. Percentage cytotoxicity for phBECs exposed to absolute ethanol titration (0.5%, 1%, 2%, 5%, and 10%) in PneumaCult-Ali medium via the basolateral compartment of the insert at 24 h and 48 h. Datas are presented in terms of mean±SEM and are normalized to the positive control 2% triton X (*N*=1 (Biological replicate), *n*=3 (Technical replicates)).

Therefore, we first exposed phBECs at day 0 to increasing concentrations of ethanol in PneumaCult-ALI medium via the basolateral compartment, incubated until 48 h, and collected basolateral compartment medium at 24 h and 48 h.

Using the LDH assay (see Figure 4), we observed cytotoxicity levels below 10% for 0.5%, 1%, and 2% absolute ethanol in the culture medium at both 24 h and 48 h. However, the cytotoxicity levels were found to be higher than 20% for 5%, and 10% absolute ethanol percentages in the culture medium at both 24 h and 48 h. From these results, we decided to continue with a maximum concentration of 1% absolute ethanol in the PneumaCult-ALI medium as vehicle, which corresponded to a maximal final concentration of 80 µM CHOL for chronic exposure.

2.2.3 Chronic CHOL treatment is variably cytotoxic in phBECs, largely due to vehicle toxicity

Figure 5

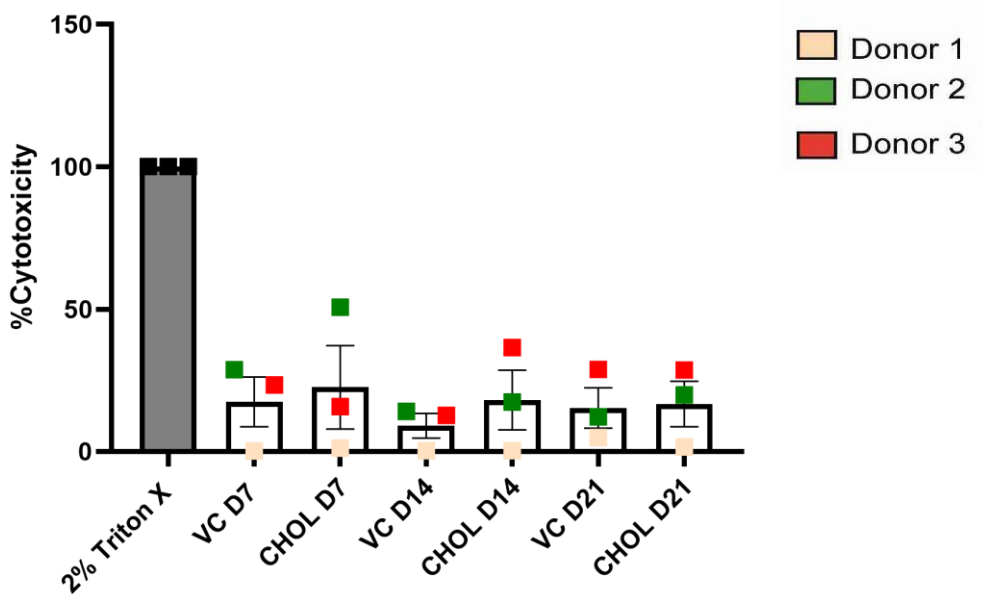

Figure 5: phBECs exposed chronically to CHOL and vehicle control-absolute ethanol shows cytotoxicity during differentiation phase. Percentage cytotoxicity for phBECs exposed to chronic CHOL and vehicle control-absolute ethanol treatment via the basolateral compartment of the insert during differentiation phase. Datas are presented in terms of mean±SEM and are normalized to the positive control 2% triton X. (*N*=3)

phBECs derived from three independent donors were treated with 80 µM CHOL chronically via the basolateral compartment of the insert during the differentiation. During chronic CHOL exposure, we collected the basolateral supernatant from both vehicle control and CHOL treatment at day 7, 14, and 21 and determined cytotoxicity using LDH assay. In a donor-dependent fashion, we observed no (less than 5 %), moderate (less than 25%) and considerable (up to

50%) cytotoxicity across all time points assessed during differentiation for both vehicle control and chronic CHOL condition (Figure 5). Therefore, the observed cytotoxicity mainly corresponded to the one caused by the vehicle control (1% absolute ethanol) and we did not monitor any additional cytotoxicity by CHOL.

2.2.4 The epithelial barrier integrity remain unchanged upon chronic CHOL exposure during phBECs differentiation

Figure 6

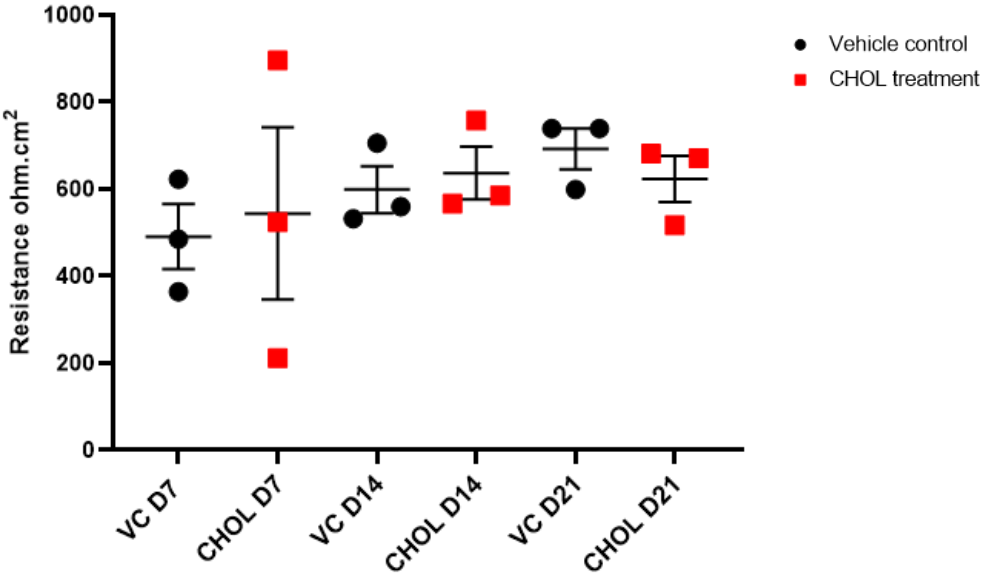

Figure 6: The epithelial barrier integrity assessment showed no differences upon chronic CHOL treatment in comparison to absolute ethanol-vehicle control during differentiation phase. TEER analysis was performed to determine the epithelial barrier integrity upon chronic CHOL and absolute ethanol-vehicle control at day 7, 14, and 21 during differentiation phase. Data are presented as mean±SEM (*N*=3). Statistical analysis was performed for chronic CHOL treatment in comparison to time-matched vehicle control at day 7, 14, and 21 using a two-tailed paired *t*-test in GraphPad Prism 9 software (San Francisco, CA, USA). No statistical significance was observed in epithelial barrier integrity upon chronic CHOL treatment in comparison to time-matched vehicle control.

Upon chronic CHOL exposure, the epithelial barrier integrity was assessed using TEER at day 7, 14 and 21 during differentiation phase. At day 7 and 14, the epithelial barrier integrity remained unchanged upon chronic CHOL treatment in comparison to vehicle control. However, we observed a high degree of variability across donors for chronic CHOL treatment at day 7 (Figure 6).

2.2.5 Transcript levels of cell type-specific markers remained largely unchanged in response to chronic CHOL treatment

Figure 7

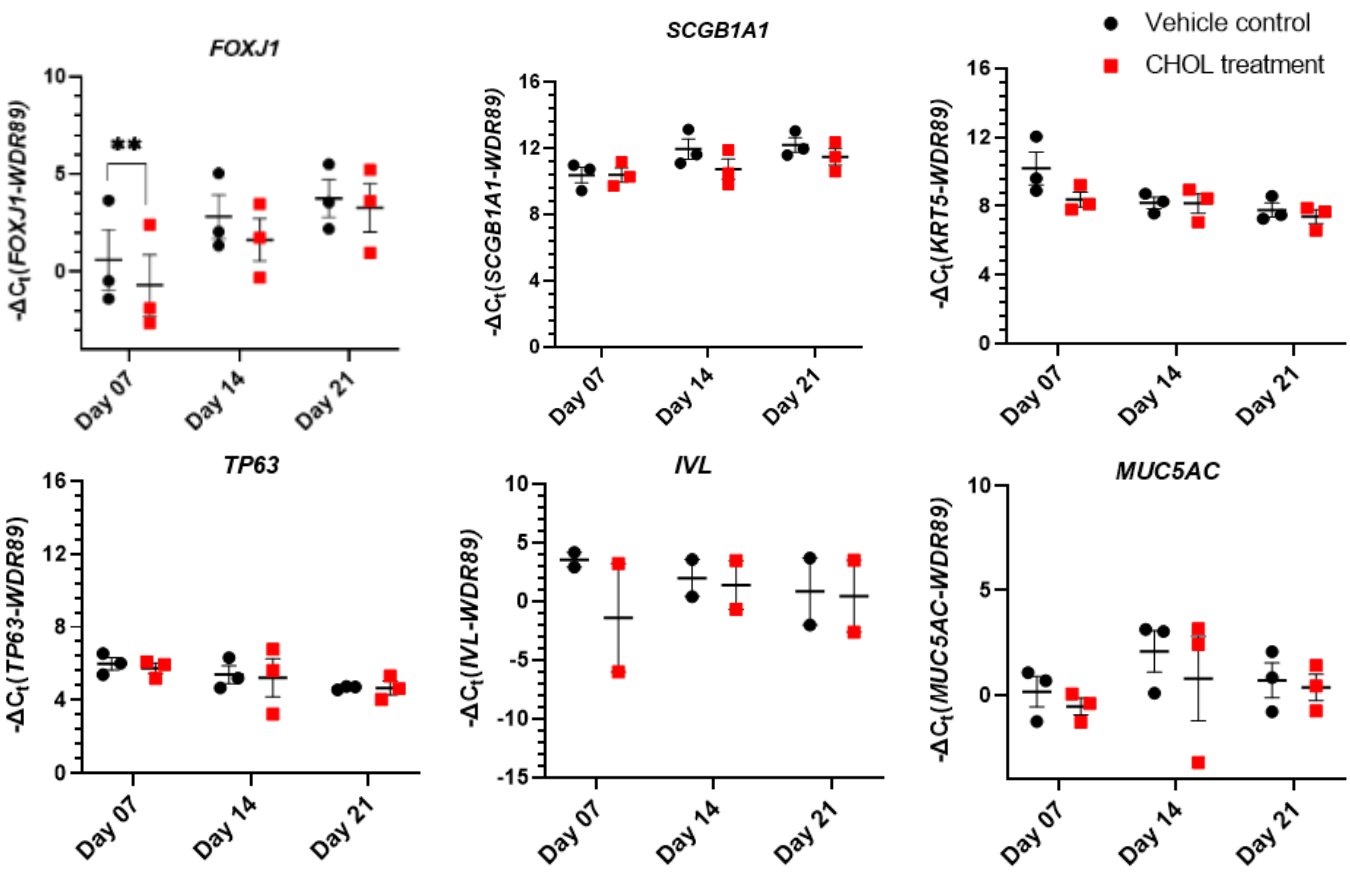

Figure 7: Chronic CHOL exposure does not cause expression changes of cell type-specific markers. qRT-PCR analysis was performed for cell type-specific markers such as *FOXJ1* (ciliated cell), *SCGB1A1* (club cell), *KRT5* and *TP63* (basal cell), *MUC5AC* (goblet cell), and squamous cell differentiation marker *IVL* (involucrin) was assessed upon chronic CHOL treatment in comparison to time-matched vehicle control during differentiation phase. Data are presented in terms of mean±SEM (*N*=3), except for *IVL* transcript analysis which were based from N=2. WD Repeat Domain 89 (*WDR89*) transcript was used as internal reference gene. Statistical analysis was performed for chronic CHOL treatment in comparison to time-matched vehicle control at day 7, 14, and 21 using a two-tailed paired *t*-test in GraphPad Prism 9 software (San Francisco, CA, USA). Significance shown for *p*-value < 0.05 (*), and *p*-value < 0.01 (**).

Upon chronic CHOL exposure, the inserts were collected at day 7, 14 and 21 and the cell type-specific markers such as *FOXJ1* (Ciliated cell), *MUC5AC* (Goblet cell), *SCGB1A1* (Club cell), and *KRT5* and *TP63* (Basal cell) were assessed at transcript level via qRT-PCR analysis. As shown in Figure 7, we did not observe any cell type-specific transcript changes for goblet, club, and basal cells upon chronic CHOL treatment in comparison to time-matched vehicle control during the differentiation phase. For *FOXJ1* transcript analysis, we observed a statistically significant downregulation upon chronic CHOL treatment in comparison to time-matched vehicle control at day7, which, however, levelled out during the later time points of the differentiation phase.

As a study had reported that CHOL treatment induces squamous cell metaplasia in rabbit tracheal epithelial cells. (Rearick & Jetten, 1986), we also included the squamous cell differentiation marker *IVL*, Involucrin upon chronic CHOL exposure, but did not see any differences in comparison to the time-matched vehicle control during the entire differentiation phase (Figure 7).

2.2.6 Chronic CHOL treatment induces an increase in the club cell population during differentiation phase

Figure 8

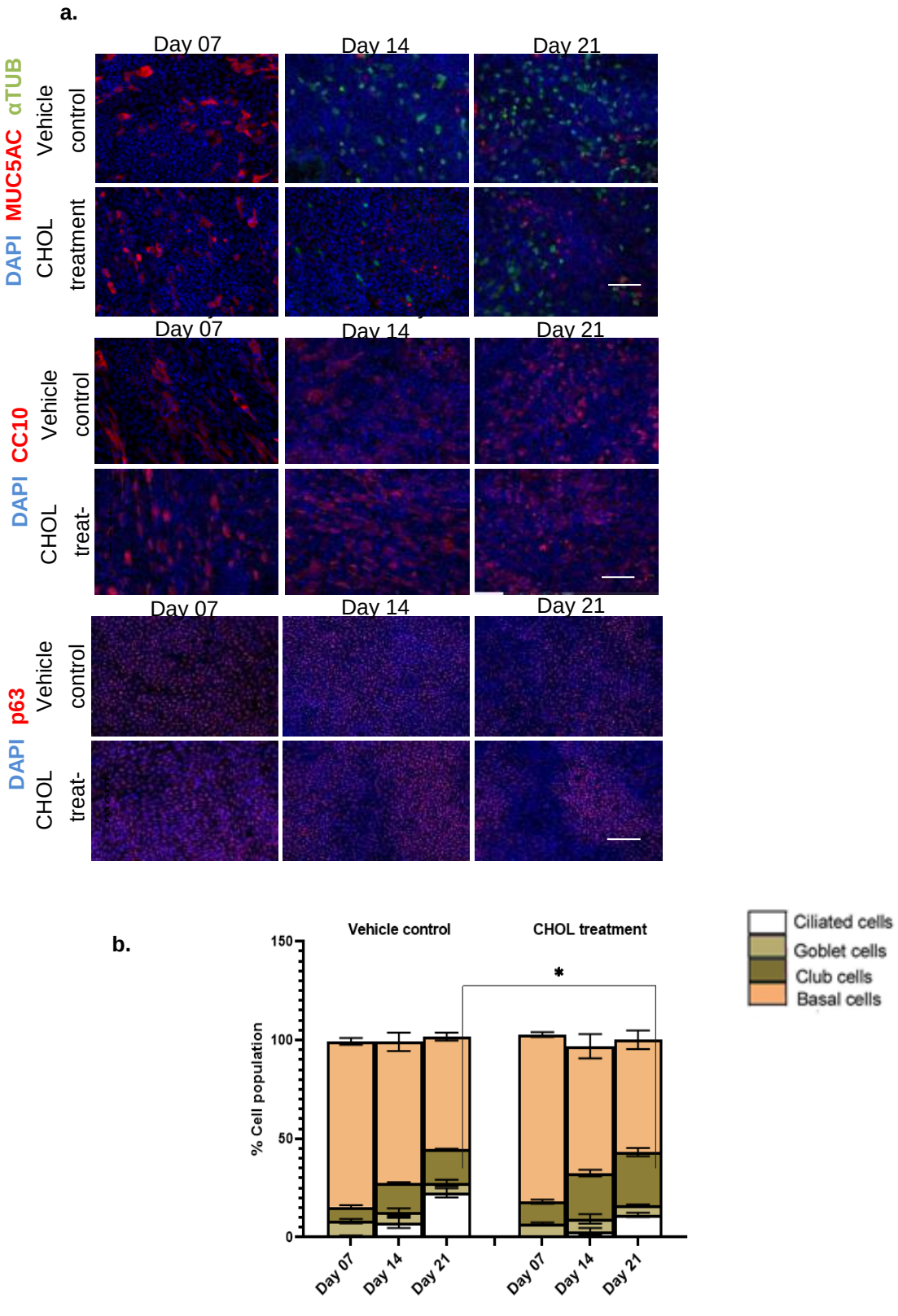

Figure 8: Increase in club cell population observed upon chronic CHOL treatment during the differentiation phase. (a) Representative immunofluorescent staining (scale bar: 50 µm) and (b) related quantification of cell type-specific markers such as αTUB (Ciliated cell), MUC5AC (Goblet cell), CC10 (Club cell), and p63 (Basal cell) upon chronic CHOL treatment in comparison to time-matched vehicle control during the differentiation phase. Data are presented in terms of mean±SEM (*N*=3). Statistical analysis was performed for chronic CHOL treatment in comparison to time-matched vehicle control at day 7, 14, and 21 using a two-tailed paired *t*-test in GraphPad Prism 9 software (San Francisco, CA, USA). Significance shown for *p*-value < 0.05 (*).

Upon chronic CHOL treatment, the cells were harvested at day 7, 14, and 21 during the differentiation phase and were stained for cell type-specific markers such as αTUB (ciliated cell), MUC5AC (goblet cell), CC10 (club cell), and p63 (basal cell), The immunofluorescent staining for cell type-specific markers and related quantification showed an increase in the club cell population at day 14 and 21 upon chronic CHOL treatment in comparison to time-matched vehicle control, and it reached statistically significant only for day 21. In addition, we also observed a decrease in the ciliated cell population at day 14 and 21 upon chronic CHOL treatment in comparison to the time-matched vehicle control but did not reach significance. Furthermore, upon chronic CHOL treatment, we did not observe any changes in the goblet and basal cell population in comparison to time-matched vehicle control during the entire differentiation phase (Figure 8 a, b).

2.2.7 Ingenuity pathway analysis from differentiating phBECs under ALI condition revealed the list of upstream regulators involved in cholesterol biosynthesis

The differentially expressed proteins from differentiating phBECs via proteome analysis were uploaded on the IPA software from Qiagen (Version: 1.8.02). The cut-off values used were: >-1 or <+1, and q value < 0.05. A total of 1371 significant hits out of 4860 proteins were enriched following these criteria, and then these enriched proteins were uploaded onto IPA software. Here, we show the list of upstream/ master regulators from IPA analysis regulating the list of molecules in the differentially expressed protein dataset (table 1).

Table 1

Upstream regulator	Molecule Type	Predicted Activation State	Activation z-score	Target Molecules in Dataset
TP53	transcription regulator		0.602	ALDH1A3, ARHGEF2, CRYAB, CYP51A1, DKK1, ECM1, FDFT1, FGFBP1, FTH1, GDF15, HMGCS1, IL1B, LOC102724788/PRODH, NDRG1, SLC2A1, SMC4, SQLE, STX6, TFRC
CDK19	kinase	Activated	2.236	ALDOC, EPHA2, FADS2, FDFT1, HMGCS1
MAP2K5	kinase	Inhibited	-2	ALDOC, CYP51A1, FDFT1, MSMO1
OGA	enzyme		1.633	ALDOC, CELSR1, FDFT1, FGFBP1, HMGCS1, MSMO1
NPPB	other		1.98	FDFT1, HMGCS1, LDLR, MSMO1
SCAP	other			FDFT1, LDLR, SCD, SQSTM1
CCL5	cytokine			IL1B, SERPINB2, SQLE

Table 1: List of upstream regulators regulating the target molecules in the dataset corresponding to cholesterol biosynthesis pathway. The target molecules marked in red corresponds to hits related to cholesterol biosynthesis pathway. Z score <-1 or >+1, q-value< 0.05.

3. Chapter 2: Establishment of a human *in vitro* model for studying airway epithelial injury and regeneration

Parts of the below mentioned work has been submitted to the journal Alternatives to Animal Experiments (ALTEX) and is currently under review: **Chakraborty A**, Mastalerz M, Marchi H, Meixner R, Hatz RA, Behr J, Lindner M, Hilgendorff A, Staab- Weijnitz CA. A human *in vitro* model for airway epithelial injury and regeneration.

3.1 Introduction

In recent years, the biomedical research on acute airways epithelial injury accompanied with successful regeneration has been largely dependent on the use of animal models, where the use of chemicals such as polidocanol (PDOC) or naphthalene (NA) leads to unspecific cell type or cell type-specific luminal depletion followed by subsequent regeneration of the damaged epithelium. (Borthwick et al., 2001; Engler et al., 2020; Gui et al., 2015; Leblond et al., 2009; Moiseenko et al., 2020; Raslan et al., 2022; Reynolds et al., 2000; Song et al., 2012) PDOC, as a strong detergent, applied intratracheally in *in vivo* leads to unspecific cell depletion leaving largely behind basal cells which then further undergo proliferation and regenerate the damaged epithelium within seven days post PDOC injury (Figure 9a) (Borthwick et al., 2001). On the other hand, NA, a non-toxic compound applied intraperitoneally *in vivo* where it undergoes club cell specific cytochrome P450 2F2 (C*yp2f2*) metabolism and leads to the formation of naphthalene-derived cytotoxic metabolites and resolves until 72 h post NA injury (Figure 9b) (Karagiannis et al., 2012; Moiseenko et al., 2020; Peake et al., 2000; Raslan et al., 2022; Song et al., 2012).

However, there are considerably major differences as we compare both human and mouse airways epithelium, for example, they differ in size, structure, cell type composition, and the progenitor cell type involved. The murine airways epithelium is pseudostratified only in the trachea region, while the bronchial airways consist of simple columnar epithelium which lacks basal cells and con-

tains progenitor club cells. In contrast, in the human lung, the pseudostratified epithelium reaches the small airways and basal cells serve as a progenitor cell type. Most importantly, the goblet cells which are present in the human airways but are rarely present in mouse airways (Hogan et al., 2014; Hong et al., 2001; Pan et al., 2019; Rock et al., 2009, 2010; Zepp & Morrisey, 2019).

Figure 9

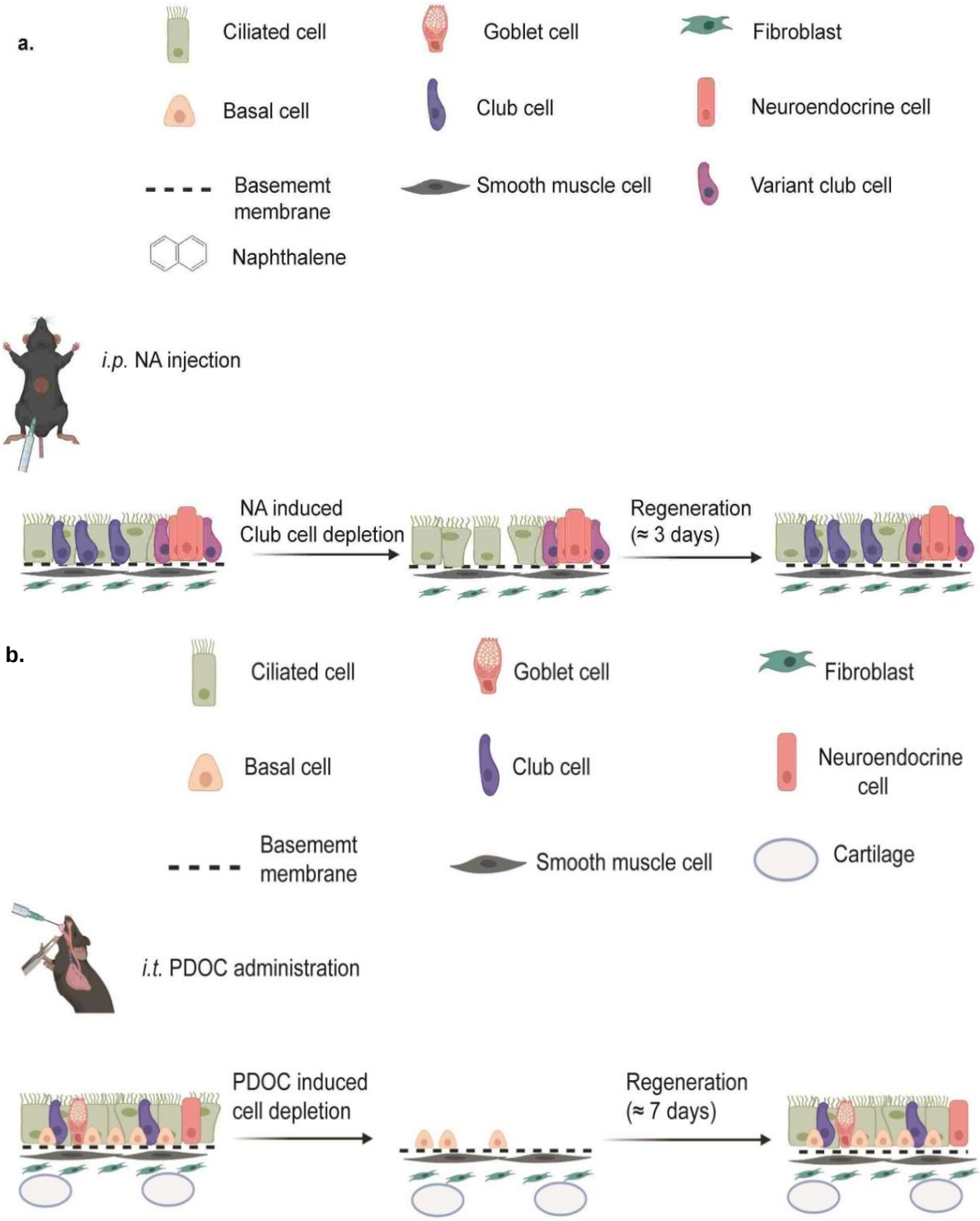

Figure 9: Schematic overview of the murine model of PDOC-induced tracheal naphthalene (NA)-induced airways injury. (a) Intratracheal (*i.t.*) application of PDOC leads to superficial epithelial cell loss up to basal membrane denudation in the mouse, followed by regeneration within 7 days. **(b)** Intraperitoneal (*i.p.*) application of NA leads to specific depletion of airways club cells, followed by regeneration within 3 days. Figure created using Biorender.

The frequent use of such acute airways' injury models is associated with pain and suffering for the animals. In 2010, the European Union adopted directive 2010/63/EU, which aims to fully replace the use of animal research with the use of alternative models. So far, to the best of our knowledge, the use of alternative models is lacking till date, therefore, we aim to develop a human *in vitro* model using primary human bronchial epithelial cells at air- liquid interface (ALI) condition to study airways epithelial injury and regeneration and thereby implement two of the 3R principle (Reduce and Replace) in this study. Here, we employed two different strategies to induce unspecific cell depletion using PDOC or specific cell-type depletion using NA and monitored subsequent regeneration. For the above-mentioned models, we determined the cell type-specific population at both transcript via qRT-PCR and protein using immunofluorescent staining. Furthermore, we also determined the epithelial barrier integrity using TEER analysis (Figure 10 a, b).

Figure 10

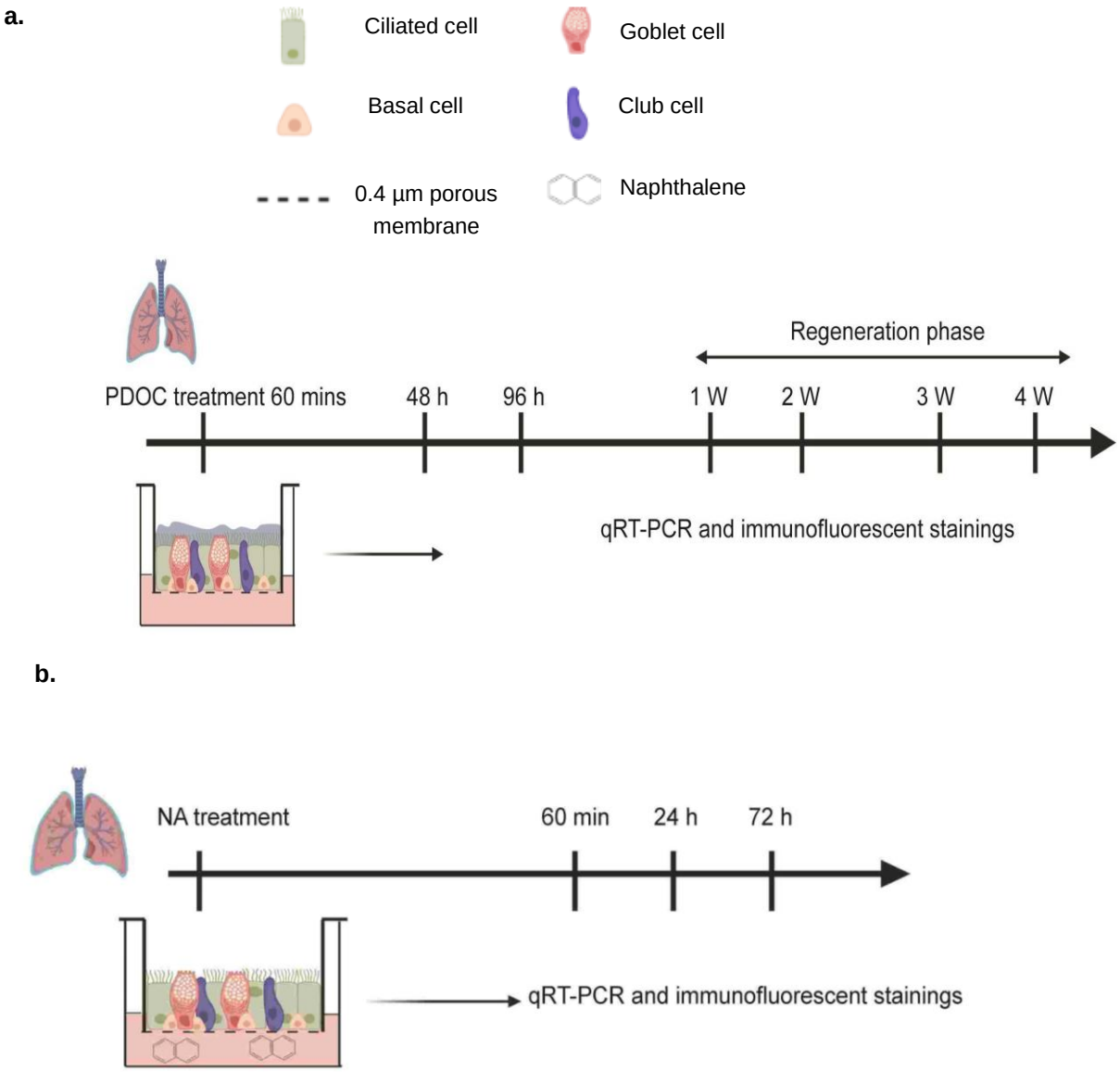

Figure 10: Schematic overview of the PDOC and NA application in *in vitro.* (a) PDOC was added apically on fully differentiated bronchial epithelial cells for 60 mins, followed by monitoring of cell depletion, barrier integrity, proliferation, and cell type composition at the indicated time points. (b) 0.35 mM NA was added in the basolateral compartment of fully differentiated bronchial epithelial cells for the above indicated incubation times, followed by monitoring of cytotoxicity and cell type composition. Figure created using Biorender.

3.2 Results

3.2.1 Fully differentiated phBECs treated with NA, at a concentration at the aqueous solubility limit, does not induce cell death

Figure 11

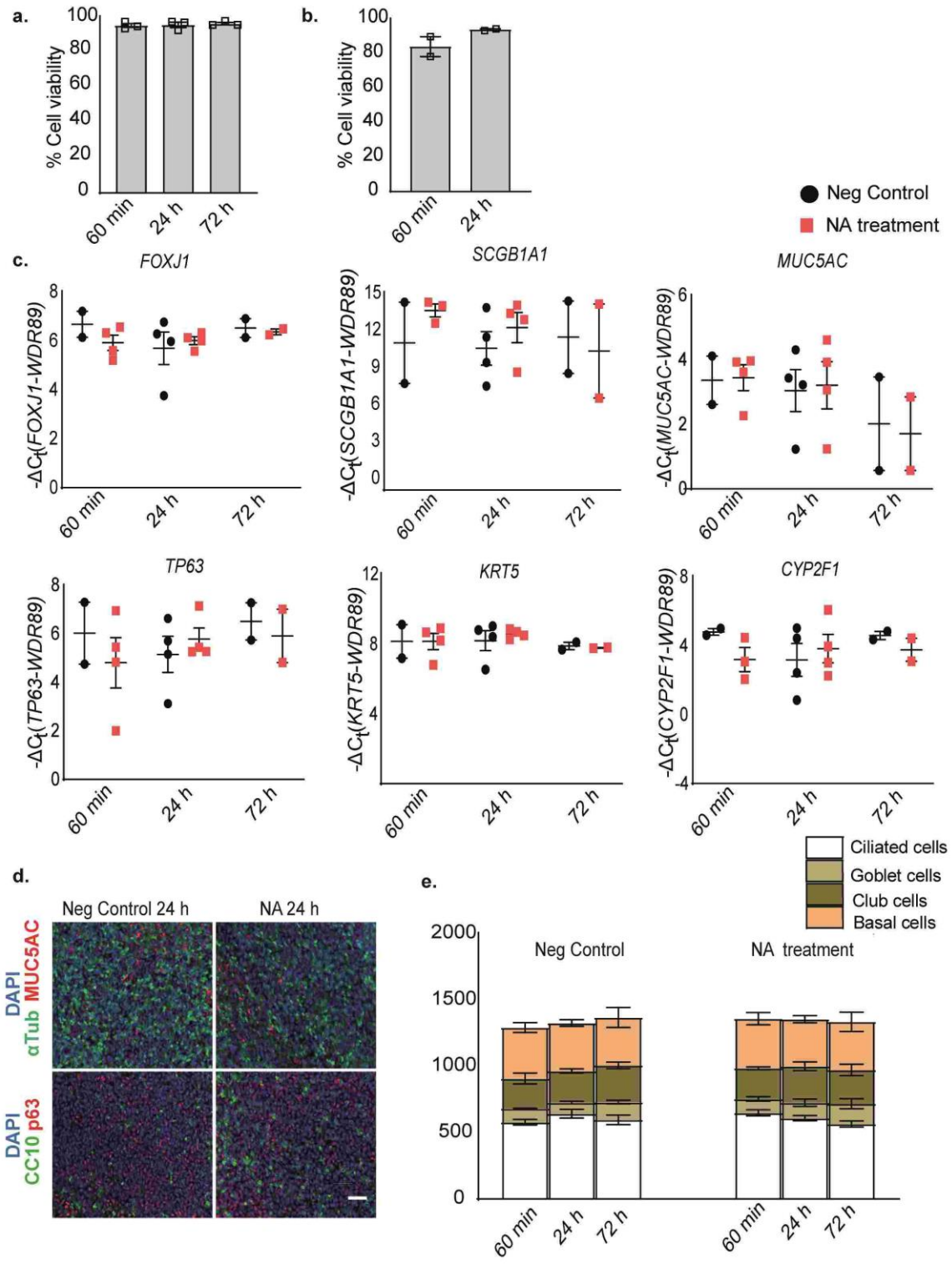

Figure 11: Naphthalene (NA) treatment fails to induce cell type-specific luminal depletion in *in vitro*. Cell viability assessment using (a) trypan blue exclusion test and (b) LDH assay post 0.35 mM NA treatment normalized to negative control for the above indicated time intervals. Data presented as mean ± SEM ($N \leq 2$). (c) Transcript analysis of cell type-specific markers such as the ciliated cell marker *FOXJ1,* the club cell marker *SCGB1A1,* the goblet cell marker *MUC5AC,* basal cell markers *KRT5* and *TP63*, and NA-metabolizing enzyme *CYP2F1*. WD Repeat Domain 89 (*WDR89*) transcript was used as internal reference gene. An outlier test was performed for *SCGB1A1* and *CYP2F1* transcript data for NA 60 min using GraphPad Prism 9 software (San Francisco, CA, USA). Statistical analysis was performed for NA 60 min and NA 24 h in comparison to negative control 24 h using a two-tailed paired *t*-test followed by Benjamini-Hochberg correction. (d) Representative immunofluorescent stainings (scale bar: 50 µm) and (e) quantification of the cell type-specific markers such as the ciliated cell marker α-tubulin (αTUB), the goblet cell marker mucin 5AC (MUC5AC), club cell-specific protein 10 (CC10) and the basal cell marker tumor protein 63 (p63) upon 0.35mM NA treatment for the above-mentioned time intervals. Statistical analysis for NA 60 min and 24 h in comparison to negative control 24 h for every cell type was performed using a two-tailed paired *t*-test followed by Benjamini-Hochberg correction. No statistical significance in cell type-specific response observed upon NA treatment in comparison to negative control.

NA, being a non-polar compound has limited solubility in aqueous solutions and a maximal water solubility of 43.9 mg/L at 34.5^0C corresponding to a concentration of 0.35 mM ("CRC Handbook of Chemistry and Physics, 2009−2010, 90th Ed.," 2009). Therefore, in efforts to use a maximal NA concentration compatible with aqueous cell culture conditions, we used a maximal soluble NA concentration of 0.35 mM NA in cell culture medium at 37^0C. Fully differentiated phBECs were treated with 0.35 mM NA at different time periods in the basolateral compartment of the insert, in analogy to the NA application *in vivo*, where NA reaches the lung via blood circulation. Upon NA treatment, we determined cell viability and cell type-specific markers at both transcript and protein levels for the indicated time points.

0.35 mM NA treatment did not affect cell viability assessed using LDH release and trypan blue exclusion test for the mentioned time points (Figure 11 a, b). qRT-PCR based quantification of cell-type specific transcript analysis (*FOXJ1* for ciliated cells, *SCGB1A1* encoding CC10 and *CYP2F1* for club cells, *MUC5AC* for goblet cells, *KRT5* and *TP63* encoding p63 for basal cells) demonstrated no changes upon NA treatment in comparison to negative control for the above indicated time intervals (Figure 11c). In agreement, the cell type-

specific marker quantification from immunofluorescent stainings (αTub for ciliated cells, MUC5AC for goblet cells, CC10 for club cells, and p63 for basal cells) remained stable upon NA treatment as compared to negative control (Figure 11 d,e). Therefore, in conclusion, treatment of differentiated phBECs with 0.35 mM NA treatment via the basolateral compartment of the insert failed to cause club cell-specific depletion *in vitro*.

For the next step, we were interested to identify other suicide enzyme substrate complexes (alternative to NA- human *CYP2F1* strategy) in depleting certain specific cell-type and understand their role in subsequent regeneration. For this, we took advantage of the above-mentioned proteomic analysis and extracted data for xenobiotic metabolizing enzymes (XMEs) of both phase I and phase II of detoxification. The listed phase I XME's contains alcohol dehydrogenases, aldehyde dehydrogenases, cytochrome P450 enzymes, NAD(P)H: quinone dehydrogenases, aldo-keto reductases, short and medium chain dehydrogenases/ reductases, and epoxide hydrolases. Phase II XME's contains glutathione S transferases, UDP-glucuronosyltransferases, and sulfotransferases. Overall, we observed an increase in expression of the above-mentioned XMEs of phase I and II during phBECs differentiation suggesting this upregulation observed is mainly due to the rise in differentiated cell types (Figure 12 and b). So, we mapped this class I and II XMEs with cell type-specific marker expression using human single cell RNA seq data (analysis performed by Meshal Ansari from unpublished data, in collaboration with Herbert Schiller). The single-cell RNA seq analysis showed the cell type-specific marker expressing both phase I and II XME's (Figure 12c). The XMEs expression were observed in differentiate cell types such as ciliated, goblet, and club cells, but the expression for XME's were low in basal cells. Therefore, the data indicates that club cells are not the main XME's expressers in the human bronchial epithelium. Hence, the above presented data did not reveal other suicide enzyme substrate complexes to induce cell-type specific depletion in the human bronchial epithelium *in vitro*.

Figure 12

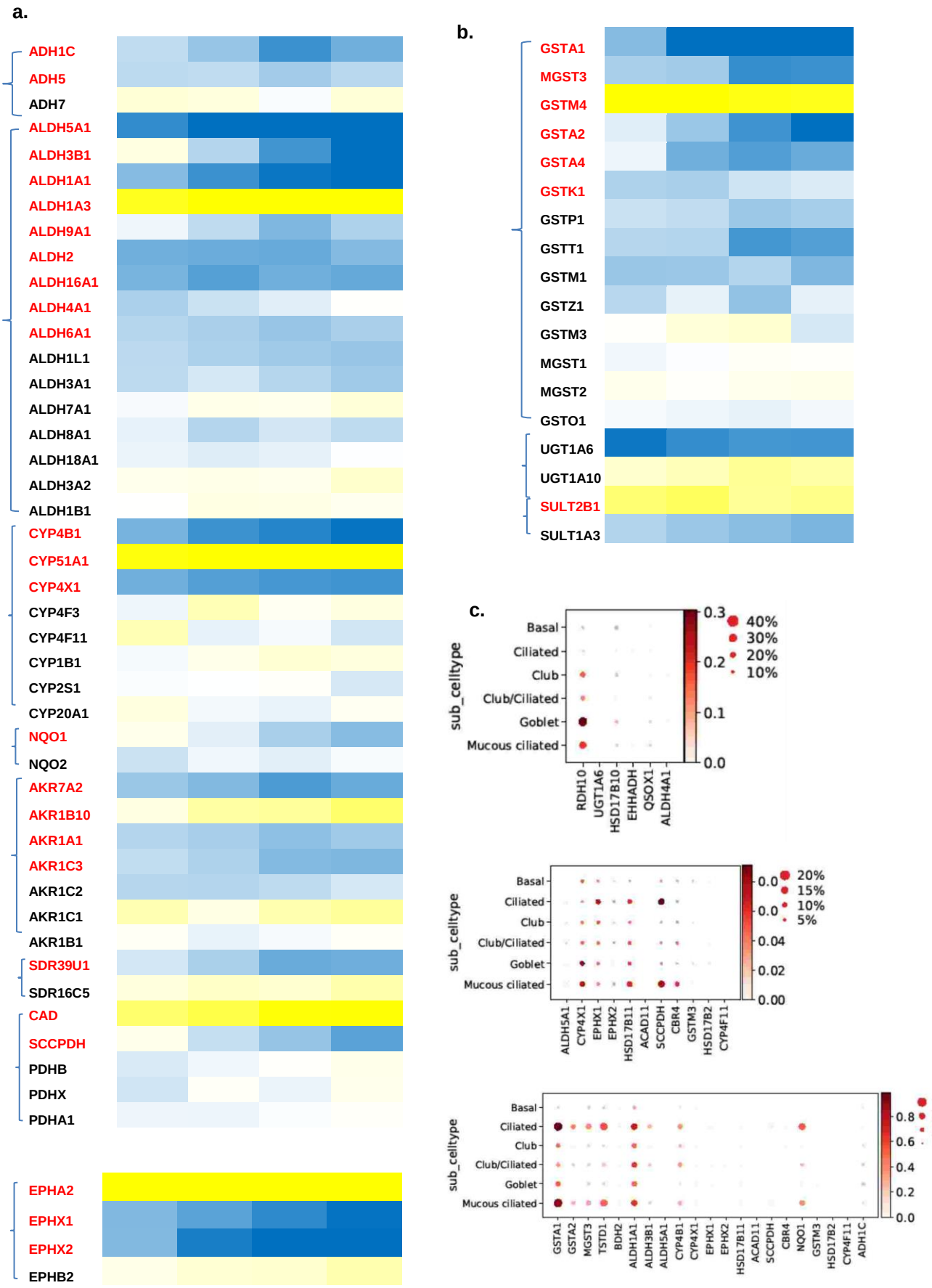
a.
ADH1C
ADH5
ADH7
ALDH5A1
ALDH3B1
ALDH1A1
ALDH1A3
ALDH9A1
ALDH2
ALDH16A1
ALDH4A1
ALDH6A1
ALDH1L1
ALDH3A1
ALDH7A1
ALDH8A1
ALDH18A1
ALDH3A2
ALDH1B1
CYP4B1
CYP51A1
CYP4X1
CYP4F3
CYP4F11
CYP1B1
CYP2S1
CYP20A1
NQO1
NQO2
AKR7A2
AKR1B10
AKR1A1
AKR1C3
AKR1C2
AKR1C1
AKR1B1
SDR39U1
SDR16C5
CAD
SCCPDH
PDHB
PDHX
PDHA1
EPHA2
EPHX1
EPHX2
EPHB2
b.
GSTA1
MGST3
GSTM4
GSTA2
GSTA4
GSTK1
GSTP1
GSTT1
GSTM1
GSTZ1
GSTM3
MGST1
MGST2
GSTO1
UGT1A6
UGT1A10
SULT2B1
SULT1A3
c.
sub_celltype
Basal
Ciliated
Club
Club/Ciliated
Goblet
Mucous ciliated
RDH10
UGT1A6
HSD17B10
EHHADH
QSOX1
ALDH4A1
40%
30%
20%
10%
0.3
0.2
0.1
0.0
ALDH5A1
CYP4X1
EPHX1
EPHX2
HSD17B11
ACAD11
SCCPDH
CBR4
GSTM3
HSD17B2
CYP4F11
20%
15%
10%
5%
0.0
0.0
0.04
0.02
0.00
GSTA1
GSTA2
MGST3
TSTD1
BDH2
ALDH1A1
ALDH3B1
ALDH5A1
CYP4B1
CYP4X1
EPHX1
EPHX2
HSD17B11
ACAD11
SCCPDH
CBR4
NQO1
GSTM3
HSD17B2
CYP4F11
ADH1C
0.8
0.6
0.4
0.2
0.0

Figure 12: Proteomic analysis and single cell RNA sequence analysis from differentiating phBECs. (a) List of phase I XME's such as alcohol dehydrogenases, aldehyde dehydrogenases, cytochrome P450 enzymes, NAD(P)H Quinone dehydrogenases, alko Keto reductases, short and medium chain dehydrogenases/ reductases, epoxide hydrolases and (b) list of phase II XME's such as glutathione S transferases, UDP-glucuronosyltransferases and sulfotransferases proteomic profile from differentiating phBECs. The proteins listed in red are significant with q-value < 0.05 (c) Single cell RNA sequence analysis: Mapping the listed phase I and II XME's with the cell type-specific marker expression from differentiating phBECs.

3.2.2 Fully differentiated phBECS treated with PDOC induces cell death in a dose-dependent manner

Figure 13

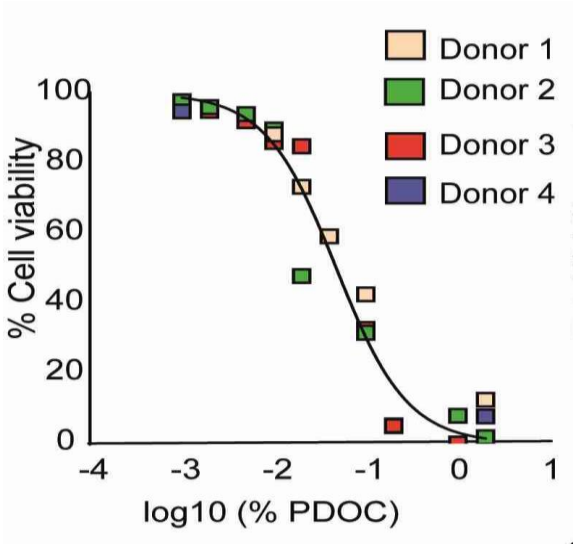

Figure 13: Epithelial injury with PDOC induces cell loss in a dose dependent manner. Trypan blue exclusion test performed to assess cell viability upon PDOC treatment. Non-linear data regression analysis was performed using the log (inhibitor) vs normalised response model (R^2: 0.9598). Data is based on *N*=4 and presented as mean ± standard deviation. Half maximal effective concentration (EC50) obtained from the analysis was 0.047 ± SD %PDOC (log 10 scale value: -1.325 ± SD)

At first, we tested a series of PDOC concentrations ranging between 0.002%-2% PDOC on the apical compartment of the insert for 60 min and assessed cell viability using the trypan blue exclusion test right after the PDOC treatment. The cell viability assessment revealed a dose-dependent decrease in the cell viability upon PDOC treatment with an effective half maximal concentration of 0.047% ± SD PDOC (-1.325 ± SD on the log 10 scale). So, we used two different PDOC concentrations for causing an injury 1) 0.04% PDOC, a concentration close to EC50, and 2) 0.1% PDOC, a concentration corresponding to cell viability around 30%, and analysed subsequent regeneration (Figure 13).

3.2.3 Fully differentiated phBECs treated with 0.04%, but not 0.1% PDOC, induces cell proliferation after marked cell loss

Figure 14

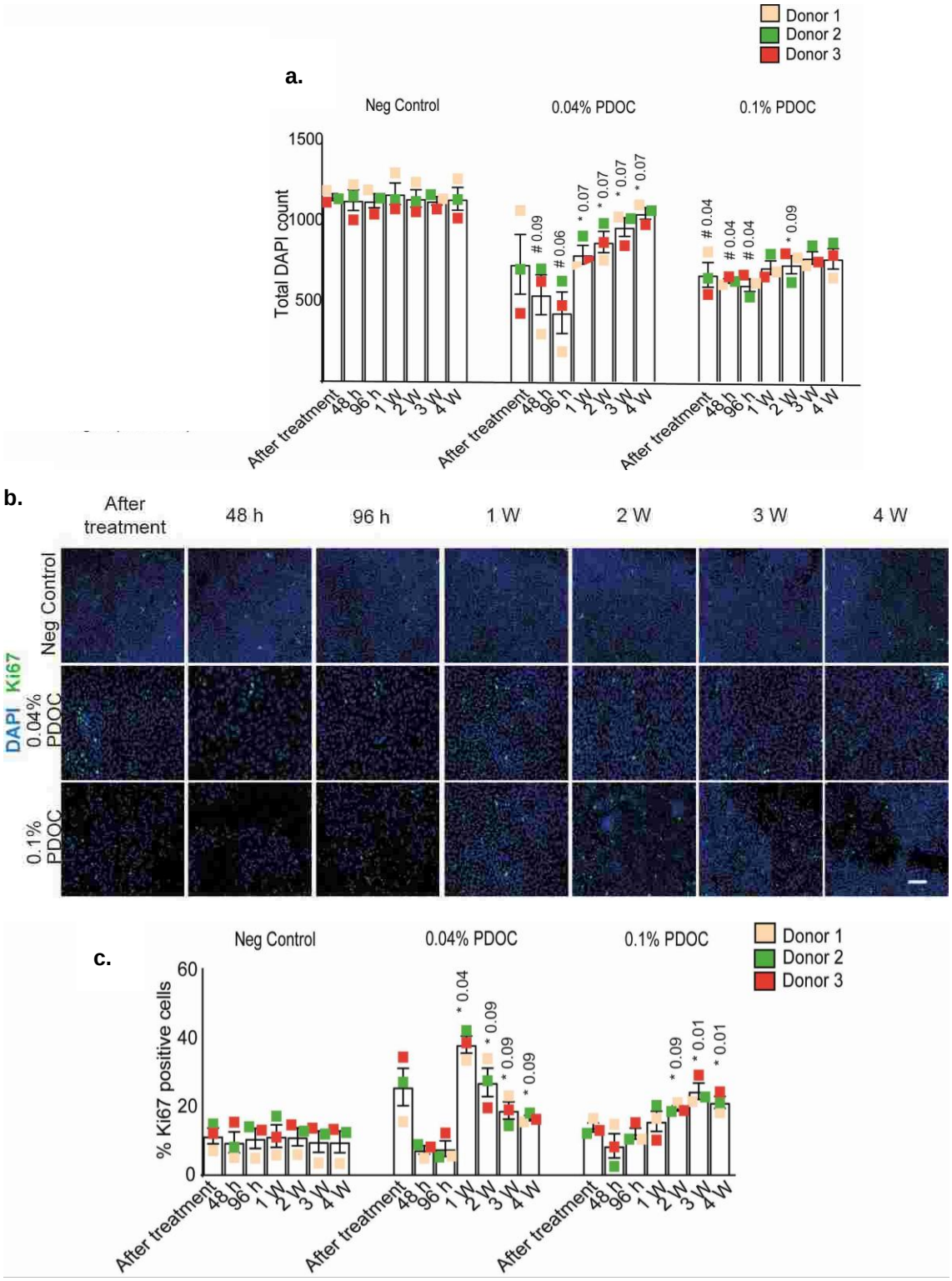

Figure 14: Epithelial injury with 0.04% PDOC, but not 0.1% PDOC, allows for cell proliferation after initial cell loss. (a) Total DAPI count from immunofluorescent staining after 0.04% and 0.1% PDOC in comparison to the time-matched negative control for the above indicated time points. Data presented as mean ± SEM (*N*=3). (b) Representative immunofluorescent staining (scale bar: 50 µm) and (c) the quantification of proliferation marker protein Ki67 post 0.04% and 0.1% PDOC in comparison to the time-matched negative control for the above indicated time intervals. Data presented as mean ± SEM (*N*=3). Statistical analysis was performed using two-tailed paired *t*-test followed by multiple testing using Benjamini-Hochberg correction, focusing on two comparisons: (1) Testing for statistically significant cell loss (#: 0.04% and 0.1% PDOC injury *vs.* time-matched negative control until 96 h); (2) Testing for statistically significant regeneration after maximal cell loss at 96 h (*: Regeneration phase *vs*. 96 h within each PDOC treatment condition). Absolute adjusted *p*-values are given above the data points.

Upon 0.04% and 0.1% PDOC injury, the cell loss and subsequent proliferation were determined by assessing total cell count based on nuclear stain DAPI and by measuring the proliferation marker protein Ki67 levels for all the mentioned time points. As expected, the total cell count remained stable throughout all the mentioned time points. However, with 0.04% PDOC injury, a significant loss of cell count was observed to about 40% of the negative control cell count. The initial cell count observed upon 0.04% PDOC was compensated by an increase in cell count in a time-dependent manner during the regeneration phase. In contrast, an epithelial injury with 0.1% PDOC also led to a significant cell count of about 50% of the negative control cell count, however, only led to a little increase in total cell count during the regeneration phase (Figure 14a).

In addition, we also analyzed the proliferation marker protein Ki67 for similar time points as mentioned above. As expected, we observed a constant proportion of about 10% at all the mentioned time points for the negative control. However, upon 0.04% PDOC injury, a sharp increase was observed right after treatment followed by its decline to baseline levels determined at both 48 and 96 h. In addition, we observed a significant rise in Ki67+ proliferative cells one week relative to 96 h maximal cell loss followed by a decrease to about 20% in a time-dependent manner over the next three weeks during the regeneration phase. For 0.1% PDOC injury, we observed a sharp decrease in the Ki67+ cells to about 10% determined at 48 h, however, we only observed a significant but modest rise in the Ki67+ cells during the last three weeks of the regeneration phase in comparison to 96 h time point (Figure 14 b, c).

3.2.4 Fully differentiated phBECs treated with 0.04%, but not 0.1% PDOC, undergoes regeneration into a full-blown bronchial epithelium and restores epithelial barrier integrity

Here, we assessed cell type-specific transcripts, quantified specific cell types at the protein level via immunofluorescent stainings, and determined epithelial barrier integrity using TEER measurements to characterize cell loss, regeneration, and understand the functional properties of the resulting epithelium in more detail. For transcript analysis, post 0.04% PDOC injury at 96 h, we observed a trend for down regulation of cell type-specific markers such as *FOXJ1* (ciliated cells), *MUC5AC* (goblet cells), and *SCGB1A1* (club cells), which reached statistical significance for only *FOXJ1* relative to the time-matched negative control (Figure 15).

During the regeneration phase, we observed a restoration in the transcript levels of *SCGB1A1, MUC5AC,* and *FOXJ1* in a time-dependent manner relative to the 96 h time point. However, we did not observe any changes in the transcript levels such as *KRT5* and *TP63* (basal cells) for all the indicated time points (Figure 15). For 0.1% PDOC injury, the transcript analysis could not be determined due to the low RNA yield for all the indicated time points (Figure 16).

Figure 15

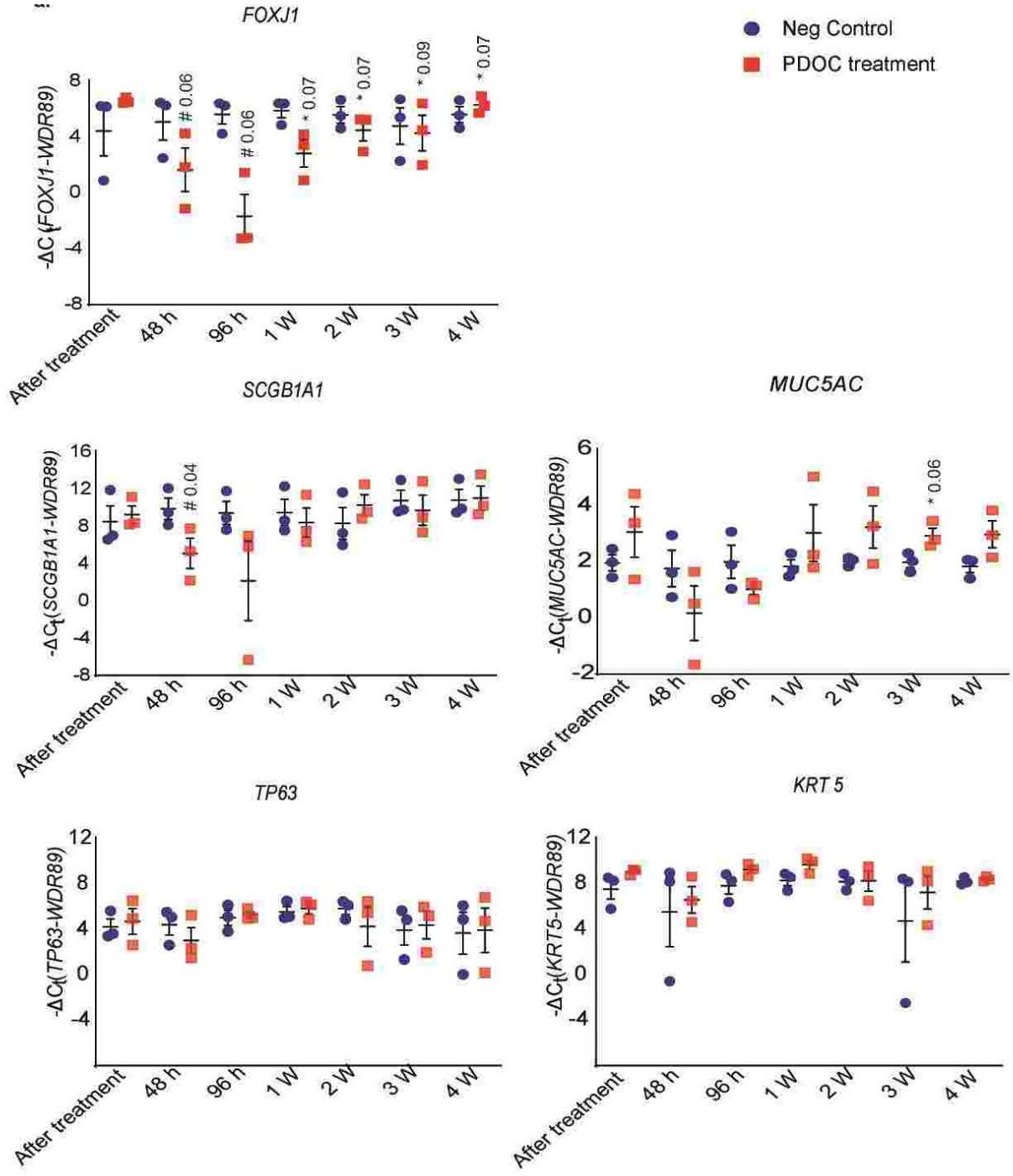

Figure 15: Epithelial injury with 0.04% PDOC, but not 0.1% PDOC, induces regeneration into a full-blown bronchial epithelium after the initial loss of differentiated cell types analysed at transcript level. Transcript analysis of cell type-specific markers such as the ciliated cell marker *FOXJ1,* the club cell marker *SCGB1A,* the goblet cell marker *MUC5AC,* and basal cell markers *KRT5* and *TP63* after 0.04 % PDOC in comparison to time-matched negative control for the above indicated time intervals. WD Repeat Domain 89 (*WDR89*) transcript was used as internal reference gene. Data presented as mean ± SEM (*N*=3). Statistical analysis was performed using two-tailed paired *t*-test followed by multiple testing using Benjamini-Hochberg

correction, focusing on two comparisons: (1) Testing for statistically significant cell loss (#: 0.04% and 0.1% PDOC injury *vs.* time-matched negative control until 96 h); (2) Testing for statistically significant regeneration after maximal cell loss at 96 h (*: Regeneration phase *vs*. 96 h within each PDOC treatment condition). Absolute adjusted *p*-values are given above the data points.

Figure 16

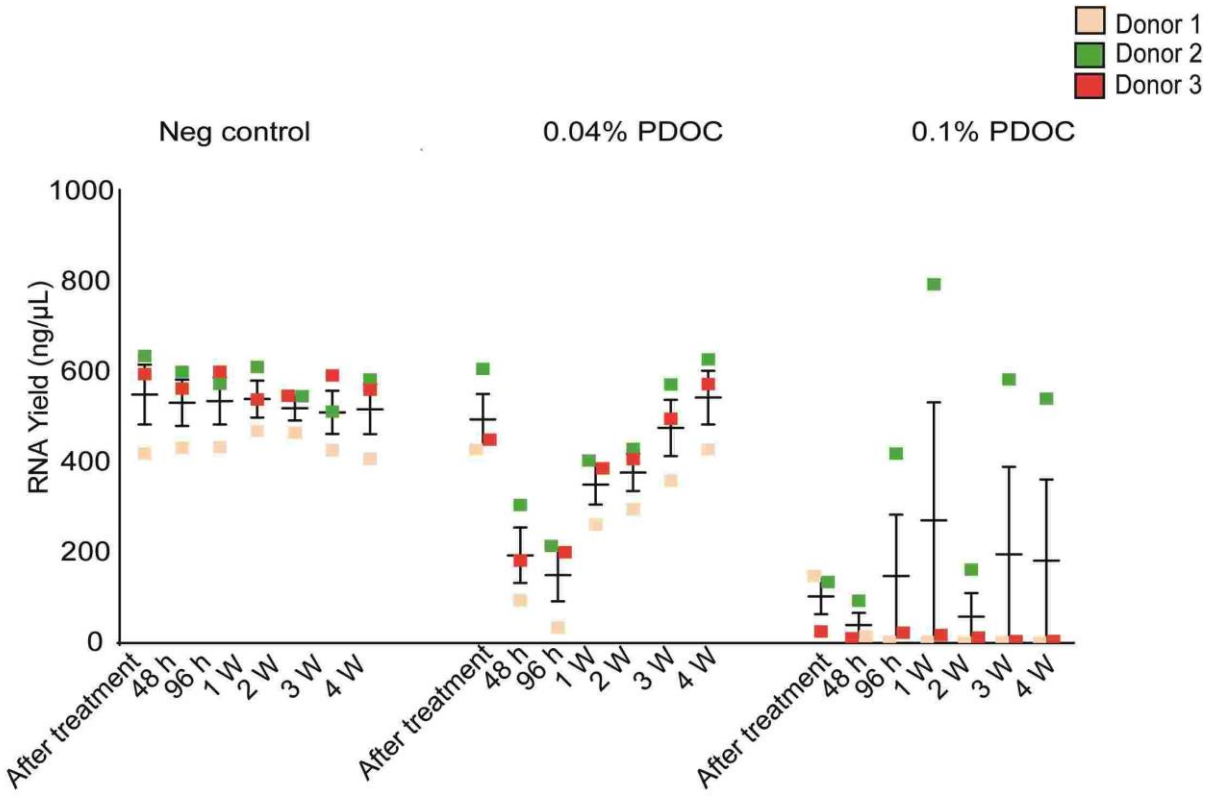

Figure 16: **Low RNA yield post 0.1% PDOC epithelial injury did not allow for transcript analysis.** Total RNA yield upon 0.04% and 0.1% PDOC in comparison to time-matched negative control for the above-mentioned time intervals. Data presented as mean ± SEM (*N*=3).

Furthermore, we also analyzed the cell type-specific markers such as the ciliated cell marker α TUB (alpha tubulin), the goblet cell marker MUC5AC (mucin5AC), the club cell marker CC10 (club cell-specific protein 10), and the basal cell marker p63 (tumor protein 63) upon 0.04% and 0.1% PDOC injury in comparison to time-matched negative control for the indicated time intervals at protein level via immunofluorescent staining's. For negative control, the cell type-specific population remained largely stable across all the indicated time points. However, with 0.04% PDOC injury, we observed a loss of differentiated cell types such as ciliated, goblet and club cells and the resulting epithelia only consisted of only p63+ basal cells at 48 and 96 h. During the regeneration phase,

we observed a rise in differentiated cell types such as club, goblet and ciliated cells, of which club and ciliated cells were only significant in a time dependent manner during the regeneration phase as compared to the 96 h time point (Figure 17 a, b).

For 0.1% PDOC treatment, we also observed a similar pattern of loss in differentiated cell types after injury and only contained p63+ basal cells at 48 and 96 h. Interestingly, during the regeneration phase, we did not observe regeneration as the cell population mainly consisted of basal cells and very few other cell types indicating failed regeneration post 0.1% PDOC injury (Figure 17 a, b).

Figure 17

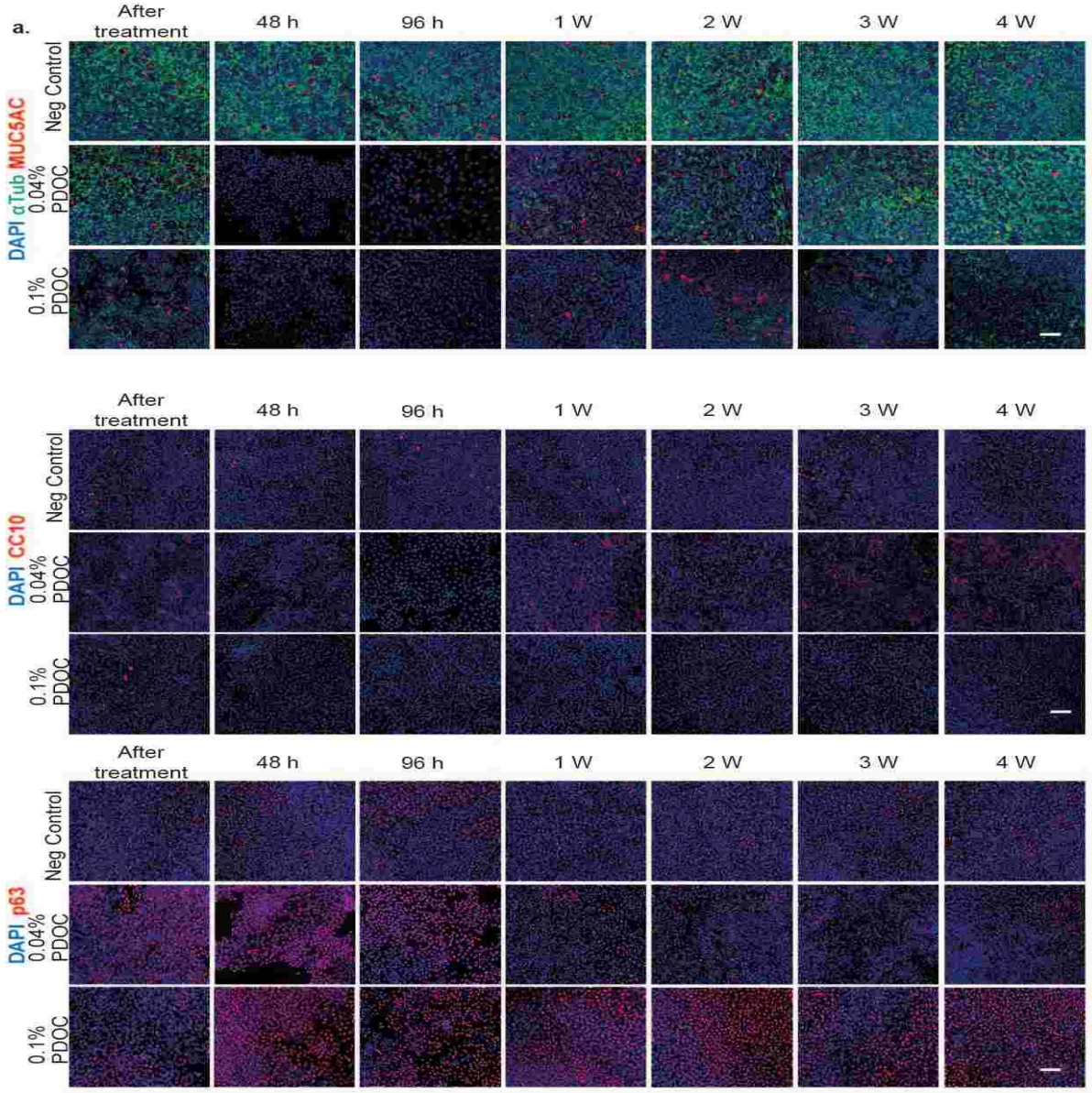
a.
After treatment
48 h
96 h
1 W
2 W
3 W
4 W
Neg Control
0.04% PDOC
0.1% PDOC
DAPI αTub MUC5AC
DAPI CC10
DAPI p63

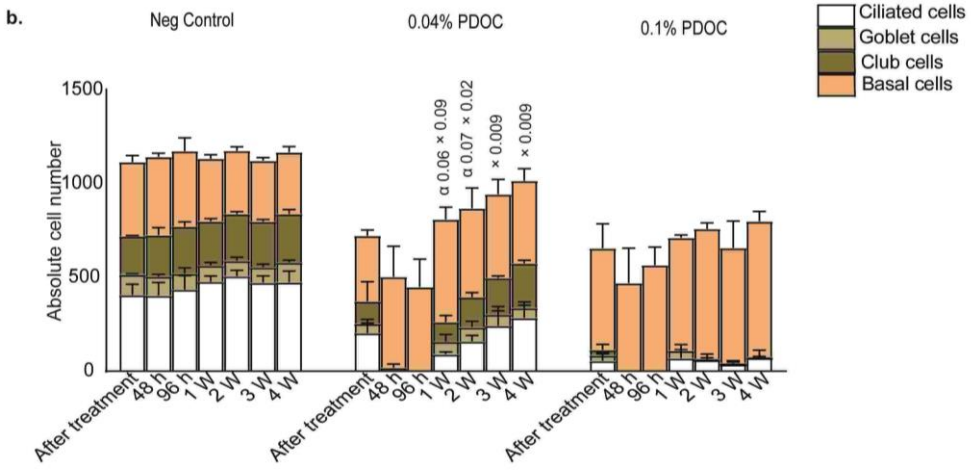
b.
Neg Control
0.04% PDOC
0.1% PDOC
Ciliated cells
Goblet cells
Club cells
Basal cells
Absolute cell number
1500
1000
500
0
α 0.06 × 0.09
α 0.07 × 0.02
× 0.009
× 0.009
After treatment
48 h
96 h
1 W
2 W
3 W
4 W

Figure 17: Epithelial injury with 0.04% PDOC, but not 0.1% PDOC, induces regeneration into a full-blown bronchial epithelium after the initial loss of differentiated cell types analysed at protein level. (a) Representative immunofluorescent staining (scale bar: 50 µm) and (b) the quantification of the cell type-specific markers such as the ciliated cell marker α TUB (alpha tubulin), the goblet cell marker MUC5AC (mucin5AC), the club cell marker CC10 (club cell-specific protein 10) and the basal cell marker p63 (tumor protein 63) after 0.04% and 0.1% PDOC in comparison to time-matched negative control for the above indicated time intervals. Data presented as mean ± SEM (*N*=3). Statistical analysis was performed using two-tailed paired *t*-test followed by multiple testing using Benjamini-Hochberg correction, focusing on two comparisons: (1) Testing for statistically significant cell loss (#: 0.04% and 0.1% PDOC injury *vs.* time-matched negative control until 96 h; see table 2); (2) Testing for statistically significant regeneration after maximal cell loss at 96 h (*: Regeneration phase *vs*. 96 h within each PDOC treatment condition). Absolute adjusted *p*-values are given above the data points. Symbols used for showing statistical significance for the individual cell-types are as follows: **α**, Ciliated cell; **β**, Goblet cell; **×**, Club cell; **$**, Basal cell.

Table 2: Statistical analysis for cell type-specific quantification upon PDOC injury and subsequent regeneration (Figure 17b)

Time point	Cell type	0.04% PDOC injury vs time-matched negative control	0.1% PDOC injury vs time-matched negative control
After treatment	Ciliated cell (α)	3×10^{-3}	4×10^{-2}
	Goblet cell (β)	ns	5×10^{-2}
	Club cell (×)	ns	4×10^{-2}
	Basal cell ($)	ns	ns
48 h	Ciliated cell (α)	3×10^{-2}	3×10^{-2}
	Goblet cell (β)	3×10^{-2}	3×10^{-2}
	Club cell (×)	7×10^{-2}	4×10^{-2}
	Basal cell ($)	ns	ns
96 h	Ciliated cell (α)	3×10^{-2}	3×10^{-2}
	Goblet cell (β)	ns	ns
	Club cell (×)	2×10^{-2}	2×10^{-2}
	Basal cell ($)	ns	ns
Time point	Cell type	0.04% PDOC regeneration phase vs 0.04% 96 h	0.1% PDOC regeneration phase vs 0.1% 96 h
1 W	Ciliated cell (α)	6×10^{-2}	ns
	Goblet cell (β)	ns	ns
	Club cell (×)	9×10^{-2}	ns
	Basal cell ($)	ns	ns
2 W	Ciliated cell (α)	7×10^{-2}	ns
	Goblet cell (β)	ns	ns
	Club cell (×)	2×10^{-2}	ns
	Basal cell ($)	ns	ns
3 W	Ciliated cell (α)	ns	ns
	Goblet cell (β)	ns	ns
	Club cell (×)	9×10^{-3}	ns
	Basal cell ($)	ns	ns
4 W	Ciliated cell (α)	ns	ns
	Goblet cell (β)	ns	ns
	Club cell (×)	9×10^{-3}	ns
	Basal cell ($)	ns	ns

ns: not significant

Figure 18

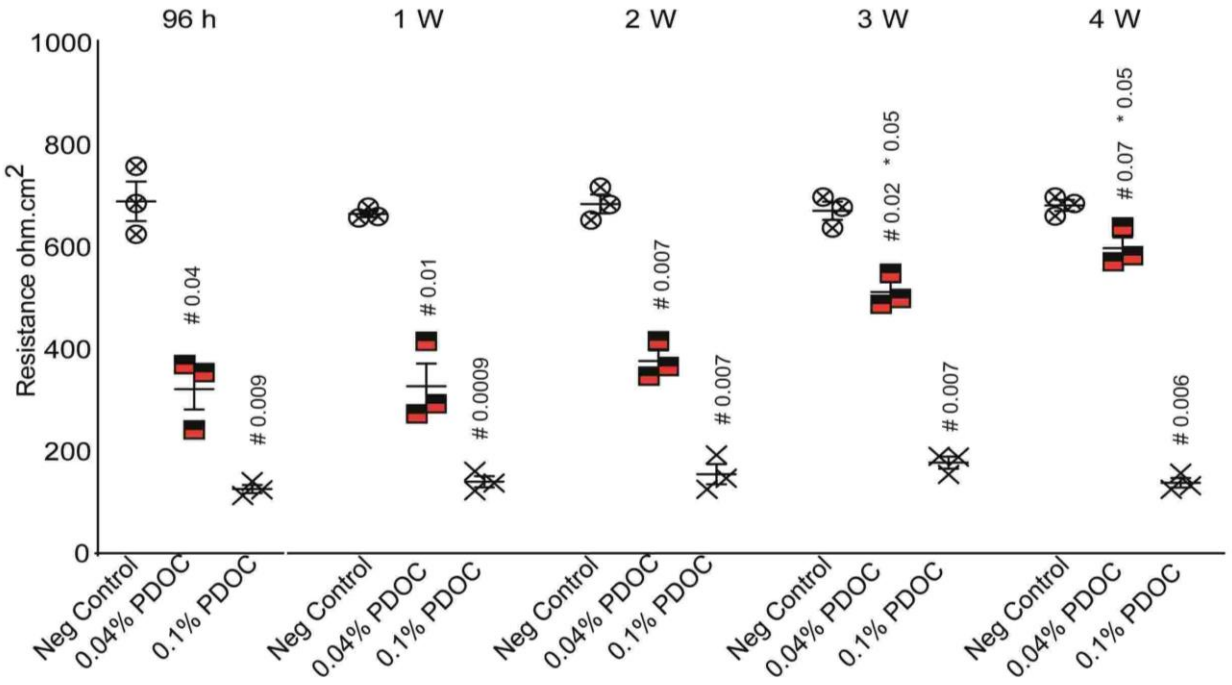

Figure 18: PDOC treatment disrupts epithelial barrier integrity after 0.04 % PDOC, but not after 0.1 % PDOC accompanied by restoration during the regeneration phase. Transepithelial electrical resistance (TEER) was performed to determine the epithelial barrier integrity post 0.04% & 0.1% PDOC treatment in comparison to time-matched negative control at 96 h and 1-4 weeks of regeneration phase. Data presented as mean ± SEM (*N*=3). Statistical analysis was performed using two-tailed paired *t*-test followed by multiple testing using Benjamini-Hochberg correction, focusing on two comparisons: (1) Testing for statistically significant cell loss (#: 0.04% and 0.1% PDOC injury *vs.* time-matched negative control until 96 h); (2) Testing for statistically significant regeneration after maximal cell loss at 96 h (*: Regeneration phase *vs*. 96 h within each PDOC treatment condition). Absolute adjusted *p*-values are given above the data points.

The epithelial barrier integrity measured using TEER remained stable across all the time points indicated in Figure 18. However, post 0.04% and 0.1% PDOC injury at 96 h, we observed a significant drop in the epithelial barrier integrity in comparison to negative control assessed using TEER. Furthermore, during regeneration phase, we observed a restoration in the epithelial barrier integrity significantly in a time dependent manner in relation to 96 h time point which is

also in agreement to the marked cell count observed upon 0.04% PDOC accompanied by proliferation during the regeneration phase (Figure 18).

For 0.1% PDOC injury at 96 h, we also observed a significant drop in the epithelial barrier integrity in comparison to negative control. However, the epithelial barrier did not restore but rather remained constantly low across the entire regeneration phase (Figure 18). Therefore, fully differentiated phBECs treated with 0.04% PDOC, but not 0.1% PDOC, incudes regeneration of the damaged epithelium which was evident due to the rise of differentiated cell types such as club, goblet and ciliated at an expense of basal cells, and restores the epithelial barrier integrity.

3.2.5 Proof-of-concept study: Notch signalling inhibition post 0.04% PDOC inhibits secretory cell formation during regeneration phase

Figure 19

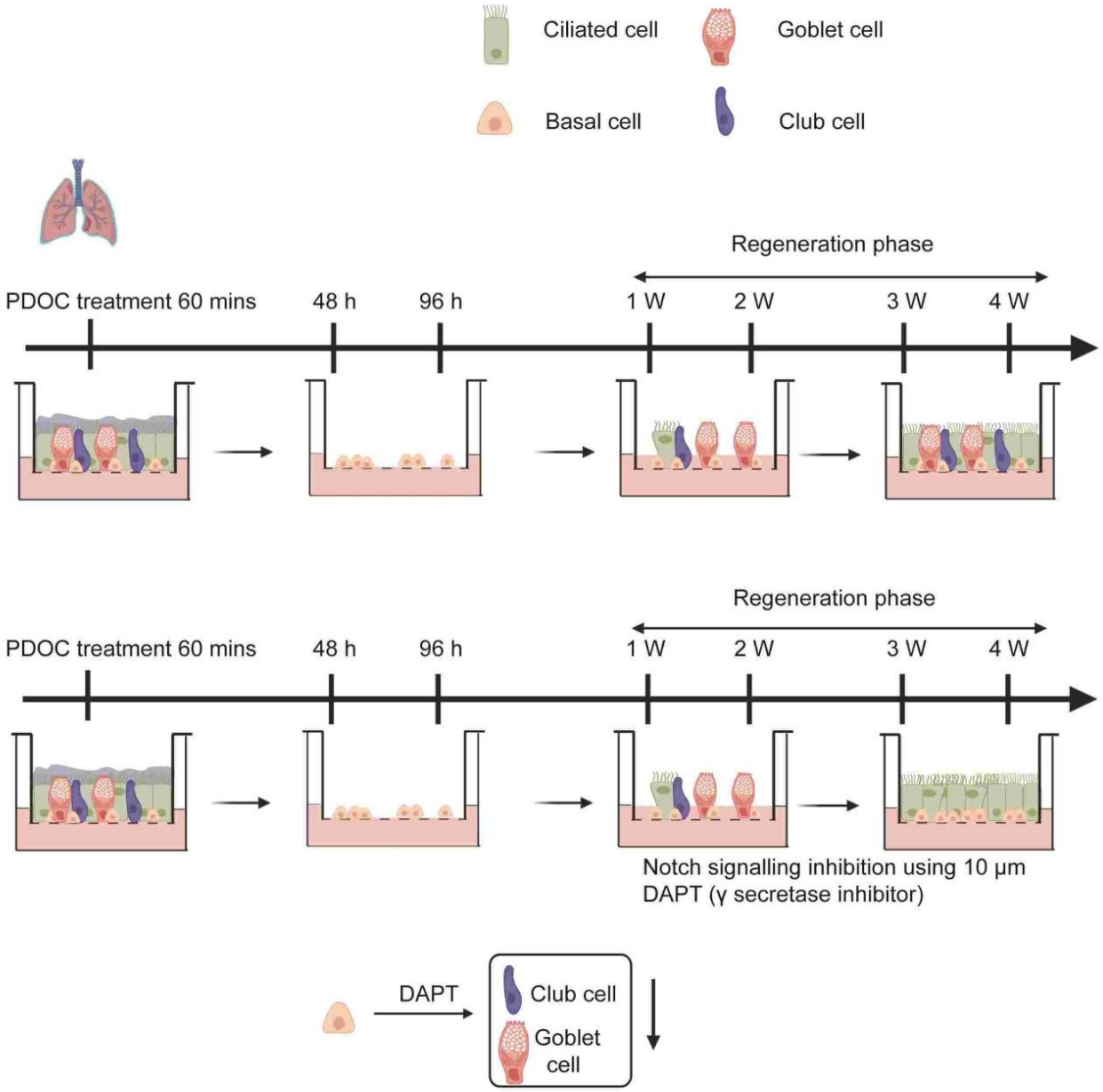

Figure 19: Proof-of-concept approach: Notch signalling inhibition using DAPT following 0.04% PDOC injury during the regeneration phase. Schematic overview of the strategy employed to inhibit Notch signalling post 0.04% PDOC treatment using 10 µM DAPT (γ-secretase inhibitor) during the regeneration phase. DMSO served as a vehicle control. Figure created using Biorender.

Notch signalling pathway inhibition favoring ciliated over the secretory cell formation has been well-known in both mouse and human airways epithelium (Gomi et al., 2015; Rock et al., 2011; Romieu et al., 2008; Xing et al., 2012; Xu et al., 2012). Therefore, to further validate the established regeneration model post 0.04% PDOC injury, as a proof-of-concept, we inhibited Notch signalling using the γ-secretase inhibitor DAPT during the entire regeneration phase and analysed the cell type-specific markers at both transcript and protein level (Figure19). For transcript analysis, we observed a downregulation of Notch target gene *HES1* in a time dependent manner upon DAPT treatment in comparison to time-matched vehicle control- DMSO. In addition, the transcript levels for cell type-specific markers for secretory cells (*SCGB1A1*, Club cell and *MUC5AC*, Goblet cell) were also found to be significantly downregulated in a time-dependent manner in relation to time-matched vehicle control-DMSO during the entire regeneration phase. On the other hand, the transcript levels of *FOXJ1* (Ciliated cell), and *TP63* and *KRT5* (Basal cell) upon DAPT treatment remain unchanged during the entire regeneration phase. Besides, we also determined the effect of DAPT treatment on the tight junction, by determining tight junction markers such as tight junction protein, *ZO1* and cadherin 1, *CDH1*. Upon DAPT treatment during the entire regeneration phase, the transcript levels of *ZO1* and *CDH1* remain unchanged in comparison to time matched DMSO vehicle control (Figure 20).

Furthermore, we also determined the effect of DAPT treatment at protein level by analysing immunofluorescent staining of cell type-specific markers such as the ciliated cell marker α TUB (alpha tubulin), the goblet cell marker MUC5AC (mucin5AC), the club cell marker CC10 (club cell-specific protein 10), the basal cell marker p63 (tumor protein 63) during the entire regeneration phase. DAPT treatment showed inhibition of secretory cell population (club and goblet) upon DAPT treatment in a time-dependent manner which is also in agreement with the transcript analysis of cell type-specific markers. And the cell composition towards the end of the regeneration phase mainly comprised of basal and ciliated cells. For DMSO vehicle control, we observed a rise in differentiated cell types such as goblet, club, and ciliated cells at an expense of basal cells in a time-dependent manner during the regeneration phase (Figure 21 a, b).

Figure 20

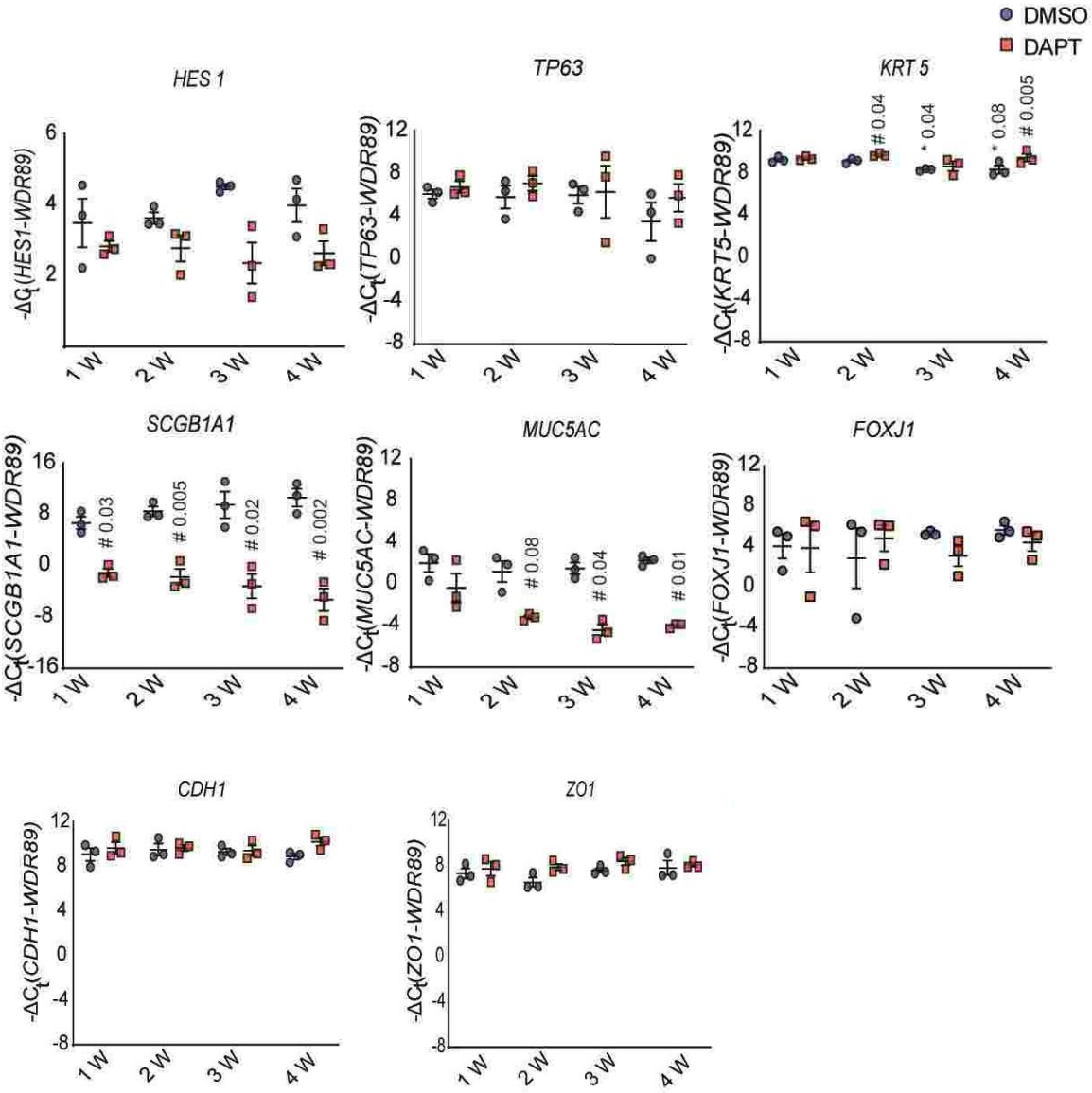

Figure 20: Proof-of-concept approach: DAPT inhibits secretory cell formation during the regeneration phase following 0.04% PDOC injury at transcript level. Transcript analysis of the Notch target gene *HES1* (hairy and enhancer of split-1), the club cell marker *SCGB1A1*, the goblet cell marker *MUC5AC,* basal cell markers *KRT5* and *TP63, the* ciliated cell marker *FOXJ1* cell and tight junction markers such as tight junction protein, *ZO1* and cadherin1, *CDH1* upon DAPT treatment in comparison to the time-matched DMSO vehicle control during the entire regeneration phase. WD Repeat Domain 89 (*WDR89*) transcript was used as internal reference gene. Data presented as mean ± SEM (*N*=3). Statistical analysis for Notch signalling inhibition was carried out using a two-tailed paired *t*-test followed by Benjamini-Hochberg correction to account for multiple testing, comparing (*) time points 2, 3, 4 W *vs.* 1 W for DMSO and DAPT condition, respectively during the regeneration phase, and comparing (#) DAPT treatment in comparison to time-matched DMSO vehicle control during the entire regeneration phase. Absolute adjusted *p*-values are given above the data points.

Figure 21

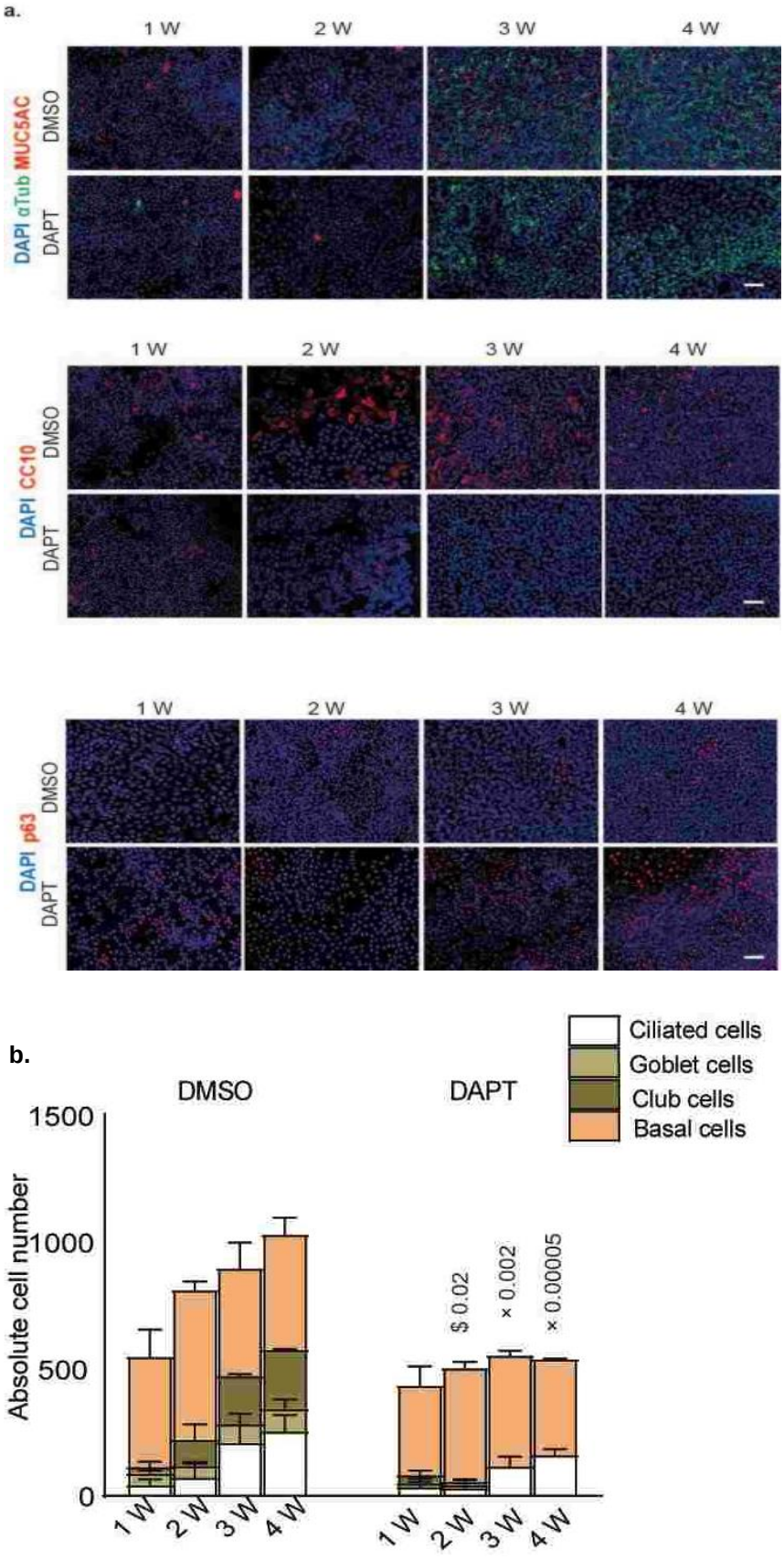
a.
1 W
2 W
3 W
4 W
DAPI αTub MUC5AC
DMSO
DAPT
DAPI CC10
DAPI p63
b.
DMSO
DAPT
Ciliated cells
Goblet cells
Club cells
Basal cells
Absolute cell number
1500
1000
500
0
$ 0.02
× 0.002
× 0.00005

Figure 21: Proof-of-concept approach: DAPT inhibits secretory cell formation during the regeneration phase following 0.04% PDOC injury at protein level. (a) Representative immunofluorescent staining (scale bar: 50 µm) and (b) the quantification of the cell type-specific markers such as the ciliated cell marker α TUB (alpha tubulin), the goblet cell marker MUC5AC (mucin5AC), the club cell marker CC10 (club cell-specific protein 10), the basal cell marker p63 (tumor protein 63) after DAPT treatment in comparison to time-matched DMSO vehicle control during the entire regeneration phase. Data presented as mean ± SEM (*N*=3). Statistical analysis for Notch signalling inhibition was carried out using a two-tailed paired *t*-test followed by Benjamini-Hochberg correction to account for multiple testing, comparing (*) time points 2, 3, 4 W *vs.* 1 W for DMSO and DAPT condition, respectively during the regeneration phase (see table 3), and comparing (#) DAPT treatment in comparison to time-matched DMSO vehicle control during the entire regeneration phase. Absolute adjusted *p*-values are given above the data points. Symbols used for showing statistical significance for specific cell-type is as follows: **α**, Ciliated cell; **β**, Goblet cell; **×**, Club cell; **$**, Basal cell.

Table 3: Statistical analysis for cell type-specific quantification upon Notch inhibition using DAPT (Figure 21b)

Time point	Cell-type	DMSO Vs DAPT	DMSO regeneration phase vs DMSO 1 W	DAPT regeneration phase vs DAPT 1 W
1 W	Ciliated cell (α)	ns		
	Goblet cell (β)	ns		
	Club cell (×)	ns		
	Basal cell ($)	ns		
2 W	Ciliated cell (α)	ns	ns	ns
	Goblet cell (β)	ns	ns	ns
	Club cell (×)	ns	ns	ns
	Basal cell ($)	2×10^{-2}	ns	ns
3 W	Ciliated cell (α)	ns	ns	ns
	Goblet cell (β)	ns	ns	9×10^{-2}
	Club cell (×)	2×10^{-3}	ns	3×10^{-2}
	Basal cell ($)	ns	ns	ns
4 W	Ciliated cell (α)	ns	ns	ns
	Goblet cell (β)	ns	ns	9×10^{-2}
	Club cell (×)	5×10^{-5}	ns	2×10^{-2}
	Basal cell ($)	ns	ns	ns

ns: not significant

Upon DAPT treatment during the regeneration phase, we assessed the epithelial barrier integrity using TEER measurements and observed the barrier integrity remained low for both DAPT treatment and DMSO vehicle control during the first week of regeneration phase. For the following weeks during regeneration phase, we observed the barrier integrity upon DAPT treatment remain constantly low in comparison to DMSO vehicle control where we observed an increase in barrier integrity in a time-dependent manner during the regeneration phase (Figure 22a). Furthermore, upon Notch signalling inhibition, we also performed total cell count analysis via nuclear stain DAPI and observed a decrease in cell count upon DAPT treatment in comparison to DMSO vehicle control, where we observed an increase in cell count in a time-dependent manner during the regeneration phase (Figure 22b).

Figure 22

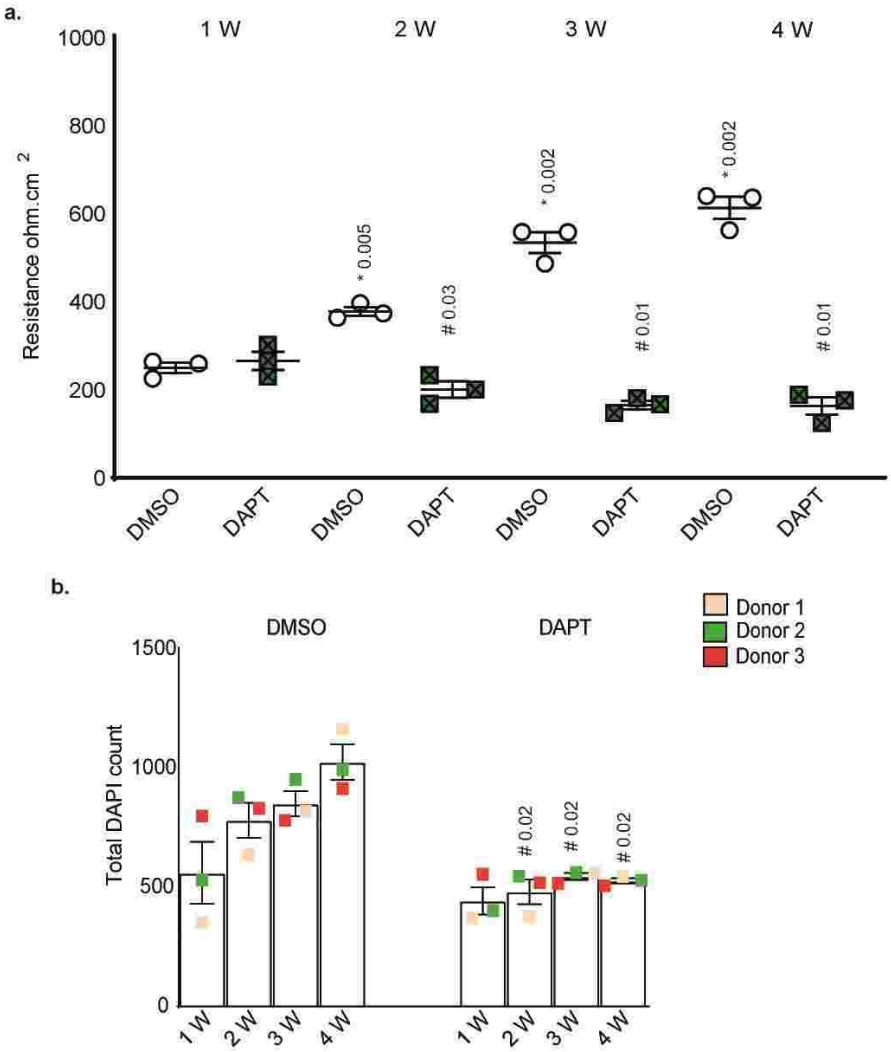

Figure 22:Proof-of-concept approach: DAPT treatment disrupts epithelial barrier integrity during regeneration phase. (a) TEER analysis was performed to determine epithelial barrier integrity upon DAPT treatment in comparison to time matched DMSO vehicle control during the entire regeneration phase. Data presented as mean ± SEM (*N*=3). (b) Total DAPI count from immunofluorescent staining upon DAPT treatment in comparison to time matched DMSO vehicle control during the entire regeneration phase. Data presented as mean ± SEM (*N*=3). For the above reported data's, the statistical analysis was performed using two-tailed paired *t*-test followed by Benjamini-Hochberg correction to account for multiple testing, comparing (*) time points 2, 3, 4 W *vs.* 1 W for DMSO and DAPT condition, respectively during the regeneration phase, and comparing (#) DAPT treatment in comparison to time-matched DMSO vehicle control during the entire regeneration phase. Absolute adjusted *p*-values are given above the data points.

4. Discussion

At first, we used the phBEC differentiation model into a fully functional bronchial epithelium and assessed the effect of the continuous supplement of CHOL during the phBEC differentiation. Chronic CHOL treatment lead to an increased in club cell population as compared to vehicle control during the differentiation phase. Next, we used the differentiated pseudostratified epithelium and established a strategy to induce an injury using 0.04% PDOC which led to a marked cell loss followed by proliferation and regeneration into a full-blown bronchial epithelium consisting of major cell types such as ciliated, club and goblet cells at an expense of basal cells. An initial drop in epithelial barrier integrity observed upon PDOC treatment and was later found to be restored during the regeneration phase. For the proof-of-concept approach, the Notch signalling inhibition was carried out on the established regeneration model post 0.04% PDOC injury lead to an inhibition of secretory cell formation such as goblet and club cells during the regeneration phase.

4.1 Effect of chronic CHOL exposure on the phBEC differentiation (from chapter 1)

In the first part of my thesis work, we took advantage of the normal human bronchial differentiation model where basal cells differentiate to a full-blown epithelium. Unbiased proteomics analysis revealed downregulation of cholesterol biosynthesis. Supplementing human bronchial epithelial cells with CHOL led to moderate but significant changes in cell type composition: Increase in club cells, probably at the expense of ciliated cells. These changes may be disease-relevant because, for instance, several studies have reported an increase in lipid-laden foam cells, basically cells containing cholesterol in a wide range of chronic lung diseases and smokers' lungs (Fessler, 2017), and in murine lungs exposed to cigarette smoke (Agudelo et al., 2020). Therefore, based on this evidence, it suggests the increase in CHOL content due to lipid dysregulation may be a common characteristic in chronic lung diseases (Kotlyarov & Kotlyarova, 2021), however, the direct impact of CHOL in human airways basal cell differentiation has not been reported so far.

Initially, we aimed to use two different concentrations of CHOL defined as physiological normal and pathological concentrations generally found in human blood (Physiological normal: 100 mg/dl (2.6 mM) and 500 mg/dl (12.9 mM)) and further use these concentrations to treat phBECs via the basolateral compartment of the insert chronically during the entire differentiation phase. The basolateral exposure route for chronic CHOL exposure offers an advantage for increased incubation time without affecting the ALI condition. For this study, we used a free form of cholesterol and dissolved in absolute ethanol at a stock concentration of 16 mM but could only manage to derive the highest possible working concentration of 80 µM CHOL for the chronic basolateral exposure.

Upon chronic CHOL treatment, we analysed the cell type-specific markers at transcript levels by qRT-PCR analysis and protein by IF stainings. For cell type-specific marker quantification via IF stainings, we observed an increase in club cell population upon chronic CHOL treatment in relation to vehicle control cells at day 14 and 21. Interestingly, a study carried out by Nomori et al., showed a significant correlation of serum levels of protein 1 (Club cell secretory protein) with serum lipids and lipoprotein including cholesterol in clinical patient samples which is in line with our reported findings (Nomori et al., 1996). Studies have reported an increased accumulation of lipid-laden cells, also known as “foam cells” in the lung of several chronic lung disease patients (Basset-Léobon et al., 2010; Wilson et al., 2011). Furthermore, a study by Jia and colleagues, showed that oxysterol, a metabolite of cholesterol involved in the inducible bronchus-associated lymphoid tissue (iBALT) formation a key contributor in the COPD pathogenesis observed in both COPD patients and cigarette smoke-exposed mice (Jia et al., 2018). Besides this experimental evidence, a meta-analysis performed by Xuan et al., showed a positive correlation between cholesterol accumulations in COPD patients (Xuan et al., 2018). Furthermore, an increase in secretory cells, such as goblet and club cells, and tight junctions’ modifications are usually observed in chronic lung diseases, namely COPD and IPF. Nevertheless, with an increase in club cell population observed upon chronic CHOL exposure, we did not observe any effect on the epithelial barrier integrity during the entire differentiation. Of note, we did observe a higher degree of variability in the TEER values, which could be caused due to donor variability.

We observed a low ciliated cell number count for both vehicle control and CHOL treatment assessed by IF stainings. At transcript level, we observed a downregulation of ciliated cell transcript *FOXJ1* upon CHOL treatment in comparison to time-matched vehicle control at day 7, but remain unchanged for the rest of the differentiation phase. During normal basal cell differentiation, the ciliated cell population corresponds to about 40-50% (Staudt et al., 2014), in contrast, we observe a lower ciliated cell number in both vehicle control- absolute ethanol and chronic CHOL treatment. Therefore, it is difficult to assess if CHOL by itself has any effect on the ciliated cell population since the vehicle control cells also has lower ciliated cell count. It is worth mentioning that the ciliated cell count remained unaffected in different vehicle control used in this study (Chapter 2: Figure 17b, Figure 21b) and also in other studies (Mastalerz et al., 2022). It suggests that the treatment with absolute ethanol itself appears to have an effect on the cell type composition. Therefore, it will be interesting in future to investigate the role of alcohol predisposition to acute lung injury and disease (Kershaw & Guidot, 2008). In near future, a negative control (without absolute ethanol) should also be differentiated alongside vehicle control-absolute ethanol and chronic CHOL conditions which will help us to better understand the overall cell type-specific response under each above-mentioned condition.

Additionally, a study reported that the accumulation of cholesterol sulfate induces squamous cell differentiation in rabbit tracheal epithelial cells (Rearick & Jetten, 1986). Therefore, we determined the squamous cell differentiation marker *IVL*, Involucrin upon chronic CHOL exposure at the transcript level. In contrast, we observed a decrease in *IVL* transcript levels during the differentiation phase suggesting that the squamous cell differentiation in phBECs upon chronic CHOL exposure.

So, in efforts to use the physiological CHOL concentrations, we performed vehicle control (absolute ethanol) titration in PneumaCult-ALI medium until 48 h and determined that 1% is the maximum tolerable absolute ethanol percentage corresponding to a working CHOL concentration of 80 µM. However, moving forward with the determined CHOL concentration, we observed increased cytotoxicity of more than 20% in both vehicle control and chronic CHOL condition. Therefore, an absolute ethanol titration should be repeated for the entire differentiation phase, and further, reassess the maximum tolerable absolute ethanol

percentage and the desired CHOL concentration for the chronic CHOL exposure.

We performed the upstream regulator analysis from differentiating phBECs at ALI condition on the IPA platform. Upon upstream regulator analysis, we found that the transcription factor, tumor protein p53 is involved in regulating the target proteins involved in the cholesterol biosynthesis pathway. p53 mutations is the key factor in human lung cancer. Abnormalities associated with p53 has been reported in the tumorigenesis of airways epithelial cells by inducing cell cycle growth arrest, senescence, and apoptosis (Mogi & Kuwano, 2011). A study carried out using mouse model showed that airways club cells are responsible for inducing senescence upon lipopolysaccharide treatment, however, the club cell-specific p53 knockout mouse model showed decreased senescence levels, suggesting the airways club cell might play a role in the p53 activation upon successive injury (Sagiv et al., 2018). Furthermore, another study demonstrated that the loss of p53 led to an increased progenitor and self-renewal capacity of airways club cells and reduced ciliated cell population *in vitro* (McConnell et al., 2016). Therefore, future studies may assess the role of p53 in the context of senescence in phBECs differentiation upon chronic CHOL treatment.

4.2 Establishment of novel human in vitro model for airway epithelial injury and regeneration (from chapter 2)

In the second part of this study, we used differentiated phBECs and carried out PDOC injury on the airway epithelium lead to a loss of differentiated cell types leaving largely behind basal cells which then underwent proliferation and regenerate the damaged epithelium between 2-4 weeks' during the regeneration phase. Several studies have reported the use of synthetic fatty acid surfactants such as PDOC, lysophosphatidylcholine, and sodium caprate have been involved in modifying tight junctions to increase paracellular permeability (Carpentieri et al., 2021; Cmielewski et al., 2017; Johnson et al., 2003; Liu et al., 2010; Parsons et al., 1998). In this study, we observed that the apical application of PDOC on the pseudostratified epithelium led to a significant drop in epithelial barrier integrity assessed using TEER, and therefore also is in line with observations in *in vivo* stated earlier. Furthermore, we observed the barrier integrity lost upon PDOC was found to be restored in a time-dependent manner

during regeneration for 0.04% PDOC, but not in 0.1% PDOC. Apical application of PDOC carried out *in vitro* was in analogy to the *i.t.* PDOC application *in vivo*, a model generally used to cause unspecific luminal cell depletion, leaving behind basal cells which then undergo proliferation, differentiation and regenerate the damaged epithelium (Borthwick et al., 2001; Engler et al., 2020; Gui et al., 2015; Leblond et al., 2009). Upon 0.04% PDOC injury, a concentration close to EC50 value, we observed a loss in differentiated cell types leaving behind only basal cells, which then underwent proliferation and regenerate the damaged epithelium during regeneration phase. For 0.1% PDOC injury, we also observed a similar trend in loss of differentiated cell types, however, only observed little proliferation and differentiation based on Ki67 and total DAPI count, and classical bronchial epithelial cell markers. Based on these observations upon 0.04% and 0.1% PDOC injury, it suggests there seems to be a threshold for PDOC injury, like a point-of-no-return, after which the regeneration fails. Therefore, strategies should be employed to understand the novel regeneration mechanisms in more detail, which may help us to overcome this point-of-no-return, however, could not be determined for this study.

The inhibition of Notch signalling abolishing secretory cell formation such as goblet and club cells is well known in both mouse and human airways. For the proof-of-concept approach, we used the established regeneration model post 0.04% PDOC injury and studied the inhibition of Notch signalling using 10 µM DAPT during the entire differentiation phase. Upon Notch signalling inhibition via DAPT treatment, we observed an inhibition of the secretory cell population while the ciliated cells remain unaffected during the regeneration phase. Furthermore, we observed a significant drop in total DAPI count and epithelial barrier integrity and remain constantly low throughout the entire differentiation phase. In contrast, for vehicle control DMSO, we observed a rise in total DAPI count and epithelial barrier integrity in a time-dependent manner during the regeneration phase. The ciliated cell number did not increase with the inhibition of secretory cell formation upon DAPT treatment during the entire regeneration phase, and therefore these may suggest that the secretory cells are required as an intermediate for the ciliated cell formation since this has always been shown by recent single-cell RNA Seq studies in the mouse (Montoro et al., 2018).

Furthermore, we determined the epithelial barrier integrity upon DAPT treatment using TEER analysis and found to be consistently low during the entire regeneration. Interestingly, studies investigating the direct impact of DAPT treatment on airways epithelial barrier integrity have not been studied yet. However, a study from Chang et al., reported that the adherens junction components such as E-cadherin (*CDH1*) were downregulation upon DAPT treatment (Chang et al., 2021). Therefore, to validate these findings, we analysed two independent cell junction components such as *ZO1* (tight junction) and *CDH1* (adherens junction) upon DAPT treatment at the transcript level, and they remained unchanged in comparison to DMSO vehicle control during the entire regeneration phase. So therefore, based on this evidence it suggests that the drop in epithelial barrier integrity observed is not due to the impact on the tight junction components, but more likely due to the consistent low cell count observed reflecting the anti-proliferative effect of DAPT treatment, which has also been observed in other cell types (Bi et al., 2016; Feng et al., 2019).

In addition to PDOC treatment, we also carried out a strategy to induce cell type-specific luminal depletion using NA *in vitro*. In murine airways, NA induced club cell specific depletion and subsequent regeneration is well established, where NA being non-toxic compound, after administration undergoes cytochrome P450 enzyme Cyp2f2 present in club cells forming cytotoxic metabolites such as NA epoxides and diols within the cell causing club cell specific depletion (Shultz et al., 1999). In this *in vitro* study, the NA application was performed in analogy to the *i.p.* NA application *in vivo* where it reaches via the blood circulation. Upon using the highest soluble NA concentration *in vitro*, we did not observe any club cell-specific inhibition at the studied time points determined at both transcript and protein levels. Human club cells use CYP2F1 to metabolize NA, and its efficiency is relatively low in comparison to mouse Cyp2f2 (Buckpitt et al., 2002; Lewis et al., 2009; Shultz et al., 1999). In agreement, a study reported by Li and colleagues used humanized CYP2F1 mouse model and studied the metabolic activation of NA and related respiratory toxicity, however, did not observe club cell-specific depletion (Li et al., 2017). Furthermore, we believe that there could be species-species differences in metabolic activation of xenobiotic compounds, which are often observed (Martignoni et al., 2006). To overcome the limitation of reduced NA metabolic activity by the human enzyme, ef-

forts could be performed to increase NA solubility by the use of protein carriers and achieve desired effects (Telange et al., 2021; Y. Wang et al., 2021).

Here, we have successfully established a human *in vitro* model where PDOC was used on the fully differentiated phBECs which induced unspecific cell depletion accompanied by subsequent regeneration. Furthermore, the established human *in vitro* model can be also used as an alternative to the frequently used *in vivo* models for studying airway epithelial injury and subsequent regeneration. We believe that the strategy employed in this model can also be performed using patient-derived phBECs, and further understand the disease-specific limitations in repair capacities upon injury. Along the same lines, the preventive measures can also be tested during normal differentiation in our model which will help us to identify the compounds and make cells more resilient towards an injury and increase the regenerative potential of the airway epithelium. The established model will allow us to perform second hit studies, for example, pHBECs can be treated chronically with compounds such as nanoparticles, cigarette smoke components or other environmental toxicants during normal differentiation and determine the repair capacity in addition to PDOC injury. Our established human *in vitro* model also serves as a platform to perform stem cell engraftment studies in patient-derived phBECs culture. COPD and cystic fibrosis-derived pHBECs have been shown to retain characteristics *in vitro* (Gindele et al., 2020; Schögler et al., 2017; Sette et al., 2021), so therefore, the PDOC concentration should be optimized to perform gene therapy or stem cell engraftment studies *in vitro*.

4.3 Conclusion

Overall, we observed an increased club cell population upon chronic CHOL exposure during phBECs differentiation suggests that CHOL might be a potential regulator of bronchial epithelial cell fate. Furthermore, we established a novel human *in vitro* model for studying airway epithelial injury and regeneration. Lastly, the results shown in this study contribute to our understanding of mechanisms involved in human bronchial epithelial injury and regeneration

5. Material and Methods

5.1 Reagents and chemicals

Cholesterol was obtained from Alfa Aesar (57-88-5) and dissolved in absolute ethanol (64-17-5, Sigma) at a stock concentration of 16 mM. Nonethylene glycol monododecyl ether (Polidocanol, PDOC) was obtained from Sigma Aldrich (CAS Number: 3055-99-0, Darmstadt, Germany) and dissolved in prewarmed 1x Hank's Balanced Salt Solution (HBSS) with calcium and magnesium at a desired working concentration (14065049, Gibco, New York, USA). Naphthalene (NA) was purchased from Sigma Aldrich (CAS number: 91-20-3) and the stock was prepared after dissolving NA in absolute ethanol (64-17-5, Sigma) at a concentration of 0.35 M.

5.2 Patient material

phBECs (n=7) of non-CLD donors were obtained from the CPC-M bioArchive at the Comprehensive Pneumology Center (CPC Munich, Germany). phBECs had been isolated from histologically normal regions adjacent to resected lung tumours. The study was approved by the local ethics committee of the Ludwig-Maximilians University of Munich, Germany (Ethic votes #333-10 and #19-630). Written informed consent was obtained for all study participants.

5.3 Primary human bronchial epithelial cell (phBEC) differentiation

For phBEC expansion, the cells (passage 2) were seeded on a type 1 collagen coated at a seeding density of 100,000-150,000 cells on 100 mm plates (Corning, 430167, New York, USA) using PneumaCult-Ex plus medium with 1 X supplement (Stemcell Technologies, 05041, Vancouver, Canada), 0.2% Hydrocortisone (Stock: 96 µg/mL) (CAS Number: H2270, Sigma) and 1% Pen/Strep (Life technologies, 10,000 U, 15140). At 80% confluency, the cells were then seeded on 12-well transwells (Corning, 3460, 12mm inserts, 12-well plate, 0.4µm Polyester Membrane, Tissue Culture Treated, Polystyrene, 1.12cm^2/transwell) at a

seeding density of 100,000 cells/insert and were expanded further under submerged conditions until they reached confluency. phBECs were then airlifted by aspirating the apical medium, and the basolateral medium was replaced with Pneumacult-ALI (Stemcell Technologies, 05002 including supplement 05003, and additives 05006) + 0.2% Heparin (Stock: 2mg/ mL) (H3149, Sigma) + 0.5% Hydrocortisone (Stock: 96 µg/mL) + 1% Pen/Strep and were differentiated for 28 days at ALI condition.

5.4 Treatments

5.4.1 Chronic cholesterol (CHOL) treatment during normal phBECs differentiation

The chronic cholesterol treatment was carried out on the basolateral compartment of the insert during normal basal cell differentiation for 28 days. The working concentration of cholesterol used for chronic exposure was 80 µM which was achieved after diluting ethanol- based cholesterol in PneumaCult-ALI medium. The vehicle control was prepared by adding the same volume of absolute ethanol in PneumaCult-Ali medium.

5.4.2 Polidocanol (PDOC) treatment on differentiated phBECs

Upon 28 days of ALI differentiation, a half maximal effective concentration (EC50) was derived for PDOC concentrations ranging from 0.002-2% PDOC in prewarmed 1x HBSS ($+Ca^{+2}/Mg^{+2}$) with a total volume of 200 µL on the apical compartment of the insert for 60 min. The apical aspiration was carried out post PDOC treatment and washed further with prewaremed 1x HBSS ($+Ca^{+2}/Mg^{+2}$) on the apical side. Prewarmed 1x HBSS ($+Ca^{+2}/Mg^{+2}$) with a total volume of 200 µL on the apical compartment of the insert for 60 min was used as a vehicle control.

5.4.3 Naphthalene (NA) treatment on differentiated phBECs

The solubility of NA is low in aqueous solution, so therefore the highest possible working concentration of NA used was 0.35 mM. Upon 28 days of ALI culture, 0.35 mM NA was used for treating phBECs via the basolateral compart of the insert for 60 min, 24 h and 72 h. The NA working concentration was achieved after diluting the appropriate volume of the ethanol- based NA stock in Pneu-

maCult-ALI medium. For vehicle control, the same volume of absolute ethanol was added to the PneumaCult-ALI medium.

5.5 Cytotoxicity assays

5.5.1 Trypan blue exclusion test

Upon PDOC or NA treatment, the cells were first washed with 1x HBSS ($+Ca^{+2}/Mg^{+2}$) on both apical and basal compartment of the inserts, aspirated and followed by the addition of 0.25% Trypsin-EDTA (25200056, Gibco) with a total volume of 500 µL on the apical compartment and 1000 µL on the basolateral compartment and incubated in the incubator for 5 mins until the cells were detached. Thereafter, the cell suspension was collected in a 50 mL falcon tube followed by additional washing step with 1x HBSS without calcium and magnesium (14170088, Gibco) on both apical and basolateral compartment of the insert and collected in the same 50 mL falcon tube with cell suspension. The cell suspension was then centrifuged at 350 g for 5 mins followed by supernatant aspiration and the cell pellet was then resuspended with PneumaCult-ALI medium, stained with trypan blue and the cell viability was assessed using heamocytometer.

5.5.2 Lactate Dehydrogenase (LDH) assay

For chronic cholesterol exposure, the apical wash and basolateral medium was collected from both vehicle control and cholesterol treatment at day 7, 14 and 21 and stored in 1.5 mL Eppendorf aliquots at $-80^{0}C$ for further use. Upon NA treatment, the basolateral compartment supernatant was collected at 60 min and 24 h and stored in 1.5 mL Eppendorf aliquots at $-80^{0}C$ for further use. The LDH release in the supernatant was determined using the cytotoxicity detection kit LDH (Roche, 11644793001, Mannheim, Germany) and used according the manufacturer's instructions. For positive control, the cells were lysed with 2% triton-X/1x HBSS ($+Ca^{+2}/Mg^{+2}$) on the apical compartment of the insert for 60 min and later the apical wash collected was used for maximal LDH release.

5.6 RNA Isolation and Real-Time Quantitative Reverse-Transcriptase PCR (qRT-PCR) Analysis

Upon CHOL, NA and PDOC treatment, the cells were washed twice with 1x HBSS (+Ca^{2+}/Mg^{2+}) on both the apical and basolateral compartment of the inserts. Thereafter, the cells were scraped from the inserts, collection of cell lysates into 1.5 mL Eppendorf and then the RNA extraction was carried out using RNeasy Mini Plus Kit (Qiagen, 74136, Venlo, Netherlands) and used according to the manufacturer's instructions. The RNA concentration was using a NanoDrop 1000 spectrophotometer determined by measuring absorbance at 260 nm (NanoDrop Tech. Inc; Wilmington, Germany). RNA was then reverse transcribed into cDNA using reverse transcriptase (Applied Biosystems, N8080018, Waltham, USA or Invitrogen, 28025013) and random hexamer primers (Applied Biosystems). 1 µg RNA was diluted up to 20 µl with DNase/RNase free water, denatured at 70°C for 10 min for the removal of secondary and tertiary RNA structures and then later incubated on ice for 5 min. 20 µl of cDNA synthesis master mix (5 mM MgCl2, 1x PCR buffer II (10x), 1 mM dGTP, 1 mM dATP, 1 mM dTTP, 1 mM dCTP, 1 U/µl RNase inhibitor, and 2.5 U/µl MuLV reverse transcriptase) was added to each sample and cDNA synthesis was performed for 60 min at 37°C, followed by 10 min incubation at 75°C. cDNA obtained was then diluted up to 200 µl with DNase/RNase-free water for the use during qRT-PCR analysis.

qRT-PCR analysis was performed in a 96-well format using a Light Cycler LC480II instrument (Roche) and LightCycler® 480 DNA SYBR Green I Master (Roche). The data were shown as - ΔC_t where ΔC_t was calculated as C_t (gene of interest) - C_t (reference gene) for each condition. WD Repeat Domain 89 (*WDR89*) and a second independent housekeeping gene Hypoxanthine guanine phosphoribosyl transferase (*HPRT*) was used as a housekeeping gene for samples obtained from CHOL, PDOC- and NA-treated phBECs.

5.7 Immunofluorescence (IF) analysis and quantification

Post CHOL, NA and PDOC treatment, the inserts were washed twice on both apical and basal side with 1x 1x HBSS (+Ca^{2+}/Mg^{2+}). After washing, the cell fixation was carried out using 3.7% paraformaldehyde (PFA) on both apical and basal side of the insert for 1 h at room temperature. Inserts were then washed with 1x DPBS (10x DPBS: 14080-055, Gibco) and stored in 1x DPBS at 4^0C for further use. The membrane containing cells were cut into six pieces and used for IF stainings as follows: Cells were first permeabilized with 0.2% Triton X-100/1x DPBS for 5 min followed by washing with 1x DPBS for 5 min, and then the cells were blocked with 5% BSA/1x DPBS for 1 h at room temperature. After blocking, the membrane containing cells were transferred to a 12-well plate, the primary antibody was applied in a total volume of 150 µL and left at 4^0C over-night. The next day, the membranes were washed three times with 1x DPBS for 5 min and then the secondary antibodies conjugated with AlexaFluor-488 and -568 together with 0.5 µg/ml 4,6-diamidino-2-phenylindole (DAPI) (1:2000 dilution) in 5% BSA/1x DPBS was added and incubated for 1 hr at room temperature covered in dark. The membrane was then washed three times with 1x DPBS and mounted in fluorescent mounting medium (Dako, S3023, Hamburg, Germany). The immunofluorescence analysis was carried out using a fluorescent microscope (Axiovert II; Carl Zeiss AG; Oberkochen, Germany). The processing of images was done using ZEN 2010 software (Carl Zeiss AG). The cell type-specific staining quantification was carried out using Imaris 7.4.0 software (Bitplane; Zurich, Switzerland).

5.8 Primer and antibodies

The list of primers used in this study was obtained from Eurofins Genomics Germany GmbH (Ebersberg, Germany) and are listed in table 4. The antibodies used in this study are listed in table 5.

Table 4: List of human primers used for qRT-PCR analysis

Gene	Forward primer Sequence (5'-3')	Reverse primer Sequence (5'-3')
WDR89	AGTACGTTCCATCCCAG-CAATCC	AGGCCATCAGATGAAC-CTGAGACT
SCGB1A1	TTCAGCGTGTCATCGAAACCC	ACAGTGAGCTTTGGGC-TATTTTT
FOXJ1	TCGTATGCCACGCTCATCTG	CTT-GTAGATGGCCGACAGGG
TP63	CCCGTTTCGTCAGAACACAC	CATAAGTCTCAC-GGCCCCTC
KRT5	GAGATCGCCACTTACCG-CAA	TGCTTGTGACAACAGA-GATGT
CYP2F1	GGCAGAGGAGAAGGAG	CTTGAACTTTTGGG-TACTTC
HES1	CTGAGCACAGAAAGTCATC	GGCTCAGACTTTCATTTATT
MUC5AC	AG-CAGGGTCCTCATGAAGGTGGAT	AATGAG-GACCCCAGACTGGCTGAA
CDH1	AACAG-GATGGCTGAAGGTGACAGA	AACTGCATTCCCGTT-GGATGAC
ZO1	CAGCCGGTCACGATCTCCT	TCCGGAGACTGCCATTGC
IVL	GGAGGTCCCATCAAAGCAAG	GCTCCTTCTGCTGTGCTCA

Table 5: List of antibodies used for Immunofluorescence analysis

Target	Host	Ref no	Provider	Dilution
αTUB	Rabbit	ab 179484	Abcam	1:500
MUC5AC	Mouse	ab 3649	Abcam	1:250
CC10	Mouse	sc 365992	Santa Cruz	1:300
	Rabbit	sc 25554	Santa Cruz	1:250
p63	Mouse	ab 735	Abcam	1:125
Ki-67	Rabbit	ab 16667	Abcam	1:500
Donkey anti-mouse (red 568)	Mouse	A10037	Thermofisher	1:500
Goat anti-rabbit (green 488)	Rabbit	A32731	Thermofisher	1:500

5.9 Trans Epithelial Electrical Resistance (TEER) measurement

During chronic CHOL exposure, the epithelial barrier integrity was assessed during normal basal cell differentiation at day 7, 14 and 21. For PDOC experiment, the epithelial barrier integrity measurement was also determined post PDOC injury at 96 h and also during the entire regeneration phase. Initially, the pre-warmed 1x HBSS (+Ca^{2+}/Mg^{2+}) was added onto the apical compartment of the insert and equilibrated at room temperature for 10 min. The measurement was performed in triplicates for each insert using Millicell-ERS-2 volt-ohm-meter (Millipore, Billerica, MA, USA) with a STX01 chopstick electrode (Millipore). Upon TEER measurement from each insert, the blank value (measurement of an insert without cells) was subtracted, and the resulting value was then multiplied with the surface area of the insert (1.12 cm^2 for 12-well transwell inserts) and the final TEER values were presented in Ω x cm^2.

5.10 Protein isolation and estimation

During phBECs differentiation, the cells were washed first with 1x HBSS on both apical and basal compartment twice and collected at day 0, 7, 14, 21 and 28 for proteomic analysis. The protein isolation was achieved by first washing the cells with cold 1x HBSS and collected into 80 µl RIPA buffer (50 mM Tris•HCl, pH 7.6, 150 mM NaCl, 1% Nonidet P-40, 0.5% sodium deoxycholate, and 0.1% SDS) with CompleteTM protease inhibitor cocktail (05892970001, Roche, Basel, Switzerland) and PhosSTOP phosphatase inhibitor cocktail (PHOSS-RO, Roche) with either a cell scratcher or a 1 ml pipette tip. The collected cells in tubes were then incubated on ice for 30 mins after which they were centrifuged at 4^0C for 15 mins at 14,000 rpm. After centrifugation, the supernatant was collected and stored in -800C. The protein concentration was estimated using the PierceTM BCA Protein Assay Kit (23225, Thermo Scientific, Rockford, USA) and used according to manufacturer's instructions.

5.11 *In silico* analysis

5.11.1 Proteomic analysis from differentiating phBECs

During normal phBECs differentiation, the inserts containing cells were collected at day 0, 7, 14, 21 and 28 and the proteins were isolated as mentioned earlier in 5.10. The isolated proteins were then sent to the PROT Research Unit Protein Science at Helmholtz Zentrum München and a non-biased proteomic analysis was performed by Juliane Merl-Pham. Upon LC-MS/MS analysis, the spectra obtained was uploaded to the Progenesis QI proteomics software (Nonlinear Dynamics, part of Waters), as described previously (Hauck et al. Molecular & Cellular Proteomics. 2010; Merl et al. Proteomics. 2012). Mascot search engine was used to identify peptides (version 2.6.1) from Swissprot human protein database resulted from the MSMS spectra (Release 2017_02, 11,451,954 residues, 20,237 sequences). The search parameters involved are as follows:

1. 20 µm fragment mass tolerance
2. 10 ppm peptide mass tolerance
3. Fixed modification was set for cysteine carbamidomethylation

4. Allowed variable modifications: Methionine oxidation or glutamine deamination
5. Allowed one missed cleavage

5.10.2 Bioinformatic analysis

The differential expression analysis for the proteome data from differentiating phBECs was kindly performed by Hannah Marchi and Ronan le Gleut from Core Facility Statistical Consulting at Helmholtz Zentrum München. The analysis was performed using statistical programming R software. Statistical analysis was performed for four time points (day 7, 14, 21 and 28) in comparison to day 0 with 4 biological replicates. Overall, the analysis was performed using Wald test with Benjamini Hochberg correction to identify the differentially expressed proteins. Significance value: $q < 0.05$.

5.10.3 Ingenuity pathway analysis (IPA)

The differential expression profile containing q-values and log fold changes from normal phBECs differentiation were uploaded to the Ingenuity Pathway Analysis platform (IPA Tool; Ingenuity®Systems, Redwood City, CA, USA; http://www.ingenuity.com). The parameters used to analyze differentially expressed proteins from differentiating phBECs are as follows:

1. Log Fold change: <-1 or >+1
2. q value: < 0.05
3. Scoring method: fischer exact test p value

A total of 1371 significant hits out of 4860 proteins were enriched fulfilling the above mentioned parameters and then these proteins were then uploaded onto the Ingenuity pathways Knowledge Base database. Next, IPA generated the information about the deregulated enriched signaling pathways, master regulators, and constructs interacting networks between proteins.

5.12 Statistical analysis

For chronic CHOL treatment, the results are presented in terms of mean± SEM from at least three biological replicates where each biological replicate was performed from cells from a different donor. The statistical analysis was performed using a paired *t*-test using GrapPad Prism version 9.0 for Windows, GraphPad Software, San Diego, California USA, www.graphpad.com. All the results presented regarding PDOC or NA experiments are presented in terms of mean ± SEM from at least three biological replicates where each biological replicate was performed from cells from a different donor. The cell viability assessment post PDOC treatment is presented in terms of mean ± SD. The statistical analysis for PDOC experiments was carried out using a two-tailed paired *t*-test (*: Regeneration phase in comparison to 96 h within each PDOC treatment condition) or paired *t*-test (#: 0.04% and 0.1% PDOC injury vs time-matched negative control until 96 h) followed by Benjamini-Hochberg correction to account for multiple testing. The statistical analysis for Notch signalling inhibition experiment was carried out using a two tailed paired *t*-test (*: Regeneration phase in comparison to 1 W for DMSO and DAPT condition respectively) or paired *t*-test (#: DAPT treatment in comparison DMSO vehicle control during regeneration phase) followed by Benjamini-Hochberg correction to account for multiple testing. The statistical analysis for NA treatment was carried out using a two tailed paired *t*-test (NA 60 min and NA 24 h in comparison to negative control 24 h) followed by Benjamini-Hochberg correction to account for multiple testing. The statistical analysis was performed using R program (Version: RStudio 2022.02.2+485 "Prairie Trillium" Release) (R Core Team, 2021). The significance level was set to 0.1 for all the analysis.

References

Adams, T. S., Schupp, J. C., Poli, S., Ayaub, E. A., Neumark, N., Ahangari, F., Chu, S. G., Raby, B. A., DeIuliis, G., Januszyk, M., Duan, Q., Arnett, H. A., Siddiqui, A., Washko, G. R., Homer, R., Yan, X., Rosas, I. O., & Kaminski, N. (2020). Single-cell RNA-seq reveals ectopic and aberrant lung-resident cell populations in idiopathic pulmonary fibrosis. *Science Advances*, *6*(28). https://doi.org/10.1126/sciadv.aba1983

Agudelo, C. W., Samaha, G., & Garcia-Arcos, I. (2020). Alveolar lipids in pulmonary disease. A review. In *Lipids in Health and Disease* (Vol. 19, Issue 1). https://doi.org/10.1186/s12944-020-01278-8

Basset-Léobon, C., Lacoste-Collin, L., Aziza, J., Bes, J. C., Jozan, S., & Courtade-Saïdi, M. (2010). Cut-off values and significance of Oil Red O-positive cells in bronchoalveolar lavage fluid. *Cytopathology*, *21*(4). https://doi.org/10.1111/j.1365-2303.2009.00677.x

BéruBé, K., Prytherch, Z., Job, C., & Hughes, T. (2010). Human primary bronchial lung cell constructs: The new respiratory models. In *Toxicology* (Vol. 278, Issue 3). https://doi.org/10.1016/j.tox.2010.04.004

Bi, P., Yue, F., Karki, A., Castro, B., Wirbisky, S. E., Wang, C., Durkes, A., Elzey, B. D., Andrisani, O. M., Bidwell, C. A., Freeman, J. L., Konieczny, S. F., & Kuang, S. (2016). Notch activation drives adipocyte dedifferentiation and tumorigenic transformation in mice. *Journal of Experimental Medicine*, *213*(10). https://doi.org/10.1084/jem.20160157

Billipp, T. E., Nadjsombati, M. S., & von Moltke, J. (2021). Tuning tuft cells: new ligands and effector functions reveal tissue-specific function. In *Current Opinion in Immunology* (Vol. 68). https://doi.org/10.1016/j.coi.2020.09.006

Borthwick, D. W., Shahbazian, M., Krantz, Q. T., Dorin, J. R., & Randell, S. H. (2001). Evidence for stem-cell niches in the tracheal epithelium. *American Journal of Respiratory Cell and Molecular Biology*, *24*(6). https://doi.org/10.1165/ajrcmb.24.6.4217

Boucherat, O., Morissette, M. C., Provencher, S., Bonnet, S., & Maltais, F. (2016). Bridging lung development with chronic obstructive pulmonary disease: Relevance of developmental pathways in chronic obstructive pulmonary disease pathogenesis. In *American Journal of Respiratory and Critical Care Medicine* (Vol. 193, Issue 4). https://doi.org/10.1164/rccm.201508-1518PP

Branchfield, K., Nantie, L., Verheyden, J. M., Sui, P., Wienhold, M. D., & Sun, X. (2016). Pulmonary neuroendocrine cells function as airway sensors to control lung immune response. *Science*, *351*(6274). https://doi.org/10.1126/science.aad7969

Buckpitt, A., Boland, B., Isbell, M., Morin, D., Shultz, M., Baldwin, R., Chan, K., Karlsson, A., Lin, C., Taff, A., West, J., Fanucchi, M., Van Winkle, L., & Plopper, C. (2002). Naphthalene-induced respiratory tract toxicity: Metabolic mechanisms of toxicity. In *Drug Metabolism Reviews* (Vol. 34, Issue 4). https://doi.org/10.1081/DMR-120015694

Carlier, F., Detry, B., Sibille, Y., & Pilette, C. (2018). *COPD epithelial phenotype shows partial reversibility in long-term primary epithelial ALI-cultures*. https://doi.org/10.1183/13993003.congress-2018.oa502

Carpentieri, C., Farrow, N., Cmielewski, P., Rout-Pitt, N., Mccarron, A., Knight, E., Parsons, D., & Donnelley, M. (2021). The Effects of Conditioning and Lentiviral

Vector Pseudotype on Short- A nd Long-Term Airway Reporter Gene Expression in Mice. *Human Gene Therapy*, *32*(15-16). https://doi.org/10.1089/hum.2021.031

Castell, J. V., Donato, M. T., & Gómez-Lechón, M. J. (2005). Metabolism and bioactivation of toxicants in the lung. The in vitro cellular approach. *Experimental and Toxicologic Pathology*, *57*(SUPPL. 1), 189–204. https://doi.org/10.1016/j.etp.2005.05.008

Chakraborty, A., Mastalerz, M., Ansari, M., Schiller, H. B., & Staab-Weijnitz, C. A. (2022). Emerging Roles of Airway Epithelial Cells in Idiopathic Pulmonary Fibrosis. *Cells*, *11*(6). https://doi.org/10.3390/cells11061050

Chang, S. F., Yang, W. H., Cheng, C. Y., Luo, S. J., & Wang, T. C. (2021). γ-secretase inhibitors, DAPT and RO4929097, promote the migration of Human Glioma Cells via Smad5-down-regulated E-cadherin Expression. *International Journal of Medical Sciences*, *18*(12), 2551–2560. https://doi.org/10.7150/ijms.50484

Cmielewski, P., Farrow, N., Devereux, S., Parsons, D., & Donnelley, M. (2017). Gene therapy for Cystic Fibrosis: Improved delivery techniques and conditioning with lysophosphatidylcholine enhance lentiviral gene transfer in mouse lung airways. *Experimental Lung Research*, *43*(9-10). https://doi.org/10.1080/01902148.2017.1395931

CRC Handbook of Chemistry and Physics, 2009−2010, 90th ed. (2009). *Journal of the American Chemical Society*, *131*(35). https://doi.org/10.1021/ja906434c

Cutz, E., Yeger, H., & Pan, J. (2007). Pulmonary neuroendocrine cell system in pediatric lung disease - Recent advances. In *Pediatric and Developmental Pathology* (Vol. 10, Issue 6). https://doi.org/10.2350/07-04-0267.1

Dang, T. P., Gazdar, A. F., Virmani, A. K., Sepetavec, T., Hande, K. R., Minna, J. D., Roberts, J. R., & Carbone, D. P. (2000). Chromosome 19 translocation, overexpression of Notch3, and human lung cancer. *Journal of the National Cancer Institute*, *92*(16). https://doi.org/10.1093/jnci/92.16.1355

Davis, J. D., & Wypych, T. P. (2021). Cellular and functional heterogeneity of the airway epithelium. In *Mucosal Immunology* (Vol. 14, Issue 5). https://doi.org/10.1038/s41385-020-00370-7

DePianto, D. J., Vander Heiden, J. A., Morshead, K. B., Sun, K. H., Modrusan, Z., Teng, G., Wolters, P. J., & Arron, J. R. (2021). Molecular mapping of interstitial lung disease reveals a phenotypically distinct senescent basal epithelial cell population. *JCI Insight*, *6*(8). https://doi.org/10.1172/jci.insight.143626

Deprez, M., Zaragosi, L. E., Truchi, M., Becavin, C., García, S. R., Arguel, M. J., Plaisant, M., Magnone, V., Lebrigand, K., Abelanet, S., Brau, F., Paquet, A., Pe'er, D., Marquette, C. H., Leroy, S., & Barbry, P. (2020). A single-cell atlas of the human healthy airways. *American Journal of Respiratory and Critical Care Medicine*, *202*(12). https://doi.org/10.1164/rccm.201911-2199OC

Dijke, P. Ten, Goumans, M. J., Itoh, F., & Itoh, S. (2002). Regulation of cell proliferation by Smad proteins. In *Journal of Cellular Physiology* (Vol. 191, Issue 1). https://doi.org/10.1002/jcp.10066

Disler, R. T., Gallagher, R. D., Davidson, P. M., Sun, S.-W., Chen, L.-C., Zhou, M., Wu, J.-H., Meng, Z.-J., Han, H.-L., Miao, S.-Y., Zhu, C.-C., Xiong, X.-Z., Reis, M. S., Sampaio, L. M. M., Lacerda, D., De Oliveira, L. V. F., Pereira, G. B. M., Pantoni, C. B. F., Di Thommazo, L., … Mistraletti, G. (2019). Factors impairing the postural balance in COPD patients and its influence upon activities of daily living. *European Respiratory Journal*, *15*(1).

Domańska, U., Klofutar, C., & Paljk, Š. (1994). Solubility of cholesterol in selected organic solvents. *Fluid Phase Equilibria*, *97*(C). https://doi.org/10.1016/0378-

3812(94)85015-1

Ekstrand-Hammarström, B., Österlund, C., Lilliehöök, B., & Bucht, A. (2007). Vitamin E down-modulates mitogen-activated protein kinases, nuclear factor-κB and inflammatory responses in lung epithelial cells. *Clinical and Experimental Immunology*, *147*(2). https://doi.org/10.1111/j.1365-2249.2006.03285.x

Engler, A. E., Ysasi, A. B., Pihl, R. M. F., Villacorta-Martin, C., Heston, H. M., Richardson, H. M. K., Thapa, B. R., Moniz, N. R., Belkina, A. C., Mazzilli, S. A., & Rock, J. R. (2020). Airway-Associated Macrophages in Homeostasis and Repair. *Cell Reports*, *33*(13). https://doi.org/10.1016/j.celrep.2020.108553

Evans, C. M., Fingerlin, T. E., Schwarz, M. I., Lynch, D., Kurche, J., Warg, L., Yang, I. V., & Schwartz, D. A. (2016). Idiopathic pulmonary fibrosis: A genetic disease that involves mucociliary dysfunction of the peripheral airways. *Physiological Reviews*, *96*(4). https://doi.org/10.1152/physrev.00004.2016

Feng, J., Wang, J., Liu, Q., Li, J., Zhang, Q., Zhuang, Z., Yao, X., Liu, C., Li, Y., Cao, L., Li, C., Gong, L., Li, D., Zhang, Y., & Gao, H. (2019). DAPT, a γ-secretase inhibitor, suppresses tumorigenesis, and progression of growth hormone-producing adenomas by targeting notch signaling. *Frontiers in Oncology*, *9*(AUG). https://doi.org/10.3389/fonc.2019.00809

Fernandez, I. E., & Eickelberg, O. (2012). New cellular and molecular mechanisms of lung injury and fi brosis in idiopathic pulmonary fi brosis. *The Lancet*, *380*(9842), 680–688. https://doi.org/10.1016/S0140-6736(12)61144-1

Fessler, M. B. (2017). A new frontier in immunometabolism cholesterol in lung health and disease. *Annals of the American Thoracic Society*, *14*. https://doi.org/10.1513/AnnalsATS.201702-136AW

Gan, H., McKenzie, R., Hao, Q., Idell, S., & Tang, H. (2014). Protein kinase D is increased and activated in lung epithelial cells and macrophages in idiopathic pulmonary fibrosis. *PLoS ONE*, *9*(7). https://doi.org/10.1371/journal.pone.0101983

Gan, H., Wang, G., Hao, Q., Jane Wang, Q., & Tang, H. (2013). Protein kinase D promotes airway epithelial barrier dysfunction and permeability through down-regulation of claudin-1. *Journal of Biological Chemistry*, *288*(52). https://doi.org/10.1074/jbc.M113.511527

Gindele, J. A., Kiechle, T., Benediktus, K., Birk, G., Brendel, M., Heinemann, F., Wohnhaas, C. T., LeBlanc, M., Zhang, H., Strulovici-Barel, Y., Crystal, R. G., Thomas, M. J., Stierstorfer, B., Quast, K., & Schymeinsky, J. (2020). Intermittent exposure to whole cigarette smoke alters the differentiation of primary small airway epithelial cells in the air-liquid interface culture. *Scientific Reports*, *10*(1). https://doi.org/10.1038/s41598-020-63345-5

Gomi, K., Arbelaez, V., Crystal, R. G., & Walters, M. S. (2015). Activation of NOTCH1 or NOTCH3 signaling skews human airway basal cell differentiation toward a secretory pathway. *PLoS ONE*, *10*(2). https://doi.org/10.1371/journal.pone.0116507

Greene, C. M., & McElvaney, N. G. (2005). Toll-like receptor expression and function in airway epithelial cells. In *Archivum Immunologiae et Therapiae Experimentalis* (Vol. 53, Issue 5).

Gu, X., Karp, P. H., Brody, S. L., Pierce, R. A., Welsh, M. J., Holtzman, M. J., & Ben-Shahar, Y. (2014). Chemosensory functions for pulmonary neuroendocrine cells. *American Journal of Respiratory Cell and Molecular Biology*, *50*(3). https://doi.org/10.1165/rcmb.2013-0199OC

Gui, L., Qian, H., Rocco, K. A., Grecu, L., & Niklason, L. E. (2015). Efficient intratracheal delivery of airway epithelial cells in mice and pigs. *American Journal*

of Physiology - Lung Cellular and Molecular Physiology, *308*(2). https://doi.org/10.1152/ajplung.00147.2014

Habermann, A. C., Gutierrez, A. J., Bui, L. T., Yahn, S. L., Winters, N. I., Calvi, C. L., Peter, L., Chung, M. I., Taylor, C. J., Jetter, C., Raju, L., Roberson, J., Ding, G., Wood, L., Sucre, J. M. S., Richmond, B. W., Serezani, A. P., McDonnell, W. J., Mallal, S. B., … Kropski, J. A. (2020). Single-cell RNA sequencing reveals profibrotic roles of distinct epithelial and mesenchymal lineages in pulmonary fibrosis. *Science Advances*, *6*(28). https://doi.org/10.1126/sciadv.aba1972

Hiemstra, P. S., Grootaers, G., van der Does, A. M., Krul, C. A. M., & Kooter, I. M. (2018). Human lung epithelial cell cultures for analysis of inhaled toxicants: Lessons learned and future directions. *Toxicology in Vitro*, *47*(September 2017), 137–146. https://doi.org/10.1016/j.tiv.2017.11.005

Hogan, B. L. M., Barkauskas, C. E., Chapman, H. A., Epstein, J. A., Jain, R., Hsia, C. C. W., Niklason, L., Calle, E., Le, A., Randell, S. H., Rock, J., Snitow, M., Krummel, M., Stripp, B. R., Vu, T., White, E. S., Whitsett, J. A., & Morrisey, E. E. (2014). Repair and regeneration of the respiratory system: Complexity, plasticity, and mechanisms of lung stem cell function. In *Cell Stem Cell* (Vol. 15, Issue 2). https://doi.org/10.1016/j.stem.2014.07.012

Hong, K. U., Reynolds, S. D., Giangreco, A., Hurley, C. M., & Stripp, B. R. (2001). Clara cell secretory protein-expressing cells of the airway neuroepithelial body microenvironment include a label-retaining subset and are critical for epithelial renewal after progenitor cell depletion. *American Journal of Respiratory Cell and Molecular Biology*, *24*(6). https://doi.org/10.1165/ajrcmb.24.6.4498

Jia, J., Conlon, T. M., Sarker, R. S., Taşdemir, D., Smirnova, N. F., Srivastava, B., Verleden, S. E., Güneş, G., Wu, X., Prehn, C., Gao, J., Heinzelmann, K., Lintelmann, J., Irmler, M., Pfeiffer, S., Schloter, M., Zimmermann, R., Hrabé de Angelis, M., Beckers, J., … Yildirim, A. Ö. (2018). Cholesterol metabolism promotes B-cell positioning during immune pathogenesis of chronic obstructive pulmonary disease. *EMBO Molecular Medicine*, *10*(5). https://doi.org/10.15252/emmm.201708349

Johnson, L. G., Vanhook, M. K., Coyne, C. B., Haykal-Coates, N., & Gavett, S. H. (2003). Safety and efficiency of modulating paracellular permeability to enhance airway epithelial gene transfer in vivo. *Human Gene Therapy*, *14*(8). https://doi.org/10.1089/104303403765255138

Karagiannis, T. C., Li, X., Tang, M. M., Orlowski, C., El-Osta, A., Tang, M. L., & Royce, S. G. (2012). Molecular model of naphthalene-induced DNA damage in the murine lung. *Human and Experimental Toxicology*, *31*(1). https://doi.org/10.1177/0960327111407228

Kershaw, C. D., & Guidot, D. M. (2008). Alcoholic lung disease. In *Alcohol Research and Health* (Vol. 31, Issue 1).

Königshoff, M., Balsara, N., Pfaff, E. M., Kramer, M., Chrobak, I., Seeger, W., & Eickelberg, O. (2008). Functional Wnt signaling is increased in idiopathic pulmonary fibrosis. *PLoS ONE*, *3*(5). https://doi.org/10.1371/journal.pone.0002142

Kotlyarov, S., & Kotlyarova, A. (2021). Molecular mechanisms of lipid metabolism disorders in infectious exacerbations of chronic obstructive pulmonary disease. In *International Journal of Molecular Sciences* (Vol. 22, Issue 14). https://doi.org/10.3390/ijms22147634

Leblond, A. L., Naud, P., Forest, V., Gourden, C., Sagan, C., Romefort, B., Mathieu, E., Delorme, B., Collin, C., Pagès, J. C., Sensebé, L., Pitard, B., & Lemarchand, P. (2009). Developing cell therapy techniques for respiratory disease: Intratracheal delivery of genetically engineered stem cells in a murine model of airway injury.

Human Gene Therapy, *20*(11), 1329–1343. https://doi.org/10.1089/hum.2009.035

Lewis, D. F. V., Ito, Y., & Lake, B. G. (2009). Molecular modelling of CYP2F substrates: Comparison of naphthalene metabolism by human, rat and mouse CYP2F subfamily enzymes. *Drug Metabolism and Drug Interactions*, *24*(2-4). https://doi.org/10.1515/DMDI.2009.24.2-4.229

Li, L., Carratt, S., Hartog, M., Kovalchuk, N., Jia, K., Wang, Y., Zhang, Q. Y., Edwards, P., Van Winkle, L., & Ding, X. (2017). Human CYP2A13 and CYP2F1 mediate naphthalene toxicity in the lung and nasal mucosa of CYP2A13/2F1-humanized mice. *Environmental Health Perspectives*, *125*(6). https://doi.org/10.1289/EHP844

Liu, C., Wong, E., Miller, D., Smith, G., Anson, D., & Parsons, D. (2010). Lentiviral airway gene transfer in lungs of mice and sheep: Successes and challenges. *Journal of Gene Medicine*, *12*(8). https://doi.org/10.1002/jgm.1481

Lopez, A. D., Shibuya, K., Rao, C., Mathers, C. D., Hansell, A. L., Held, L. S., Schmid, V., & Buist, S. (2006). Chronic obstructive pulmonary disease: Current burden and future projections. *European Respiratory Journal*, *27*(2). https://doi.org/10.1183/09031936.06.00025805

Martignoni, M., Groothuis, G. M. M., & de Kanter, R. (2006). Species differences between mouse, rat, dog, monkey and human CYP-mediated drug metabolism, inhibition and induction. *Expert Opinion on Drug Metabolism and Toxicology*, *2*(6), 875–894. https://doi.org/10.1517/17425255.2.6.875

Mastalerz, M., Dick, E., Chakraborty, A., Hennen, E., Schamberger, A. C., Schröppel, A., Lindner, M., Hatz, R., Behr, J., Hilgendorff, A., Schmid, O., & Staab-Weijnitz, C. A. (2022). Validation of in vitro models for smoke exposure of primary human bronchial epithelial cells. *American Journal of Physiology - Lung Cellular and Molecular Physiology*, *322*(1). https://doi.org/10.1152/ajplung.00091.2021

McConnell, A. M., Yao, C., Yeckes, A. R., Wang, Y., Selvaggio, A. S., Tang, J., Kirsch, D. G., & Stripp, B. R. (2016). p53 Regulates Progenitor Cell Quiescence and Differentiation in the Airway. *Cell Reports*, *17*(9). https://doi.org/10.1016/j.celrep.2016.11.007

McGuire, J. K., Li, Q., & Parks, W. C. (2003). Matrilysin (matrix metalloproteinase-7) mediates E-cadherin ectodomain shedding in injured lung epithelium. *American Journal of Pathology*, *162*(6). https://doi.org/10.1016/S0002-9440(10)64318-0

Minagawa, S., Araya, J., Numata, T., Nojiri, S., Hara, H., Yumino, Y., Kawaishi, M., Odaka, M., Morikawa, T., Nishimura, S. L., Nakayama, K., & Kuwano, K. (2011). Accelerated epithelial cell senescence in IPF and the inhibitory role of SIRT6 in TGF-β-induced senescence of human bronchial epithelial cells. *American Journal of Physiology - Lung Cellular and Molecular Physiology*, *300*(3). https://doi.org/10.1152/ajplung.00097.2010

Mogi, A., & Kuwano, H. (2011). TP53 mutations in nonsmall cell lung cancer. In *Journal of Biomedicine and Biotechnology* (Vol. 2011). https://doi.org/10.1155/2011/583929

Moiseenko, A., Vazquez-Armendariz, A. I., Kheirollahi, V., Chu, X., Tata, A., Rivetti, S., Günther, S., Lebrigand, K., Herold, S., Braun, T., Mari, B., De Langhe, S., Kwapiszewska, G., Günther, A., Chen, C., Seeger, W., Tata, P. R., Zhang, J. S., Bellusci, S., & El Agha, E. (2020). Identification of a Repair-Supportive Mesenchymal Cell Population during Airway Epithelial Regeneration. *Cell Reports*, *33*(12). https://doi.org/10.1016/j.celrep.2020.108549

Montoro, D. T., Haber, A. L., Biton, M., Vinarsky, V., Lin, B., Birket, S. E., Yuan, F., Chen, S., Leung, H. M., Villoria, J., Rogel, N., Burgin, G., Tsankov, A. M., Waghray, A., Slyper, M., Waldman, J., Nguyen, L., Dionne, D., Rozenblatt-Rosen,

O., … Rajagopal, J. (2018). A revised airway epithelial hierarchy includes CFTR-expressing ionocytes. *Nature*, *560*(7718). https://doi.org/10.1038/s41586-018-0393-7

Mou, H., Yang, Y., Riehs, M. A., Barrios, J., Shivaraju, M., Haber, A. L., Montoro, D. T., Gilmore, K., Haas, E. A., Paunovic, B., Rajagopal, J., Vargas, S. O., Haynes, R. L., Fine, A., Cardoso, W. V., & Ai, X. (2021). Airway basal stem cells generate distinct subpopulations of PNECs. *Cell Reports*, *35*(3). https://doi.org/10.1016/j.celrep.2021.109011

National Cholesterol Education Program (NCEP). (2001). Executive summary of the Third Report of the National Cholesterol Education Programme. *(Ncep)*, *285*(19).

Nomori, H., Horio, H., Takagi, M., Kobayashi, R., & Hirabayashi, Y. (1996). Clara cell protein correlation with hyperlipidemia. *Chest*, *110*(3). https://doi.org/10.1378/chest.110.3.680

Pan, H., Deutsch, G. H., & Wert, S. E. (2019). Comprehensive anatomic ontologies for lung development: A comparison of alveolar formation and maturation within mouse and human lung. *Journal of Biomedical Semantics*, *10*(1). https://doi.org/10.1186/s13326-019-0209-1

Parsons, D. W., Grubb, B. R., Johnson, L. G., & Boucher, R. C. (1998). Enhanced in vivo airway gene transfer via transient modification of host barrier properties with a surface-active agent. *Human Gene Therapy*, *9*(18). https://doi.org/10.1089/hum.1998.9.18-2661

Peake, J. L., Reynolds, S. D., Stripp, B. R., Stephens, K. E., & Pinkerton, K. E. (2000). Alteration of pulmonary neuroendocrine cells during epithelial repair of naphthalene-induced airway injury. *American Journal of Pathology*, *156*(1). https://doi.org/10.1016/S0002-9440(10)64728-1

Pini, L., Pinelli, V., Modina, D., Bezzi, M., Tiberio, L., & Tantucci, C. (2014). Central airways remodeling in COPD patients. *International Journal of COPD*, *9*. https://doi.org/10.2147/COPD.S52478

Plasschaert, L. W., Žilionis, R., Choo-Wing, R., Savova, V., Knehr, J., Roma, G., Klein, A. M., & Jaffe, A. B. (2018). A single-cell atlas of the airway epithelium reveals the CFTR-rich pulmonary ionocyte. *Nature*, *560*(7718). https://doi.org/10.1038/s41586-018-0394-6

Plataki, M., Koutsopoulos, A. V., Darivianaki, K., Delides, G., Siafakas, N. M., & Bouros, D. (2005). Expression of apoptotic and antiapoptotic markers in epithelial cells in idiopathic pulmonary fibrosis. *Chest*, *127*(1), 266–274. https://doi.org/10.1378/chest.127.1.266

Prasse, A., Binder, H., Schupp, J. C., Kayser, G., Bargagli, E., Jaeger, B., Hess, M., Rittinghausen, S., Vuga, L., Lynn, H., Violette, S., Jung, B., Quast, K., Vanaudenaerde, B., Xu, Y., Hohlfeld, J. M., Krug, N., Herazo-Maya, J. D., Rottoli, P., … Kaminski, N. (2019). BAL Cell Gene Expression Is Indicative of Outcome and Airway Basal Cell Involvement in Idiopathic Pulmonary Fibrosis. *https://doi.org/10.1164/rccm.201712-2551OC*, *199*(5), 622–630. https://doi.org/10.1164/RCCM.201712-2551OC

R Core Team. (2021). R Core Team 2021 R: A language and environment for statistical computing. R foundation for statistical computing. https://www.R-project.org/. In *R Foundation for Statistical Computing* (Vol. 2).

Rackley, C. R., & Stripp, B. R. (2012). Building and maintaining the epithelium of the lung. In *Journal of Clinical Investigation* (Vol. 122, Issue 8). https://doi.org/10.1172/JCI60519

Rane, C. K., Jackson, S. R., Pastore, C. F., Zhao, G., Weiner, A. I., Patel, N. N.,

Herbert, D. R., Cohen, N. A., & Vaughan, A. E. (2019). Development of solitary chemosensory cells in the distal lung after severe influenza injury. *American Journal of Physiology - Lung Cellular and Molecular Physiology*, *316*(6). https://doi.org/10.1152/ajplung.00032.2019

Raslan, A. A., Oh, Y. J., Jin, Y. R., & Yoon, J. K. (2022). R-Spondin2, a Positive Canonical WNT Signaling Regulator, Controls the Expansion and Differentiation of Distal Lung Epithelial Stem/Progenitor Cells in Mice. *International Journal of Molecular Sciences*, *23*(6), 3089. https://doi.org/10.3390/ijms23063089

Rearick, J. I., & Jetten, A. M. (1986). Accumulation of cholesterol 3-sulfate during in vitro squamous differentiation of rabbit tracheal epithelial cells and its regulation by retinoids. *Journal of Biological Chemistry*, *261*(30). https://doi.org/10.1016/s0021-9258(18)66956-x

Reynolds, S. D., Giangreco, A., Power, J. H. T., & Stripp, B. R. (2000). Neuroepithelial bodies of pulmonary airways serve as a reservoir of progenitor cells capable of epithelial regeneration. *American Journal of Pathology*, *156*(1), 269–278. https://doi.org/10.1016/S0002-9440(10)64727-X

Rock, J. R., Gao, X., Xue, Y., Randell, S. H., Kong, Y. Y., & Hogan, B. L. M. (2011). Notch-dependent differentiation of adult airway basal stem cells. *Cell Stem Cell*, *8*(6). https://doi.org/10.1016/j.stem.2011.04.003

Rock, J. R., Onaitis, M. W., Rawlins, E. L., Lu, Y., Clark, C. P., Xue, Y., Randell, S. H., & Hogan, B. L. M. (2009). Basal cells as stem cells of the mouse trachea and human airway epithelium. *Proceedings of the National Academy of Sciences of the United States of America*, *106*(31). https://doi.org/10.1073/pnas.0906850106

Rock, J. R., Randell, S. H., & Hogan, B. L. M. (2010). Airway basal stem cells: A perspective on their roles in epithelial homeostasis and remodeling. In *DMM Disease Models and Mechanisms* (Vol. 3, Issues 9-10). https://doi.org/10.1242/dmm.006031

Rokicki, W., Rokicki, M., Wojtacha, J., & Dzeljijli, A. (2016). The role and importance of club cells (Clara cells) in the pathogenesis of some respiratory diseases. *Kardiochirurgia I Torakochirurgia Polska*, *13*(1). https://doi.org/10.5114/kitp.2016.58961

Romieu, I., Castro-Giner, F., Kunzli, N., & Sunyer, J. (2008). Air pollution, oxidative stress and dietary supplementation: A review. *European Respiratory Journal*, *31*(1), 179–196. https://doi.org/10.1183/09031936.00128106

Rooney, C., & Sethi, T. (2011). The epithelial cell and lung cancer: The link between chronic obstructive pulmonary disease and lung cancer. *Respiration*, *81*(2). https://doi.org/10.1159/000323946

Sagiv, A., Bar-Shai, A., Levi, N., Hatzav, M., Zada, L., Ovadya, Y., Roitman, L., Manella, G., Regev, O., Majewska, J., Vadai, E., Eilam, R., Feigelson, S. W., Tsoory, M., Tauc, M., Alon, R., & Krizhanovsky, V. (2018). p53 in Bronchial Club Cells Facilitates Chronic Lung Inflammation by Promoting Senescence. *Cell Reports*, *22*(13). https://doi.org/10.1016/j.celrep.2018.03.009

Salvi, S. S., & Barnes, P. J. (2009). Chronic obstructive pulmonary disease in non-smokers. In *The Lancet* (Vol. 374, Issue 9691). https://doi.org/10.1016/S0140-6736(09)61303-9

Sauleda, J., Núñez, B., Sala, E., & Soriano, J. (2018). Idiopathic Pulmonary Fibrosis: Epidemiology, Natural History, Phenotypes. *Medical Sciences*, *6*(4). https://doi.org/10.3390/medsci6040110

Schamberger, A. C., Staab-Weijnitz, C. A., Mise-Racek, N., & Eickelberg, O. (2015). Cigarette smoke alters primary human bronchial epithelial cell differentiation at the

air-liquid interface. *Scientific Reports*, *5*, 1–9. https://doi.org/10.1038/srep08163

Schögler, A., Blank, F., Brügger, M., Beyeler, S., Tschanz, S. A., Regamey, N., Casaulta, C., Geiser, T., & Alves, M. P. (2017). Characterization of pediatric cystic fibrosis airway epithelial cell cultures at the air-liquid interface obtained by non-invasive nasal cytology brush sampling. *Respiratory Research*, *18*(1). https://doi.org/10.1186/s12931-017-0706-7

Seibold, M. A., Smith, R. W., Urbanek, C., Groshong, S. D., Cosgrove, G. P., Brown, K. K., Schwarz, M. I., Schwartz, D. A., & Reynolds, S. D. (2013). The Idiopathic Pulmonary Fibrosis Honeycomb Cyst Contains A Mucocilary Pseudostratified Epithelium. *PLoS ONE*, *8*(3). https://doi.org/10.1371/JOURNAL.PONE.0058658

Selman, M., & Pardo, A. (2014). Revealing the pathogenic and aging-related mechanisms of the enigmatic idiopathic pulmonary fibrosis: An integral model. *American Journal of Respiratory and Critical Care Medicine*, *189*(10). https://doi.org/10.1164/rccm.201312-2221PP

Sette, G., Cicero, S. Lo, Blaconà, G., Pierandrei, S., Bruno, S. M., Salvati, V., Castelli, G., Falchi, M., Fabrizzi, B., Cimino, G., De Maria, R., Biffoni, M., Eramo, A., & Lucarelli, M. (2021). Theratyping cystic fibrosis in vitro in ALI culture and organoid models generated from patient-derived nasal epithelial conditionally reprogrammed stem cells. *European Respiratory Journal*, *58*(6). https://doi.org/10.1183/13993003.00908-2021

Shaykhiev, R. (2019). Emerging biology of persistent mucous cell hyperplasia in COPD. In *Thorax* (Vol. 74, Issue 1). https://doi.org/10.1136/thoraxjnl-2018-212271

Shaykhiev, R., Sackrowitz, R., Fukui, T., Zuo, W. L., Chao, I. W., Strulovici-Barel, Y., Downey, R. J., & Crystal, R. G. (2013). Smoking-induced CXCL14 expression in the human airway epithelium links chronic obstructive pulmonary disease to lung cancer. *American Journal of Respiratory Cell and Molecular Biology*, *49*(3). https://doi.org/10.1165/rcmb.2012-0396OC

Shultz, M. A., Choudary, P. V., & Buckpitt, A. R. (1999). Role of murine cytochrome P-450 2F2 in metabolic activation of naphthalene and metabolism of other xenobiotics. *Journal of Pharmacology and Experimental Therapeutics*, *290*(1).

Smirnova, N. F., Schamberger, A. C., Nayakanti, S., Hatz, R., Behr, J., & Eickelberg, O. (2016). Detection and quantification of epithelial progenitor cell populations in human healthy and IPF lungs. *Respiratory Research*, *17*(1). https://doi.org/10.1186/s12931-016-0404-x

Song, H., Yao, E., Lin, C., Gacayan, R., Chen, M. H., & Chuang, P. T. (2012). Functional characterization of pulmonary neuroendocrine cells in lung development, injury,and tumorigenesis. *Proceedings of the National Academy of Sciences of the United States of America*, *109*(43), 17531–17536. https://doi.org/10.1073/pnas.1207238109

Springer, J., Scholz, F. R., Peiser, C., Groneberg, D. A., & Fischer, A. (2004). SMAD-signaling in chronic obstructive pulmonary disease: Transcriptional down-regulation of inhibitory SMAD 6 and 7 by cigarette smoke. *Biological Chemistry*, *385*(7). https://doi.org/10.1515/BC.2004.080

Staudt, M. R., Rogalski, A., Tilley, A. E., Kaner, R. J., Harvey, B., & Crystal, R. G. (2014). Smoking Is Associated With A Loss Of Ciliated Cells Throughout The Airways. *AmJ Resp Crit Care Med - Meeting Abstracts*.

Strine, M. S., & Wilen, C. B. (2022). Tuft cells are key mediators of interkingdom interactions at mucosal barrier surfaces. In *PLoS Pathogens* (Vol. 18, Issue 3). https://doi.org/10.1371/journal.ppat.1010318

Sunday, M. E., Shan, L., & Subramaniam, M. (2004). Immunomodulatory functions of

the diffuse neuroendocrine system: Implications for bronchopulmonary dysplasia. In *Endocrine Pathology* (Vol. 15, Issue 2). https://doi.org/10.1385/ep:15:2:091

Telange, D. R., Jain, S. P., Pethe, A. M., & Kharkar, P. S. (2021). Egg White Protein Carrier-Assisted Development of Solid Dispersion for Improved Aqueous Solubility and Permeability of Poorly Water Soluble Hydrochlorothiazide. *AAPS PharmSciTech*, *22*(3). https://doi.org/10.1208/s12249-021-01967-2

Thomas, B., Koh, M. S., O'Callaghan, C., Allen, J. C., Rutman, A., Hirst, R. A., Connolly, J., Low, S. Y., Thun How, O., Chian Min, L., Lim, W. T., Lin Ean Oon, L., He, Q., Teoh, O. H., & Lapperre, T. S. (2021). Dysfunctional Bronchial Cilia Are a Feature of Chronic Obstructive Pulmonary Disease (COPD). *COPD: Journal of Chronic Obstructive Pulmonary Disease*, *18*(6). https://doi.org/10.1080/15412555.2021.1963695

Tilley, A. E., Harvey, B. G., Heguy, A., Hackett, N. R., Wang, R., O'Connor, T. P., & Crystal, R. G. (2009). Down-regulation of the notch pathway in human airway epithelium in association with smoking and chronic obstructive pulmonary disease. *American Journal of Respiratory and Critical Care Medicine*, *179*(6). https://doi.org/10.1164/rccm.200705-795OC

Timm, M., Saaby, L., Moesby, L., & Hansen, E. W. (2013). Considerations regarding use of solvents in in vitro cell based assays. *Cytotechnology*, *65*(5). https://doi.org/10.1007/s10616-012-9530-6

Vaughan, A. E., Brumwell, A. N., Xi, Y., Gotts, J. E., Brownfield, D. G., Treutlein, B., Tan, K., Tan, V., Liu, F. C., Looney, M. R., Matthay, M. A., Rock, J. R., & Chapman, H. A. (2014). Lineage-negative progenitors mobilize to regenerate lung epithelium after major injury. *Nature 2014 517:7536*, *517*(7536), 621–625. https://doi.org/10.1038/nature14112

Wang, G. F., Lai, M. D., Yang, R. R., Chen, P. H., Su, Y. Y., Lv, B. J., Sun, L. P., Huang, Q., & Chen, S. Z. (2006). Histological types and significance of bronchial epithelial dysplasia. *Modern Pathology*, *19*(3). https://doi.org/10.1038/modpathol.3800553

Wang, I. M., Stepaniants, S., Boie, Y., Mortimer, J. R., Kennedy, B., Elliott, M., Hayashi, S., Loy, L., Coulter, S., Cervino, S., Harris, J., Thornton, M., Raubertas, R., Roberts, C., Hogg, J. C., Crackower, M., O'Neill, G., & Paré, P. D. (2008). Gene expression profiling in patients with chronic obstructive pulmonary disease and lung cancer. *American Journal of Respiratory and Critical Care Medicine*, *177*(4). https://doi.org/10.1164/rccm.200703-390OC

Wang, Y., Sun, R., Xu, X., Du, M., Zhu, B., & Wu, C. (2021). Mechanism of enhancing the water-solubility and stability of curcumin by using self-assembled cod protein nanoparticles at an alkaline pH. *Food and Function*, *12*(24). https://doi.org/10.1039/d1fo02833b

Watkins, D. N., Berman, D. M., Burkholder, S. G., Wang, B., Beachy, P. A., & Baylin, S. B. (2003). Hedgehog signalling within airway epithelial progenitors and in small-cell lung cancer. *Nature*, *422*(6929). https://doi.org/10.1038/nature01493

Weichselbaum, M., Sparrow, M. P., Hamilton, E. J., Thompson, P. J., & Knight, D. A. (2005). A confocal microscopic study of solitary pulmonary neuroendocrine cells in human airway epithelium. *Respiratory Research*, *6*. https://doi.org/10.1186/1465-9921-6-115

Westhoff, B., Colaluca, I. N., D'Ario, G., Donzelli, M., Tosoni, D., Volorio, S., Pelosi, G., Spaggiari, L., Mazzarol, G., Viale, G., Pece, S., & Di Fiore, P. P. (2009). Alterations of the Notch pathway in lung cancer. *Proceedings of the National Academy of Sciences of the United States of America*, *106*(52). https://doi.org/10.1073/pnas.0907781106

Wilson, A. M., Nair, P., Hargreave, F. E., Efthimiadis, A. E., Anvari, M., & Allen, C. J. (2011). Lipid and smoker's inclusions in sputum macrophages in patients with airway diseases. *Respiratory Medicine*, *105*(11). https://doi.org/10.1016/j.rmed.2011.07.011

Wistuba, I. I., Berry, J., Behrens, C., Maitra, A., Shivapurkar, N., Milchgrub, S., Mackay, B., Minna, J. D., & Gazdar, A. F. (2000). Molecular changes in the bronchial epithelium of patients with small cell lung cancer. *Clinical Cancer Research*, *6*(7).

Xing, Y., Li, A., Borok, Z., Li, C., & Minoo, P. (2012). NOTCH1 is required for regeneration of Clara cells during repair of airway injury. *Stem Cells*, *30*(5). https://doi.org/10.1002/stem.1059

Xu, K., Moghal, N., & Egan, S. E. (2012). Notch signaling in lung development and disease. *Advances in Experimental Medicine and Biology*, *727*. https://doi.org/10.1007/978-1-4614-0899-4_7

Xuan, L., Han, F., Gong, L., Lv, Y., Wan, Z., Liu, H., Zhang, D., Jia, Y., Yang, S., Ren, L., & Liu, L. (2018). Association between chronic obstructive pulmonary disease and serum lipid levels: A meta-analysis. *Lipids in Health and Disease*, *17*(1). https://doi.org/10.1186/s12944-018-0904-4

Zandvoort, A., Postma, D. S., Jonker, M. R., Noordhoek, J. A., Vos, J. T. W. M., van der Geld, Y. M., & Timens, W. (2006). Altered expression of the Smad signalling pathway: Implications for COPD pathogenesis. *European Respiratory Journal*, *28*(3). https://doi.org/10.1183/09031936.06.00078405

Zepp, J. A., & Morrisey, E. E. (2019). Cellular crosstalk in the development and regeneration of the respiratory system. In *Nature Reviews Molecular Cell Biology* (Vol. 20, Issue 9). https://doi.org/10.1038/s41580-019-0141-3

Zou, J., Li, Y., Yu, J., Dong, L., Husain, A. N., Shen, L., & Weber, C. R. (2020). Idiopathic pulmonary fibrosis is associated with tight junction protein alterations. *Biochimica et Biophysica Acta - Biomembranes*, *1862*(5). https://doi.org/10.1016/j.bbamem.2020.183205

List of abbreviations

AT I: Alveolar type I cells

AT II: Alveolar type II cells

ALI: Air-liquid interface

BSA: Bovine Serum Albumin

CHOL: Cholesterol

COPD: Chronic Obstructive Pulmonary Disease

DPBS: Dulbecco's Phosphate-Buffered Saline

ECM: Extracellular Matrix Components

EC50: Half maximal effective concentration

HBSS: Hanks' Balanced Salt Solution

IPA: Ingenuity Pathway Analysis

IF: Immunofluorescent

IPF: Idiopathic Pulmonary Fibrosis

LDH: Lactate Dehydrogenease Assay

NA: Naphthalene

phBECs: Primary human bronchial epithelial cells

PDOC: Polidocanol

PNECs: Pulmonary neuroendocrine cells

qRT-PCR: Quantitative Real-Time Reverse-Transcriptase PCR

TEER: Trans Epithelial Electrical Resistance

WHO: World Health Organization

XME's: Xenobiotic Metabolizing Enzymes

List of Figures

List of tables

List of publications

Chakraborty A, Mastalerz M, Ansari M, Schiller HB, Staab-Weijnitz CA. Emerging Roles of Airway Epithelial Cells in Idiopathic Pulmonary Fibrosis. Cells. 2022 Mar 19;11(6):1050. doi: 10.3390/cells11061050. PMID: 35326501; PMCID: PMC8947093.

Mastalerz M, Dick E, **Chakraborty A**, Hennen E, Schamberger AC, Schröppel A, Lindner M, Hatz R, Behr J, Hilgendorff A, Schmid O, Staab-Weijnitz CA. Validation of in vitro models for smoke exposure of primary human bronchial epithelial cells. Am J Physiol Lung Cell Mol Physiol. 2022 Jan 1;322(1):L129-L148. doi: 10.1152/ajplung.00091.2021. Epub 2021 Oct 20. PMID: 34668416.

Berthold EJ, Lauer YM, **Chakraborty A**, von Brunn B, Hilgendorff A, Hatz RA, Behr J, Hausch F, Staab- Weijnitz CA, von Brunn A. Effects of immunophilin inhibitors and non-immunosuppressive analogs on coronavirus replication in human infection models Frontiers in Cellular and Infection Microbiology journal. . https://doi.org/10.3389/fcimb.2022.958634

Nakayama M, Marchi H, Dimitrieva AM, **Chakraborty A**, Hennen E, Gleut RL, Ruppert C, Guenther A, Kahnert K, Behr J, Hilgendorff A, Hauck S, Adler H, Staab- Weijnitz CA. Quantitative proteomics of differentiated primary bronchial epithelial cells from COPD and control show novel host factors post-influenza A virus infection Frontiers in Microbiology, 2023, 13. doi:10.3389/fmicb.2022.957830.

Acknowledgements

I would like to thank my doctoral supervisor PD Dr. Claudia Staab-Weijnitz for giving me this opportunity to work on this project. I would also like to thank for her constant support and feedback sessions throughout my PhD journey which has helped me to improve scientifically. It has been a great learning curve for me, and I believe that the things I have learned over the past four years will be of great benefit in the near future. I would also like to thank her for the CPC research school activities and training during PhD studies. You have always motivated and inspired us in the lab. Thank you Claudia ☺ ☺

I would like to thank my Thesis Advisory Committee members Prof Dr. Alexander Dietrich and Prof Dr. Scott Randell for their valuable discussions and inputs in this project. Special thanks go to the CPC bioarchive team for providing valuable human material for this work.

I would like to thank my former and current lab members: Elisabeth Hennen, Elisabeth Dick, Ceylan Onursal, Michal Mastalerz, Karolina Pijadina, Natalia Christina Cabeza-Boeddinghaus, Emilia Berthold, Marie Zoeller, Juliana Giraldo, and Misako Nakayama. I am grateful to have met such people in the lab. You all have been very supportive and helpful throughout my PhD journey. You guys are the driving force for keeping up the team spirit in the lab.

Coffee buddies: Aydan, Bikram, Andy, Shruthi, Pushkar, Vijay, Ceylan, Haifeng, Michal, Valeria, Johannes, Tankut, Shuboshree, Georgia, Sabine, Safwan, Ravinder, Christopher, Sezer, Mahesh, Arunima Sengupta, and Prajakta Oak. I would like to thank you all for such a great time that we have spent altogether. I will surely cherish these memories in the future. I wish you all great success in your scientific career in the near future.

I would also like to take a moment and thank my girlfriend Aydan whom I actually met during my PhD journey. Thank you for being very supportive and motivating throughout the PhD journey. Best wishes for your PhD too.

I thank my former lab supervisors Prof Dr. Lena Palmberg, Dr. Swapna Upadhyay, and Dr. Koustav Ganguly, where I first learned about the air-liquid interface cell culture and it has been a strong foundation for my PhD work. I would also like to take this opportunity and thank my friends and colleagues from my master's program: Sabbir, David, Mike, Heeteak, Edwin, Mizanur, Karlhans, Malin, and Tania.

Special thanks to all the administrative staff: Sophie, Silke, Karin, Kaori, and Jocelyne who have always been supportive and helpful.

Lastly, I would like to thank my family members Anindita, Shubhra, and Dr. Anjan kumar Chakraborty for their unconditional support and motivation throughout this journey.